

JAERI-Data/Code



JP0550105

2005-002



PROGRAMS OPTMAN AND SHEMMAN VERSION 8 (2004)

March 2005

Efrem Sh. SOUKHOVITSKI*, Satoshi CHIBA, Osamu IWAMOTO,
Keiichi SHIBATA, Tokio FUKAHORI and Gennadij B. MOROGOVSKIJ*

日本原子力研究所
Japan Atomic Energy Research Institute

本レポートは、日本原子力研究所が不定期に公刊している研究報告書です。
入手の問合せは、日本原子力研究所研究情報部研究情報課（〒319-1195 茨城県那珂郡東海村）あて、
お申し越しください。なお、このほかに財団法人原子力弘済会資料センター（〒319-1195 茨城県那珂郡
東海村日本原子力研究所内）で複写による実費頒布をおこなっております。

This report is issued irregularly.

Inquiries about availability of the reports should be addressed to Research Information Division,
Department of Intellectual Resources, Japan Atomic Energy Research Institute, Tokai-mura, Naka-
gun, Ibaraki-ken 319-1195, Japan.

Programs OPTMAN and SHEMMAN Version 8 (2004)

Efrem Sh. SOUKHOVITSKI*, Satoshi CHIBA, Osamu IWAMOTO⁺,
Keiichi SHIBATA⁺, Tokio FUKAHORI⁺ and Gennadij B. MOROGOVSKIJ*

Advanced Science Research Center
(Tokai Site)
Japan Atomic Energy Research Institute
Tokai-mura, Naka-gun, Ibaraki-ken

(Received January 27, 2005)

This report gives a description of the theory, computational algorithms, input and output formats of modernized coupled-channels optical model code OPTMAN based on wave functions of the soft-rotator model. An accompany code SHEMMAN is also explained which is used to obtain nuclear Hamiltonian parameters to reproduce low-lying collective levels of even-even nuclei in terms of the soft-rotator model. The report describes ideas and algorithms developed to make OPTMAN and SHEMMAN quicker and more accurate, new user-friendly interface generated for OPTMAN, and covers an activity performed under Project Agreement B-521 with the International Science and Technology Center (Moscow), financing party of which is Japan.

Keywords: Nuclear Reactions, σ_{tot} , (n,n), (n,n'), (p,p), (p,p'), $\sigma_{p,nonel}$, OPTMAN, Soft-rotator Model, Collective Level Structure, Coupled-channels Method, ISTC B-521, Theory, Numerical Algorithms, Interface, Inputs-outputs

⁺ Department of Nuclear Energy System, Tokai Research Establishment
* Joint Institute for Energy and Nuclear Research (Belarus)

プログラム OPTMAN 及び SHEMMAN 第8版 (2004)

日本原子力研究所先端基礎研究センター

Efrem Sh. Soukhovitski* 千葉 敏・岩本 修 +

柴田 恵一 +・深堀 智生 +・Gennadij B. Morogovskij*

(2005年1月27日受理)

軟回転体模型ハミルトニアンに基づくチャンネル結合光学模型によって原子核の集団励起構造と反応断面積を記述する計算コード OPTMANにおいて用いられている理論、数値計算手法と入出力フォーマットの説明を行う。同時に軟回転体模型によって原子核ハミルトニアンのパラメータを求めるコード SHEMMAN の説明も行う。本研究は、国際科学技術センター (ISTC モスクワ) のプロジェクト B-521 として、日本のサポートの下で行われている。本プロジェクトにより OPTMAN における数値計算アルゴリズムは完全に改訂され、またユーザーフレンドリーなインターフェースが設けられた。

日本原子力研究所(東海駐在) : 〒319-1195 茨城県那珂郡東海村白方白根2-4

+ 東海研究所エネルギーシステム研究部

* エネルギー及び原子核共同研究所(ペラルーシ)

Contents

1.	Introduction	1
2.	Description of the Soft-rotator Model	2
3.	Optical Potential and Channel Coupling	8
	3.1 The Main Essence of the CC Built on Soft-rotator Nuclear Model	11
4.	Solutions of Scattering Problems	12
	4.1 Accurate Solution of Coupled-channels System for Radial Functions and Matching	12
	4.2 Iterative Approach to Solve a System of Coupled Equations	14
	4.3 Asymptotic Wave Functions Used to be Matched with Numerical Solutions	16
5.	C-matrix and Coupled-channels Optical Model Predictions	17
	5.1 Legendre Polynomial Expansion of Angular Distributions of Scattered Particles	18
6.	Energy Dependence of Optical Potential Parameters	19
7.	Relativistic Generalization of Non-relativistic Schrödinger Equation	21
8.	Potential Adjustment	21
9.	Analysis of B(E2) Data	22
10.	Program OPTMAN	22
	10.1 Program Description	22
	10.2 Input Data	30
	10.3 Examples of Input Files	41
	10.3.1 Input for the Rigid-rotator Model	41
	10.3.2 Input for the Soft-rotator Model	47
	10.4 User-friendly Input Interface	51
	10.5 Running the Code OPTMAN and Description of Output Files	57
11.	Program SHEMMAN	70
	11.1 Input Data	71
	11.2 An Example of Input File	72
	11.3 Running the SHEMMAN Code	74
12.	Conclusions	74
	Acknowledgements	75
	References	76

目 次

1. 序論	1
2. 軟回転体模型の説明	2
3. 光学ポテンシャルとチャンネル結合法	8
3.1 軟回転体模型に基づくチャンネル結合法の特徴	11
4. 散乱問題の解	12
4.1 動径波動関数に対する結合方程式の正確な解と接続	12
4.2 チャンネル結合方程式に対する繰り返し解法	14
4.3 数値解と接続させる漸近波動関数	16
5. C-行列とチャンネル結合光学模型による断面積計算	17
5.1 散乱粒子の角度分布に対するルジャンドル多項式展開	18
6. 光学ポテンシャルパラメータのエネルギー依存性	19
7. 非相対論的シュレーディンガー方程式の相対論的一般化	21
8. ポテンシャルの調整	21
9. B(E2) データの解析	22
10. プログラム OPTMAN	22
10.1 プログラムの説明	22
10.2 入力データ	30
10.3 入力ファイルの例	41
10.3.1 剛回転体模型に対する入力	41
10.3.2 軟回転体模型に対する入力	47
10.4 初心者用入力インターフェース	51
10.5 OPTMAN コードの実行と出力ファイルの説明	57
11. プログラム SHEMMAN	70
11.1 入力データ	71
11.2 入力データ例	72
11.3 SHEMMAN コードの実行	74
12. 結論	74
謝辞	75
参考文献	76

1 Introduction

For more than twenty years, an original coupled-channels optical model code OPTMAN has been developed at Joint Institute of Energy and Nuclear Research to investigate nucleon-nucleus interaction mechanisms and as a basic tool for nuclear data evaluation for reactor design and other applications. Results of such activities for, e.g., ^{235}U , ^{239}Pu , ^{236}U , ^{233}U , ^{238}Pu etc., were included in evaluated Nuclear Data Library BROND[1] of former Soviet Union. Except for the standard rigid rotator and harmonic vibrator coupling schemes encoded in widely-used JUPITER[2] and ECIS[3] codes, level-coupling schemes based on a non-axial soft-rotator model are included for the even-even nuclei in OPTMAN. This allows account of stretching of soft nuclei by rotations, which results in change of equilibrium deformations for excited collective states compared with that of the ground state. This is a critical point for reliable predictions[4, 5, 6] based on the coupled-channels method.

Over many years, OPTMAN was improved and used for evaluation of reactor oriented nuclear data. So it was written originally considering only neutrons as the projectile with possible upper incident energy of about 20MeV. In 1995-1998, this code was successfully used as a theoretical base for nuclear data evaluation for minor actinides carried out in the framework of ISTC Project CIS-03-95, financial party of which was Japan. In 1997 OPTMAN code was installed at Nuclear Data Center of Japan Atomic Energy Research Institute and an active collaboration started. After that time, many new options were added to the code following demands from a broad range of applications: power reactors, shielding design, radiotherapy, transmutations of nuclear wastes and nucleosynthesis.

Calculations with OPTMAN are now possible both for neutrons and protons as the projectile, and the upper incident nucleon energy is extended to at least 200 MeV[7]. Current version of soft-rotator model of OPTMAN takes account of the non-axial quadrupole, octupole and hexadecapole deformations, and β_2 , β_3 and γ -vibrations with account of nuclear volume conservation. With this option, OPTMAN is able to analyze the collective level structure, E2, E3, E4 γ -transition probabilities and reaction data in a self-consistent manner, which makes results of such analyses more reliable. We have found that this model was flexible enough so that OPTMAN can be applied not only to heavy rotational nuclei[8, 9], but can be applied very successfully even to a very light nucleus, namely ^{12}C [10, 11] and light one ^{28}Si [12], and also to vibrational nuclei such as ^{52}Cr [13], ^{56}Fe [14, 15] and ^{58}Ni [16]. In the mean time, energy dependence of the optical potential has been continuously improved with a guidance by physical principles. Now, such features as the high-energy saturation behaviour consistent with Dirac phenomenology[17], relativistic generalization of Elton[18] and Madland[19], and properties stemming from the nuclear matter theory[20] are taken into consideration.

Therefore, OPTMAN has capabilities applicable for analyses of nucleon interaction with light, medium and heavy nuclei for a wide energy range, which will be crucially important to fulfill many nuclear-data demands. Nevertheless, the code, especially the mathematical algorithms, is not described in detail before, so it may be still a “black box” for most of the users. On the other hand, large computational resources available today made a complete modernization of the code possible. Furthermore,

currently available theoretical approaches were included with some new, more accurate advanced mathematical solutions and algorithms. They have made the code a user-friendly program complex for coupled-channels optical model calculations.

This report is intended as a manual of the codes OPTMAN and SHEMMAN, giving details of the soft-rotator theory, physical ideas and computation algorithms developed and incorporated into modernized codes, description of input and output files, allowing easy running, understanding and using of OPTMAN outputs. Some parts of this report, especially the theory part, have duplication with our previous report[21], but we include them here so that this report alone can serve as a stand-alone manual of OPTMAN and SHEMMAN. Also, typological errors in our previous report are corrected in this manual.

The report covers the activity performed under the Project Agreement B-521 with the International Science and Technology Center (Moscow). The financing party for the Project is Japan.

2 Description of the Soft-rotator Model

We assume that the low-lying excited states observed in even-even non-spherical nuclei can be described as a combination of rotation, β -quadrupole and octupole vibrations, and γ -quadrupole vibration. Instant nuclear shapes that correspond to such excitations can be presented [22, 23] in a body-fixed system as:

$$\begin{aligned}
 R(\theta', \varphi') &= R_0 r_\beta(\theta', \varphi') \\
 &= R_0 \left\{ 1 + \sum_{\lambda\mu} \beta_{\lambda\mu} Y_{\lambda\mu}(\theta', \varphi') \right\} \\
 &= R_0 \left\{ 1 + \beta_2 \left[\cos \gamma Y_{20}(\theta', \varphi') + \frac{1}{\sqrt{2}} \sin \gamma (Y_{22}(\theta', \varphi') + Y_{2-2}(\theta', \varphi')) \right] \right. \\
 &\quad + \beta_3 \left[\cos \eta Y_{30}(\theta', \varphi') + \frac{1}{\sqrt{2}} \sin \eta (Y_{32}(\theta', \varphi') + Y_{3-2}(\theta', \varphi')) \right] \\
 &\quad \left. + b_{40} Y_{40}(\theta', \varphi') + \sum_{\mu=2,4} b_{4\mu} (Y_{4\mu}(\theta', \varphi') + Y_{4-\mu}(\theta', \varphi')) \right\}. \tag{1}
 \end{aligned}$$

To simplify the calculations, we assume that internal octupole variables satisfy additional conditions:

$$\beta_{3\pm 1} = \beta_{3\pm 3} = 0, \beta_{32} = \beta_{3-2}, \tag{2}$$

which are admissible in the case for the first excited states [24].

The Hamiltonian \hat{H} of the soft-rotator model consists of the kinetic energy terms for the rotation of the non-axial nuclei with quadrupole, hexadecapole and octupole deformations, the β_2 -, γ -quadrupole and octupole vibrations, and the vibrational potentials ignoring a coupling between the three vibration modes [5]:

$$\hat{H} = \frac{\hbar^2}{2B_2} \left\{ \hat{T}_{\beta_2} + \frac{1}{\beta_2^2} \hat{T}_\gamma \right\} + \frac{\hbar^2}{2} \hat{T}_r + \frac{\hbar^2}{2B_3} \hat{T}_{\beta_3} + \frac{\beta_{20}^4}{\beta_2^2} V(\gamma) + V(\beta_2) + V(\beta_3), \tag{3}$$

where

$$\hat{T}_{\beta_2} = -\frac{1}{\beta_2^4} \frac{\partial}{\partial \beta_2} \left(\beta_2^4 \frac{\partial}{\partial \beta_2} \right), \quad (4)$$

$$\hat{T}_\gamma = -\frac{1}{\sin 3\gamma} \frac{\partial}{\partial \gamma} \left(\sin 3\gamma \frac{\partial}{\partial \gamma} \right), \quad (5)$$

$$\hat{T}_{\beta_3} = -\frac{1}{\beta_3^3} \frac{\partial}{\partial \beta_3} \left(\beta_3^3 \frac{\partial}{\partial \beta_3} \right). \quad (6)$$

The symbol \hat{T}_r denotes the operator for rotation energy of deformed nuclei expressed in terms of the angular momentum operator and principal moments of inertia

$$\hat{T}_r = \sum_{i=1}^3 \frac{\hat{I}_i^2}{J_i} = \sum_{i=1}^3 \frac{\hat{I}_i^2}{J_i^{(2)} + J_i^{(3)} + J_i^{(4)}}. \quad (7)$$

Here, $J_i^{(\lambda)}$ stands for the principal moments of inertia in the direction of the i -th axis in the body-fixed system due to quadrupole, octupole and hexadecapole deformations depending on $\lambda=2, 3$ and 4, respectively. The symbol \hat{I}_i denotes the projection of the angular momentum operator on the i -th axis of the body-fixed coordinate, β_{20} the quadrupole equilibrium deformation parameter at the ground state (G.S.) and B_λ the mass parameter for multipolarity of λ . The eigenfunctions Ω of operator (3) are defined in a space of six dynamical variables: $0 \leq \beta_2 < \infty$, $-\infty < \beta_3 < \infty$, $\frac{n\pi}{3} \leq \gamma \leq \frac{(n+1)\pi}{3}$, $0 \leq \theta_1 \leq 2\pi$, $0 \leq \theta_2 \leq \pi$ and $0 \leq \theta_3 < 2\pi$ with the volume element $d\tau = \beta_2^4 \beta_3^3 |\sin 3\gamma| d\beta_2 d\beta_3 d\gamma d\theta_1 \sin \theta_2 d\theta_2 d\theta_3$. Here $\beta_\lambda^2 = \sum \beta_{\lambda\mu} \beta_{\lambda\mu}^*$ is the measure of nucleus deformation with multipolarity λ . Below we consider nuclei that are hard with respect to octupole transverse and hexadecapole vibrations.

For nuclei of shapes determined by Eq. (1), $J_i^{(\lambda)}$ is given by[25]

$$J_i^{(2)} = 4B_2 \beta_2^2 \sin^2(\gamma - 2/3\pi i), \quad (i = 1..3) \quad (8)$$

$$J_1^{(3)} = 4B_3 \beta_3^2 \left(\frac{1}{2} \cos^2 \eta + \frac{\sqrt{15}}{4} \sin 2\eta + 1 \right), \quad (9)$$

$$J_2^{(3)} = 4B_3 \beta_3^2 \left(\frac{1}{2} \cos^2 \eta - \frac{\sqrt{15}}{4} \sin 2\eta + 1 \right), \quad (10)$$

$$J_3^{(3)} = 4B_3 \beta_3^2 \sin^2 \eta, \quad (11)$$

$$J_1^{(4)} = 4B_4 \left(\frac{5}{2} b_{40}^2 + 4b_{42}^2 + b_{44}^2 + \frac{3}{2} \sqrt{10} b_{40} b_{42} + \sqrt{7} b_{42} b_{44} \right), \quad (12)$$

$$J_2^{(4)} = 4B_4 \left(\frac{5}{2} b_{40}^2 + 4b_{42}^2 + b_{44}^2 - \frac{3}{2} \sqrt{10} b_{40} b_{42} - \sqrt{7} b_{42} b_{44} \right), \quad (13)$$

$$J_3^{(4)} = 4B_4 (2b_{42}^2 + 8b_{44}^2) \quad (14)$$

with $b_{4\mu}$ that can be presented as [26]:

$$b_{40} = \beta_4 \left(\sqrt{7/12} \cos \delta_4 + \sqrt{5/12} \sin \delta_4 \cos \gamma_4 \right), \quad (15)$$

$$b_{42} = -\beta_4 \sqrt{1/2} \sin \delta_4 \sin \gamma_4, \quad (16)$$

$$b_{44} = \beta_4 \sqrt{1/2} \left(\sqrt{5/12} \cos \delta_4 - \sqrt{7/12} \sin \delta_4 \cos \gamma_4 \right) \quad (17)$$

with parameters η , δ_4 , and γ_4 determining the non-axiality of octupole and hexadecapole deformations.

For convenience, let us rewrite the operator \hat{T}_r as

$$\hat{T}_r = \frac{1}{4B_2\beta_2^2} \sum_{i=1}^3 \frac{\hat{I}_i^2}{j_i^{(2)} + a_{32}j_i^{(3)} + a_{42}j_i^{(4)}}, \quad (18)$$

where $j_i^{(\lambda)} = J_i^{(\lambda)}/4B_\lambda\beta_\lambda^2$ and $a_{\lambda 2} = (B_\lambda/B_2)(\beta_\lambda/\beta_2)^2$. To solve the Schrödinger equation in a perturbative way, we expand Eq. (18) around the minima of the potential energy of the quadrupole and octupole vibrations, *i.e.* β_{20} , γ_0 and β_{30} :

$$\begin{aligned} \hat{T}_r = & \frac{1}{4B_2\beta_2^2} \sum_{i=1}^3 \left\{ \left. \frac{\hat{I}_i^2}{j_i^{(2)} + a_{32}j_i^{(3)} + a_{42}j_i^{(4)}} \right|_{\substack{\beta_2=\beta_{20} \\ \gamma=\gamma_0 \\ \beta_3=\beta_{30}}} \right. \\ & + \frac{\partial}{\partial\gamma} \left[\left. \frac{\hat{I}_i^2}{j_i^{(2)} + a_{32}j_i^{(3)} + a_{42}j_i^{(4)}} \right] \right|_{\substack{\beta_2=\beta_{20} \\ \gamma=\gamma_0 \\ \beta_3=\beta_{30}}} (\gamma - \gamma_0) \\ & + \frac{\partial}{\partial a_{32}} \left[\left. \frac{\hat{I}_i^2}{j_i^{(2)} + a_{32}j_i^{(3)} + a_{42}j_i^{(4)}} \right] \right|_{\substack{\beta_2=\beta_{20} \\ \gamma=\gamma_0 \\ \beta_3=\beta_{30}}} 2a_{320} \left[\frac{\beta_3 \mp \beta_{30}}{\pm\beta_{30}} - \frac{\beta_2 - \beta_{20}}{\beta_{20}} \right] + \dots \\ & - \frac{\partial}{\partial a_{42}} \left[\left. \frac{\hat{I}_i^2}{j_i^{(2)} + a_{32}j_i^{(3)} + a_{42}j_i^{(4)}} \right] \right|_{\substack{\beta_2=\beta_{20} \\ \gamma=\gamma_0 \\ \beta_3=\beta_{30}}} 2a_{420} \left[\frac{\beta_2 - \beta_{20}}{\beta_{20}} \right] + \dots \right\}, \end{aligned} \quad (19)$$

where $a_{\lambda 20} = (B_\lambda/B_2)(\beta_{\lambda 0}/\beta_{20})^2$ and sign \pm in front of β_{30} denotes that we bear in mind that even-even octupole deformed nuclei must have two minima at $\pm\beta_{30}$ of the potential energy that correspond to two symmetric octupole shapes. These nuclei are characterized by the double degeneration of levels, which is washed out as a result of tunneling transition through a barrier separating those nuclear shapes with opposite values of octupole deformation which is expressed as [27, 28]:

$$V(\beta_3) + \frac{3\hbar^2}{8B_3\beta_3^2} = \frac{\hbar^2}{2B_3\mu_\epsilon^4\beta_2} (\epsilon \mp \epsilon_0)^2. \quad (20)$$

Owing to centrifugal forces caused by nuclear rotation, equilibrium octupole deformation changes as $\beta_3 = \beta_2\epsilon$ in direct proportion to β_2 . It is shown in Ref. [29] that, along with the choice of potential in the form of Eq. (20), this enables us to reproduce various patterns of level-energy intervals observed experimentally for positive and negative parity bands of even-even nuclei

Let us solve the Schrödinger equation in the zeroth order approximation for the expansion of the rotational-energy operator \hat{T}_r . Assuming that $\Omega = (\beta_2^{-2}\beta_3^{-3/2})/\sqrt{\sin 3\gamma}u$, we arrive at the following equation for u ,

$$\begin{aligned} -\frac{\hbar^2}{2B_2} \frac{\partial^2 u}{\partial\beta_2^2} - \frac{\hbar^2}{2B_3\beta_2^2} \frac{\partial^2 u}{\partial\epsilon^2} - \frac{\hbar^2}{2B_2\beta_2^2} \frac{\partial^2 u}{\partial\gamma^2} + \frac{\hbar^2}{2B_2\beta_2^2} \frac{1}{4} \sum_{i=1}^3 \frac{\hat{I}_i^2}{j_i^{(2)} + a_{32}j_i^{(3)} + a_{42}j_i^{(4)}} \Big|_{\substack{\beta_2=\beta_{20} \\ \gamma=\gamma_0 \\ \beta_3=\beta_{30}}} u \\ + \left[V(\beta_2) + \frac{\hbar^2}{2B_3\mu_\epsilon^4\beta_2^2} (\epsilon \mp \epsilon_0)^2 + \frac{\beta_{20}^4}{\beta_2^2} V(\gamma) - \frac{\hbar^2}{2B_2\beta_2^2} \frac{9}{4} \frac{1 + \sin^2 3\gamma}{\sin^2 3\gamma} \right] u = Eu. \end{aligned} \quad (21)$$

The quadrupole and octupole variables in (21) are separated now. Therefore, the function u can be factorized into these variables. Thus we can write as

$$u = \psi^\pm(\beta_2, \gamma, \Theta) \varphi_{n_{\beta_3}}^\pm(\epsilon), \quad (22)$$

where

$$\varphi_{n_{\beta_3}}^{\pm}(\epsilon) = \frac{C_{n_{\beta_3}}}{\sqrt{2}} [\chi_{n_{\beta_3}}(\tau_{\epsilon}^+) \pm \chi_{n_{\beta_3}}(\tau_{\epsilon}^-)], \quad (23)$$

$$\tau_{\epsilon}^{\pm} = \epsilon \mp \epsilon_0. \quad (24)$$

Here $\chi_{n_{\beta_3}}(\tau_{\epsilon}^{\pm})$ are oscillator functions that satisfy the equation:

$$\left[-\frac{\hbar^2}{2B_3} \frac{\partial^2}{\partial \epsilon^2} + \frac{\hbar^2}{2B_3 \mu_{\epsilon}^4} (\epsilon \mp \epsilon_0)^2 \right] \chi_{n_{\beta_3}}(\tau_{\epsilon}^{\pm}) = \hbar \omega_{\epsilon} (n + 1/2) \chi_{n_{\beta_3}}(\tau_{\epsilon}^{\pm}), \quad (25)$$

where the frequency is given by $\omega_{\epsilon} = \hbar/(B_3 \mu_{\epsilon}^2)$, $n_{\beta_3} = 0, 1, 2, \dots$ and $C_{n_{\beta_3}}$ is the normalization constant. The superscript \pm on the eigenfunctions of Eq. (23) specifies their symmetry under the transformation $\epsilon_0 \rightarrow -\epsilon_0$. Nuclear states of positive parity are described by symmetric combinations of the oscillator functions, while states of negative parity are represented by antisymmetric combinations.

The function $\psi^{\pm}(\beta_2, \gamma, \Theta)$ satisfies the equation

$$\begin{aligned} & \frac{\hbar^2 \beta_2^2}{2B_2} \frac{\partial^2 \psi^{\pm}}{\partial \beta_2^2} + \frac{\hbar^2}{2B_2} \frac{\partial^2 \psi^{\pm}}{\partial \gamma^2} - \frac{\hbar^2}{2B_2} \frac{1}{4} \sum_{i=1}^3 \frac{\hat{I}_i^2}{j_i^{(2)} + a_{32} j_i^{(3)} + a_{42} j_i^{(4)}} \Bigg|_{\substack{\beta_2 = \beta_{20} \\ \gamma = \gamma_0 \\ \beta_3 = \beta_{30}}} \psi^{\pm} \\ & - \left[\beta_2^2 V(\beta_2) + \beta_{20}^4 V_0(\gamma) - \frac{\hbar^2}{2B_2} \frac{9}{4} \frac{1 + \sin^2 3\gamma}{\sin^2 3\gamma} + E_{n_{\beta_3}}^{\pm} - E \beta_2^2 \right] \psi^{\pm} = 0, \end{aligned} \quad (26)$$

where $E_{n_{\beta_3}}^{\pm} = \hbar \omega_{\epsilon}(n_{\beta_3} + 1/2) \mp \delta_n$ is the energy of octupole longitudinal surface vibrations, and $2\delta_n$ is the energy splitting of a doubly degenerate level due to the tunneling effect.

The only difference between equation (26) and the analogous equation (considered in detail in [5]) for vibrational and rotational state of positive parity in non-axial deformed even-even nuclei is due to the necessity of taking account of the dependence of the eigenfunctions of the rotation operator \hat{T}_r on the parity of the states under consideration. If K is even (as in our case), these functions have the form

$$\Phi_{IM\tau}^{\pm}(\Theta) = \sum_{K \geq 0} |IMK, \pm\rangle A_{IK}^{\tau}, \quad (27)$$

where

$$|IMK, \pm\rangle = ((2I+1)/(16\pi^2(1+\delta_{K0})))^{1/2} [D_{MK}^I(\Theta) \pm (-1)^I D_{M-K}^I(\Theta)], \quad (28)$$

the symbol $D_{M \pm K}^I(\Theta)$ being the rotation function. In even-even nuclei, rotational bands formed by positive parity levels are described by the wave functions $|IMK, +\rangle$ of a rigid rotator, which transform according to the irreducible representation A of the D_2 group. Bands formed by negative-parity levels with even K are described by the functions $|IMK, -\rangle$ that realize the irreducible representation B_1 of the same group [29].

Using the results from [5], we can obtain the eigenvalues of the nuclear Hamiltonian predicting the energies of rotational-vibrational states (with allowance for the quadrupole and octupole deformability

of an even-even nucleus in the zeroth order approximation of \hat{T}_r expansion) in the form

$$\begin{aligned} E_{I\tau n_\gamma n_{\beta_3} n_{\beta_2}}^\pm &= \hbar\omega_0 \left\{ \left(\nu_{I\tau n_\gamma n_{\beta_3} n_{\beta_2}}^\pm + 1/2 \right) \times \left(4 - 3/P_{I\tau n_\gamma n_{\beta_3}}^\pm \right)^{1/2} \right. \\ &\quad + \frac{1}{2} \frac{\mu_{\beta_{20}}^2}{P_{I\tau n_\gamma n_{\beta_3}}^{\pm 2}} \left[\frac{2}{\mu_{\gamma_0}^2} (\nu_{n_\gamma} - \nu_{0_\gamma}) + \varepsilon_{I\tau}^\pm + \epsilon_{n_{\beta_3}}^\pm - \epsilon_{0_{\beta_3}}^+ \right] \\ &\quad \left. + \frac{1}{2} \frac{\mu_{\beta_{20}}^6}{P_{I\tau n_\gamma n_{\beta_3}}^{\pm 6}} \left[\frac{2}{\mu_{\gamma_0}^2} (\nu_{n_\gamma} - \nu_{0_\gamma}) + \varepsilon_{I\tau}^\pm + \epsilon_{n_{\beta_3}}^\pm - \epsilon_{0_{\beta_3}}^+ \right]^2 \right\}, \end{aligned} \quad (29)$$

where $\epsilon_{n_{\beta_3}}^\pm = \frac{2B_2}{\hbar^2} E_{n_{\beta_3}}^\pm$, and $P_{I\tau n_\gamma n_{\beta_3}}^\pm$ is a root of the equation

$$\left(P_{I\tau n_\gamma n_{\beta_3}}^\pm - 1 \right) P_{I\tau n_\gamma n_{\beta_3}}^{\pm 3} = \mu_{\beta_{20}}^4 \left[\frac{2}{\mu_{\gamma_0}^2} (\nu_{n_\gamma} - \nu_{0_\gamma}) + \varepsilon_{I\tau}^\pm + \epsilon_{n_{\beta_3}}^\pm - \epsilon_{0_{\beta_3}}^+ \right], \quad (30)$$

where $\hbar\omega_0$, $\mu_{\beta_{20}}$, μ_{γ_0} and γ_0 are the model parameters to be adjusted to reproduce experimentally-known band structures. The $\hbar\omega_0$ parameter denotes an overall scale factor of the level energies, $\mu_{\beta_{20}}$, μ_{γ_0} and μ_ϵ are related to the elasticity constants of β_2 -, γ - and octupole vibrations, respectively and γ_0 is the equilibrium point of the γ -vibration.

Other quantities in the above equation are to be determined in the following way. The quantity ν_{n_γ} denotes the eigenvalue of the γ -vibration corresponding to the quantum number of n_γ . The quantity $\varepsilon_{I\tau}^\pm$ is the eigenvalues of the asymmetric-rotator Hamiltonian[30, 31] corresponding to the first term of the r.h.s. of Eq. (19),

$$\hat{T}_r^0 \Phi_{IM\tau}^\pm = \varepsilon_{I\tau}^\pm \Phi_{IM\tau}^\pm. \quad (31)$$

The symbol ν_{n_γ} is determined by a system of two equations corresponding to the boundary conditions for γ -vibrations, and n_γ is the number of the solutions:

$$\begin{cases} v_{\nu_{n_\gamma}} \left[-\frac{\sqrt{2}}{\mu_{\gamma_0}} \left(\frac{\pi}{3} n - \gamma_0 \right) \right] = 0 \\ v_{\nu_{n_\gamma}} \left[-\frac{\sqrt{2}}{\mu_{\gamma_0}} \left(\frac{\pi}{3} (n+1) - \gamma_0 \right) \right] = 0 \end{cases}, \quad (32)$$

where $v_{\nu_{n_\gamma}}$ denotes a solution of an oscillator equation

$$\left[\frac{d^2}{dy^2} + \nu_{n_\gamma} + \frac{1}{2} - \frac{y^2}{4} \right] v_{n_\gamma} = 0, \quad (33)$$

which is a linear combination of two independent solutions:

$$v_{n_\gamma}(y) = c_{n_\gamma} \left[D_{\nu_{n_\gamma}}(y) + a_{n_\gamma} V_{\nu_{n_\gamma}}(y) \right], \quad (34)$$

where $D_{\nu_{n_\gamma}}$ denotes the well-known Weber function (see [32]). The symbol $\nu_{I\tau n_\gamma n_{\beta_3} n_{\beta_2}}^\pm$ is determined also by the boundary conditions (32). For the β_2 variable, however, one of the boundaries is at infinity where the function V in the above equation diverges. Therefore, this reduces the possible solution of equation (33) to be

$$v_\nu(y) = c_\nu D_\nu(y), \quad (35)$$

so that $\nu_{I\tau n_\gamma n_{\beta_3} n_{\beta_2}}^\pm$ is determined by the following equation at $\beta_2 = 0$,

$$D_{\nu_{I\tau n_\gamma n_{\beta_3} n_{\beta_2}}^\pm} \left[-\frac{\sqrt{2}P_{I\tau n_\gamma n_{\beta_3}}^\pm}{\mu_{\beta_{20}}} \left(4 - \frac{3}{P_{I\tau n_\gamma n_{\beta_3}}^\pm} \right)^{1/4} \right] = 0. \quad (36)$$

Finally, we can write the full wave function for the soft-rotator Hamiltonian as

$$\begin{aligned} \Omega_{IM\tau n_\gamma n_{\beta_3} n_{\beta_2}}^\pm &= C_{I\tau n_\gamma n_{\beta_3} n_{\beta_2}}^\pm \frac{C_{n_{\beta_3}}}{\sqrt{2}} \frac{\beta_2^{-2} \beta_3^{-3/2}}{\sqrt{\sin 3\gamma}} \sum_{K \geq 0} |IMK, \pm\rangle A_{IK}^\tau \\ &\times D_{\nu_{I\tau n_\gamma n_{\beta_3} n_{\beta_2}}^\pm} \left[\frac{\sqrt{2}}{\beta_{20} \mu_{\beta_{2_I\tau n_\gamma n_{\beta_3}}}^\pm} (\beta_2 - \beta_{2_I\tau n_\gamma n_{\beta_3}}^\pm) \right] \\ &\times v_{n_\gamma} \left[\frac{\sqrt{2}}{\mu_{\gamma_0}} (\gamma - \gamma_0) \right] [\chi_{n_{\beta_3}}(\tau_\epsilon^+) \pm \chi_{n_{\beta_3}}(\tau_\epsilon^-)], \end{aligned} \quad (37)$$

with

$$\beta_{2_I\tau n_\gamma n_{\beta_3}}^\pm = \beta_{20} P_{I\tau n_\gamma n_{\beta_3}}^\pm, \quad (38)$$

which denotes the equilibrium deformation of the stretched rotating nucleus for state $I\tau n_\gamma n_{\beta_3}$ and

$$\frac{1}{\mu_{\beta_{2_I\tau n_\gamma n_{\beta_3}}}^{\pm 4}} = \frac{1}{\mu_{\beta_{20}}^4} + \frac{3 \left[\frac{2}{\mu_{\gamma_0}^2} (\nu_{n_\gamma} - \nu_{0_\gamma}) + \varepsilon_{I\tau}^\pm + \epsilon_{n_{\beta_3}}^\pm - \epsilon_{0_{\beta_3}}^\pm \right]}{P_{I\tau n_\gamma n_{\beta_3}}^{\pm 4}}, \quad (39)$$

with $\mu_{\beta_{2_I\tau n_\gamma n_{\beta_3}}}^\pm$ being the nucleus softness for this state. The correction $\Delta E_{I\tau n_\gamma n_{\beta_3} n_{\beta_2}}^\pm$ to the energy of rotational-vibrational states due to linear terms of expansion (19) can be easily calculated by a perturbative way. If we consider $n_{\beta_3} = 0$ (as states with $n_{\beta_3} \geq 1$ lie above the experimentally resolved ones), this correction is given by

$$\begin{aligned} \Delta E_{I\tau n_\gamma n_{\beta_3} (=0) n_{\beta_2}}^\pm &= \hbar\omega_0 \frac{\mu_{\beta_{20}}^2}{\beta_{20}^2} \left\{ \frac{B_3 \epsilon_0^2 \langle \Phi_{IM\tau}^\pm(\theta) | \sum_{i=1}^3 \frac{\partial}{\partial a_{32}} \left[\frac{\hat{I}_i^2}{j_i^{(2)} + a_{32} j_i^{(3)} + a_{42} j_i^{(4)}} \right] \rangle}{B_2} \Big|_{\substack{\beta_2 = \beta_{20} \\ \gamma = \gamma_0 \\ \beta_3 = \beta_{30}}} |\Phi_{IM\tau}^\pm(\theta)\rangle \right. \\ &\times \left\{ \left[\frac{e^{-\epsilon_0^2/\mu_\epsilon^2}}{1 \pm e^{-\epsilon_0^2/\mu_\epsilon^2}} \left(\frac{\mu_\epsilon}{\epsilon_0 \sqrt{\pi}} \pm \frac{\mu_\epsilon}{\epsilon_0 \sqrt{\pi}} \mp 1 \right) - \frac{\text{erfc}(\epsilon_0/\mu_\epsilon)}{1 \pm e^{-\epsilon_0^2/\mu_\epsilon^2}} \right] J_{I\tau n_\gamma n_{\beta_3} n_{\beta_2}}^\pm (1/y^2) - J_{I\tau n_\gamma n_{\beta_3} n_{\beta_2}}^\pm [(y-1)/y^2] \right\} \\ &- \frac{B_4}{B_2} \beta_2^2 \langle \Phi_{IM\tau}^\pm(\theta) | \sum_{i=1}^3 \frac{\partial}{\partial a_{42}} \left[\frac{\hat{I}_i^2}{j_i^{(2)} + a_{32} j_i^{(3)} + a_{42} j_i^{(4)}} \right] \rangle \Big|_{\substack{\beta_2 = \beta_{20} \\ \gamma = \gamma_0 \\ \beta_3 = \beta_{30}}} |\Phi_{IM\tau}^\pm(\theta)\rangle \times J_{I\tau n_\gamma n_{\beta_3} n_{\beta_2}}^\pm [(y-1)/y^2] \left. \right\} \quad (40) \end{aligned}$$

where

$$\begin{aligned} J_{I'\tau' n'_\gamma n'_{\beta_3} n'_{\beta_2}}^\pm [f(y)] &= \int_0^\infty f(y) D_{\nu_{I'\tau' n'_\gamma n'_{\beta_3} n'_{\beta_2}}^\pm} \left[\frac{\sqrt{2}}{\mu_{\beta_{2_I'\tau' n'_\gamma n'_{\beta_3}}}^\pm} (y - P_{I'\tau' n'_\gamma n'_{\beta_3}}^\pm) \right] \\ &\times D_{\nu_{I'\tau' n'_\gamma n'_{\beta_3} n'_{\beta_2}}^\pm} \left[\frac{\sqrt{2}}{\mu_{\beta_{2_I'\tau' n'_\gamma n'_{\beta_3}}}^\pm} (y - P_{I'\tau' n'_\gamma n'_{\beta_3}}^\pm) \right] dy \\ &\times \left\{ \int_0^\infty D_{\nu_{I\tau n_\gamma n_{\beta_3} n_{\beta_2}}^\pm}^2 \left[\frac{\sqrt{2}}{\mu_{\beta_{2_I\tau n_\gamma n_{\beta_3}}}^\pm} (y - P_{I\tau n_\gamma n_{\beta_3}}^\pm) \right] dy \right\}^{-1/2} \\ &\times \left\{ \int_0^\infty D_{\nu_{I'\tau' n'_\gamma n'_{\beta_3} n'_{\beta_2}}^\pm}^2 \left[\frac{\sqrt{2}}{\mu_{\beta_{2_I'\tau' n'_\gamma n'_{\beta_3}}}^\pm} (y' - P_{I'\tau' n'_\gamma n'_{\beta_3}}^\pm) \right] dy' \right\}^{-1/2}. \quad (41) \end{aligned}$$

3 Optical Potential and Channel Coupling

Multipoles of the deformed nuclear potential arising from the deformed nuclear shape are determined by expanding it in a Taylor series, considering ($\sum_{\lambda\mu} \beta_{\lambda\mu} Y_{\lambda\mu}(\theta', \varphi')$) in Eq.(1) to be small:

$$V(r, R(\theta', \varphi')) = V(r, R_0) + \sum_{t=1}^{\max} \frac{\partial^t V(r, R)}{\partial R^t} \Big|_{R(\theta', \varphi')=R_0} \frac{R_0^t}{t!} (\sum_{\lambda\mu} \beta_{\lambda\mu} Y_{\lambda\mu}(\theta', \varphi'))^t, \quad (42)$$

in which body fixed coordinates (θ', φ') can be easily converted to the Laboratory ones by using the rotation function D :

$$Y_{\lambda\nu}(\theta', \varphi') = \sum_{\nu} D_{\mu\nu}^{\lambda*} Y_{\lambda\mu}(\theta, \varphi), \quad (43)$$

so that coupling potential can be written in a form:

$$V_{coupl}(r, \theta, \varphi, \gamma, \beta_{\lambda}) = \sum_{t-m-n \geq 0} v^t(r) \beta_{\lambda}^{t-m-n} \beta_{\lambda'}^m \cdot \beta_{\lambda''}^n \cdot \sum_{\nu\mu} Q_{\nu\mu}^{(tm \cdots n\lambda'\lambda''\cdots\lambda''')} * Y_{\nu\mu}(\theta, \varphi). \quad (44)$$

Here, $v^t(r) = \frac{\partial^t V(r, R)}{\partial R^t} \Big|_{R(\theta', \varphi')=R_0}$ with the deformed optical nuclear potential taken to be a standard spherical form, but now with the account of deformed instant nuclear shapes:

$$\begin{aligned} V(r, R(\theta', \varphi')) &= -V_R f_R(r, R(\theta', \varphi')) \\ &\quad + i \left\{ 4W_D a_D \frac{d}{dr} f_D(r, R(\theta', \varphi')) - W_V [\alpha f_V(r, R(\theta', \varphi')) + (1-\alpha) f_W(r, R(\theta', \varphi'))] \right\} \\ &\quad + \left(\frac{\hbar}{\mu_{\pi} c} \right)^2 (V_{SO} + iW_{SO}) \frac{1}{r} \frac{d}{dr} f_{SO}(r, R(\theta', \varphi')) \boldsymbol{\sigma} \cdot \boldsymbol{\ell} + V_{Coul}(r, R(\theta', \varphi')), \end{aligned} \quad (45)$$

where the form factors are given as

$$f_i = \frac{1}{1 + \exp \left[\frac{r - R_i(\theta', \varphi')}{a_i} \right]}, \quad R_i(\theta', \varphi') = R_i^0 r_{\beta}(\theta', \varphi') = r_i A^{1/3} r_{\beta}(\theta', \varphi'), \quad (46)$$

$$f_W = \exp \left\{ - \left[\frac{r - R_W(\theta', \varphi')}{a_W} \right]^2 \right\}, \quad R_W(\theta', \varphi') = R_W^0 r_{\beta}(\theta', \varphi') = r_W A^{1/3} r_{\beta}(\theta', \varphi'), \quad (47)$$

with $r_{\beta}(\theta', \varphi')$ as defined by Eq. (1). The subscripts $i = R, V, D$ and so denote the real volume, imaginary volume, imaginary surface and real spin-orbit potentials.

For the reasons mentioned above, we need the potential expansion expressed with an evident dependence on deformation. For Coulomb potential $V_{Coul}(r, R(\theta', \varphi'))$, such expansion with an evident dependence on the deformations becomes possible as we follow the suggestion of Satchler *et al.* [33], using a multipole expansion of the Coulomb potential V_{Coul} for a charged ellipsoid with a uniform charge density within the Coulomb radius R_C and zero outside. Up to the second order of $\sum \beta_{\lambda\mu} Y_{\lambda\mu}$, it reads:

$$\begin{aligned} V_{Coul}(r, R(\theta', \varphi')) &= \frac{ZZ'e^2}{2R_c} \left[3 - \frac{r^2}{R_C^2} \right] \theta(R_C - r) + \frac{ZZ'e^2}{r} \theta(r - R_C) \\ &\quad + \sum_{\lambda\mu} \frac{3ZZ'e^2}{2\lambda+1} \left[r^{\lambda} R_C^{-(\lambda+1)} \theta(R_C - r) + R_C^{\lambda} r^{-(\lambda+1)} \theta(r - R_C) \right] (\beta_{\lambda\mu} Y_{\lambda\mu}) \\ &\quad + \sum_{\lambda\mu} \frac{3ZZ'e^2}{2\lambda+1} \left[(1-\lambda)r^{\lambda} R_C^{-(\lambda+1)} \theta(R_C - r) + (\lambda+2)R_C^{\lambda} r^{-(\lambda+1)} \theta(r - R_C) \right] \\ &\quad \times \sum_{\lambda'\lambda''} \frac{\hat{\lambda}'\hat{\lambda}''}{(4\pi)^{1/2}\hat{\lambda}} (\lambda'\lambda''00 | \lambda0) \sum_{\mu} (\beta_{\lambda'} \otimes \beta_{\lambda''})_{\lambda\mu} Y_{\lambda\mu}, \end{aligned} \quad (48)$$

where Z' , Z are charges of incident particle and nucleus, $\hat{\lambda} = (2\lambda + 1)^{1/2}$, while the symbol \otimes means the vector addition, *i.e.*

$$(\beta_{\lambda'} \otimes \beta_{\lambda''})_{\lambda\mu} = \sum_{\mu'\mu''} (\lambda' \lambda'' \mu' \mu'' | \lambda \mu) \beta_{\lambda' \mu'} \beta_{\lambda'' \mu''} \quad (49)$$

and $\theta(r) = 1$, if $r > 0$ and $\theta(r) = 0$, if $r < 0$. This form of expansion gives contributions to $v^t(r)$ for $t = 1$ and 2 in addition to the couplings coming from the nuclear potential.

Coulomb potential deformation results in a dependence on r of the coupling potential multipoles as $r^{-\lambda-1}$ so that induced error for matching at radius R must be of order of $R^{-\lambda}$, and hence the matching radius must be significantly increased or Coulomb correction procedure must be applied[34]. As potential multipole λ determines angular momentum transfer, it is important for excitation of the $J^\pi = 2^+$ level (for ground state with $J^\pi = 0^+$) but much less for levels with higher spins.

The Coulomb potential used in the present work included some modifications to formula (48). Instead of the spherical term, which is $\frac{ZZ'e^2}{2R_c} \left[3 - \frac{r^2}{R_c^2} \right] \theta(R_C - r) + \frac{ZZ'e^2}{r} \theta(r - R_C)$ for uniform charge density within the Coulomb radius R_C , one can use a spherical term of the Coulomb potential calculated by taking account of the diffuseness of the charge distribution with a charge density form factor equal to $f_C = [1 + \exp(r - R_C)/a_C]^{-1}$. Our model involves quadrupole, octupole and hexadecapole instant nuclear deformations, *i.e.* the Coulomb expansion of the potential can in principle give additional coupling strength between collective states with an angular momentum transfer of 0 to 8. However, in the Coulomb expansion used in this model, we truncate the dynamic square terms which lead to zero angular momentum transfer. This is equivalent to introducing a dynamic negative deformation β_{00} in the radial expansion given in Eq. (1):

$$\beta_{00} = - \sum_{\lambda} (-1)^{\lambda} \frac{\hat{\lambda}}{(4\pi)^{1/2}} (\beta_{\lambda} \otimes \beta_{\lambda})_{00}, \quad (50)$$

which is required as a condition to conserve the nuclear volume, *i.e.* the nuclear charge [30]. This correction is necessary to have the correct asymptotic behavior for the spherical term of the Coulomb potential which must be equal to $ZZ'e^2/r$. The additional coupling due to the Coulomb potential was obtained in the same manner as for the nuclear one [35] with deformed radii as described above.

As we consider $\beta_{\lambda\mu}$ to be dynamic in the soft-rotator nuclear model, nuclear shape described in Eq. (1) will violate nuclear mass conservation. To conserve nuclear mass for uniform nuclear density case, one must add a dynamic negative deformation β_{00} to the radial expansion given in Eq. (1). This is required as the condition to conserve the nuclear volume[30] which is equivalent to mass and nuclear charge conservation for uniform nuclear and charge density case adopted in [30]. So the radius describing shape of nuclei with constant volume becomes

$$R(\theta', \varphi') = R_0 \left\{ 1 + \beta_{00} Y_{00} + \sum_{\lambda\mu} \beta_{\lambda\mu} Y_{\lambda\mu}(\theta', \varphi') \right\} \quad (51)$$

Additional β_{00} deformation leads to additional zero nuclear potential multipole that couples levels with equal spin and parity I^π .

In case of nuclear density with diffuseness, one must use the following zero multipole deformation β'_{00} to conserve nuclear mass[36].

$$\beta'_{00} = -\left(\frac{R_0}{2a}\right)\beta_{00} \frac{\int \frac{\partial^2 f(r, R, a)}{\partial x^2} \Big|_{x_0} r^2 dr}{\int \frac{\partial f(r, R, a)}{\partial x} \Big|_{x_0} r^2 dr} \quad (52)$$

Here $f(r, R, a) = f(x)$ denotes the nuclear density form factor, $x = \frac{r-R}{a}$, and $x_0 = \frac{r-R_0}{a}$. We can write the above equation as follows since integrals in it are just constants,

$$\beta'_{00} = C_\beta \beta_{00}. \quad (53)$$

In our code we use nuclear real potential form factor $f_R(r, R, a)$ instead of nuclear density form factor. As C_β appears to be close to unity, we take substitution of nuclear density form factor by real potential one as an acceptable approximation. Such an approximation leads to simultaneous conservation of nuclear volume and real potential volume integral in nuclear shape oscillations, so there is an additional reason to use it. Thus, considering nuclear mass and charge conservations, the multipoles of the deformed nuclear potential arising from deformed nuclear shape are determined by expanding nuclear potential in a Taylor series, now considering $(\beta'_{00}Y_{00} + \sum \beta_{\lambda\mu}Y_{\lambda\mu}(\theta', \varphi'))$ in Eq.(1) to be small:

$$V(r, R(\theta', \varphi')) = V(r, R_0) + \sum_{t=1}^{\max} \frac{\partial^t V(r, R)}{\partial R^t} \Big|_{R(\theta', \varphi')=R_0} \frac{R_0^t}{t!} (\beta'_{00}Y_{00} + \sum_{\lambda\mu} \beta_{\lambda\mu}Y_{\lambda\mu}(\theta', \varphi'))^t, \quad (54)$$

One can see that account of nuclear volume conservation leads to additional zero multipole term starting with the first derivative of the nuclear potential, which will additionally couple states with equal spins and parity I^π and themselves. This term is proportional to $(\beta_{\lambda\mu})^2$ and must be taken into account, as account of terms up to $(\beta_{\lambda\mu})^4$ is necessary to describe experimental data consistently[37].

Starting with full wave function which is defined by wave functions of nucleon + nuclei system[2]

$$\begin{aligned} \Psi^\pm &= r^{-1} \sum_{Jnl_n j_n} R_{Jnl_n j_n}(r) |(l_n s)j_n; I_n \tau n_{\beta_2} n_{\gamma} n_{\beta_3}; JM\rangle \\ &\equiv r^{-1} \sum_{Jnl_n j_n} R_{Jnl_n j_n}(r) \sum_{m_{j_n}, M_{I_n}} (j_n I_n m_{j_n} M_n | JM) \mathcal{Y}_{l_n j_n m_{j_n}} \Omega_{I_n M_n \tau n_{\gamma} n_{\beta_3} n_{\beta_2}}^\pm \end{aligned} \quad (55)$$

and inserting it in the Schrödinger equation we obtain the equation for radial wave functions:

$$\left(\frac{d^2}{dr^2} - \frac{l(l+1)}{r^2} + k_n^2 - \frac{2\mu V_{centr}(r)}{\hbar^2} \right) R_{nlj}(r) = \frac{2\mu}{\hbar^2} \sum_{n'l'j'} V_{nlj, n'l'j'}(r) R_{n'l'j'}(r) \quad (56)$$

with a coupling potential $V_{nlj, n'l'j'}(r)$ for coupling built on soft-rotator nuclear Hamiltonian wave functions:

$$\begin{aligned}
V(r)_{nlj,n'l'j'} &= \langle (ls)j; I\tau n_{\beta_2} n_{\gamma} n_{\beta_3}; JM | \sum_{t-m-n \geq 0} v^t(r) \beta_{\lambda}^{t-m-n} \beta_{\lambda'}^m \cdot \beta_{\lambda''}^n \\
&\quad \times \sum_{\nu\mu} Q_{\nu\mu}^{(tm \cdots n\lambda'\lambda''\cdots\lambda''')} * Y_{\nu\mu}(\theta, \varphi) | (l's)j'; I'\tau' n'_{\beta_2} n'_{\gamma} n'_{\beta_3}; JM \rangle \\
&= (-1)^{J-I'-s+j+j'+(l'-l)/2} \frac{1}{\sqrt{4\pi}} ll' \hat{j} \hat{j}' \\
&\quad \times \sum_t v^t(r) \sum_{t-m-n \geq 0} \langle f | \beta_{\lambda}^{t-m-n} \beta_{\lambda'}^m \cdot \beta_{\lambda''}^n | i \rangle \\
&\quad \times \sum_{\nu} (ll'00|\nu0) W(jIj'I; \nu J) W(ljl'j'; s\nu) \\
&\quad \times \langle I\tau n_{\gamma} || Q_{\nu\mu}^{(tm \cdots n\lambda'\lambda''\cdots\lambda''')} * || I'\tau' n'_{\gamma} \rangle. \tag{57}
\end{aligned}$$

Here $|i\rangle$ and $|f\rangle$ are parts of initial and final states nuclear wave functions depending on different modes of variables β_{λ} , while $|I\tau n_{\gamma}\rangle$ is the rest part of the full nuclear wave function, holding dependence of nuclear level rotational quantum numbers I , τ and non-axiality γ -oscillations.

In rigid rotator or harmonic oscillator case, system of coupled equations has the same form as Eq. (56), but coupling potential $V(r)_{nlj,n'l'j'}$ differs and can be found in [2].

3.1 The Main Essence of the CC Built on Soft-rotator Nuclear Model

As our wave functions are factorized to different oscillation modes, the matrix element in the fourth line of Eq. (57) can be also factorized:

$$\langle f | \beta_{\lambda}^{t-m-n} \beta_{\lambda'}^m \cdot \beta_{\lambda''}^n | i \rangle = \langle f_{\lambda} | \beta_{\lambda}^{t-m-n} | i_{\lambda} \rangle \langle f_{\lambda'} | \beta_{\lambda'}^m | i_{\lambda'} \rangle \cdots \langle f_{\lambda''} | \beta_{\lambda''}^n | i_{\lambda''} \rangle. \tag{58}$$

Here $|i_{\lambda}\rangle$ and $|f_{\lambda}\rangle$ stand for factorized parts of initial and final states nuclear wave functions, describing λ -multipole oscillations.

In Rigid-rotor case:

$$\langle f_{\lambda} | \beta_{\lambda}^t | i_{\lambda} \rangle = \langle G.S. | \beta_{\lambda}^t | G.S. \rangle = (\langle f_{\lambda} | \beta_{\lambda} | i_{\lambda} \rangle)^t = \beta_{\lambda}^t = \beta_{\lambda G.S.}^t.$$

In case of soft-rotator wave functions:

$$\langle f_{\lambda} | \beta_{\lambda}^t | i_{\lambda} \rangle \neq \langle f'_{\lambda} | \beta_{\lambda}^t | i'_{\lambda} \rangle \neq \langle G.S. | \beta_{\lambda}^t | G.S. \rangle \neq (\langle f_{\lambda} | \beta_{\lambda}^t | i_{\lambda} \rangle)^t \neq \beta_{\lambda G.S.}^t.$$

Usually for initial and final states from one band :

$$\langle f_{\lambda} | \beta_{\lambda}^t | i_{\lambda} \rangle / \langle G.S. | \beta_{\lambda}^t | G.S. \rangle > 1,$$

but it can be less than unity for interband case.

For quadrupole oscillations $\langle f_{\lambda=2} | \beta_2^t | i_{\lambda=2} \rangle = \beta_{20}^t J_{I\tau n_{\gamma} n_{\beta_3} n_{\beta_2}}^{\pm} [y^t]$, with $J_{I'\tau' n'_{\gamma} n'_{\beta_3} n'_{\beta_2}}^{\pm} [f(y)]$ determined by Eq.(41). So it is easy to understand that enhancement of the coupling strength compared with the rigid-rotator model [2] arises because the dynamic variables in the expansion of deformed nuclear optical potential are averaged over the wave functions of the appropriate collective nuclear shape

motions given by the solutions of the soft-rotator model Hamiltonian. Such enhancement is equal to $\langle i_\lambda | \beta_\lambda^t | f_\lambda \rangle / \beta_{\lambda G.S.}^t$, and this ratio is usually greater than unity, as a soft-rotating nucleus is rotating with increasing velocity for collective states with higher spins I and thus is increasingly stretched due to the centrifugal force, so that equilibrium deformations $\beta_{\lambda I \tau}$ for states with higher spins I are greater than equilibrium G.S. deformation $\beta_{\lambda G.S.}$. As the deformation potential energy $V(\beta_\lambda)$ of the soft-rotator model in terms of nuclear softness μ_λ is considered to be $\sim \frac{1}{\mu_\lambda^4} (\beta_\lambda - \beta_{\lambda G.S.})^2$, the coupling enhancement is larger for nuclei with larger softness μ_λ and vanishes for nuclei with small μ_λ . Of course this also concerns the functions $\cos \gamma$ and $\sin \gamma$ appearing in matrix element $\langle I \tau n_\gamma || Q_{\nu \mu}^{(tm \cdots n \lambda' \lambda'' \cdots \lambda''')} * || I' \tau' n'_\gamma \rangle$ of Eq.(57), which are in turn averaged over non-axiality γ -vibrations eigenfunctions. Such enhancements are different for different combinations of initial and final states, and also depend on the powers of potential expansion t . In this way, the soft-rotator model predicts the redistribution of coupling strength, *i.e.* the particle current between the channels, which in turn changes the estimates of direct level excitation cross sections compared to rigid-rotor or harmonic-vibrational models.

4 Solutions of Scattering Problems

Let us rewrite system of equations (56) in a more convenient form:

$$\frac{d^2 f_j(r)}{dr^2} = \sum_k V_{jk}(r) f_k(r). \quad (59)$$

To solve the scattering problem, we need to find the normalized solutions $f n_j^i(r)$ which, in asymptotic region where nuclear forces become absent, must become an incoming plane wave with a unit current plus an outgoing wave in initial (i) channel and pure outgoing waves in all other final (j) channels

$$f n_j^i(r) = \delta_{ij} F_{l_j}(\eta, r) + \sqrt{\frac{k_i}{k_j}} C_{ij} (F_{l_j}(\eta, r) + iG_{l_j}(\eta, r)), \quad (60)$$

where $F_l(\eta, r)$ and $G_l(\eta, r)$ are Coulomb functions, that are already normalized to a unit current, and C_{ij} -matrix describes scattering. The symbol η denotes the Sommerfeld parameter

$$\eta = \frac{Z' Z e^2 \mu}{\hbar^2 k}. \quad (61)$$

where symbols Z , Z' , μ and k denote projectile charge number, target charge number, reduced mass and wave number, respectively.

4.1 Accurate Solution of Coupled-channels System for Radial Functions and Matching

Solutions, determining C_{ij} -matrix, can be found if we have a system of independent solutions $f_j^m(r)$ of Eq. (59), each vanishing at the origin, number of which is equal to the number of coupled equations N : $m = 1, N$. In the vicinity of the origin, the central potential may be considered to be constant and

is equal to its value at the origin $V_{centr}(0)$, while coupling terms $V_{nlj,n'l'j'}(r)$ and Coulomb potential vanish. Therefore, Eq. (56) reduces to:

$$\left(\frac{d^2}{dr^2} - \frac{l(l+1)}{r^2} + k_n^2 - \frac{2\mu V_{centr}(0)}{\hbar^2} \right) R_{nlj}(r) = 0 \quad (62)$$

It is easy to see that solutions of the above equation will be independent if they depend on r at the origin as:

$$f_j^m(r) = \delta_{mj} r^{(l_j+1)}, \quad (63)$$

This dependence can be used as boundary conditions for integrating Eq. (59) to get its necessary independent solutions.

OPTMAN code uses Störmer[38] algorithm for step by step integration from the origin to the matching radius:

$$\begin{aligned} f_j^m(r+h) &= 2f_j^m(r) - f_j^m(r-h) + h^2 \left[229 \sum_k V_{jk}(r) f_k^m(r) \right. \\ &\quad - 176 \sum_k V_{jk}(r-h) f_k^m(r-h) + 194 \sum_k V_{jk}(r-2h) f_k^m(r-2h) \\ &\quad \left. - 96 \sum_k V_{jk}(r-3h) f_k^m(r-3h) + 19 \sum_k V_{jk}(r-4h) f_k^m(r-4h) \right]. \end{aligned} \quad (64)$$

Note that above we are integrating system of homogeneously coupled equations and using that $f_j''(r) = \sum_k V_{jk}(r) f_k(r)$.

In case of N coupled equations, number of arithmetic operations for one step integration of one system line (e.g., each j) is proportional to $N \times (M + L)$, where M is the number of operations necessary to calculate coupling potential V_{jk} , and L (~ 10) denotes number of arithmetic operations necessary to make summations and multiplications for each k for one step integrations using Eq. (64) with all components preliminary prepared. Then number of arithmetic operations for one step integration for all system lines is proportional to $N \times N \times (M + L)$. If K is the number of integration steps, number of arithmetic operations necessary to get one independent solution of coupled equation system is proportional to $N^2 \times (M + L) \times K$. Finally we need $N^3 \times (M + L) \times K$ to get N independent solutions necessary for matching. So number of arithmetic operations in suggested algorithm and thus computational time grows as the number of coupled equations in the power of three. In case for three levels with spins $0^+, 2^+, 4^+$, $N = \sum_I (2I+1)$ is equal to 15. If we include 6^+ level in coupling scheme, N becomes 28, almost twice so that N^3 and thus necessary computational time becomes ~ 8 times longer. Soft-rotator model describes at least collective levels from 3-4 low lying bands, including negative parity one. It is shown that coupling of the first levels from these bands cannot be ignored in reliable optical calculations. For such calculations N may be 50 and more. One can evaluate typical number of arithmetic operations, thus computational time, considering that typical number of integration steps from origin to the matching radius is about 100-200 and numbers of operations necessary to calculate coupling potential V_{jk} , Eq. (57) due to its complicity are about 60 for neutrons and 180 for protons, yet

most potential elements V_{jk} are to be calculated in advance and can be used repeatedly. Such algorithm requests about $\sim 10^9$ arithmetic operations to solve typical coupled-channels system of equations. Note that running scattering problem we need solutions for a number of coupled-channels systems for each spin and parity J^π , giving significant contribution to calculated cross-sections (about 100 for 200 MeV incident energies). It can be concluded that suggested algorithm is rather time consuming. Looking at Eq. (64) one can see that for one step integration for any of integrated solutions $f_j^m(r)$ potential $V_{jk}(r)$ is the same, so once it is organized we can perform one step integration for all solutions $f_j^m(r)$ simultaneously. In this case number of arithmetic operations necessary for integration for all independent solutions reduces to $N^2 \times (M + L) \times K + N^2 \times (N - 1) \times L \times K = N^2 \times K \times (M + L + (N - 1) \times L)$. One can see that for large N suggested algorithm of simultaneous $f_j^m(r)$ functions integration is about $M/L \approx 6 - 20$ times quicker. This quicker algorithm is now realized in subroutine SOSIT.

After independent solutions $f_j^m(r)$ are found, one can easily get C_{ij} -matrix, matching the solutions to have the desired asymptotic wave functions behavior. Matching approach used in our code is suggested by[3].

We consider that numerical solution $f_j^m(r)$ is a linear combination of the normalized solutions $fn_j^i(r)$, each having an incoming plane wave with a unit current only for channel i , so that for asymptotic radius R region we can write:

$$f_j^m(R \pm h) = \sum_i a_{mi} \left\{ F_j(R \pm h) \delta_{ij} + \sqrt{\frac{k_i}{k_j}} C_{ij} [F_j(R \pm h) + iG_j(R \pm h)] \right\}. \quad (65)$$

Then, we can determine matrices

$$\begin{aligned} A_{mj} &\equiv \frac{f_j^m(R + h)G_j(R - h) - f_j^m(R - h)G_j(R + h)}{F_j(R + h)G_j(R - h) - F_j(R - h)G_j(R + h)} = \sum_i a_{mi} \left\{ \delta_{ij} + i\sqrt{\frac{k_i}{k_j}} C_{ij} \right\} \\ B_{mj} &\equiv \frac{f_j^m(R + h)F_j(R - h) - f_j^m(R - h)G_j(R - h)}{F_j(R + h)G_j(R - h) - F_j(R - h)G_j(R + h)} = - \sum_i a_{mi} \sqrt{\frac{k_i}{k_j}} C_{ij}, \end{aligned} \quad (66)$$

giving matching equations:

$$B_{mj} = - \sum_i (A_{mi} + iB_{mi}) \sqrt{\frac{k_i}{k_j}} C_{ij}. \quad (67)$$

One can see that it is necessary to invert $(A_{mi} + iB_{mi})$ matrix with complex elements determined by Eq. (66) to get C_{ij} elements.

The normalized solutions $fn_j^i(r)$ can be easily determined as:

$$fn_j^i(r) = - \sum_{k,m} \sqrt{\frac{k_i}{k_k}} C_{ik} B_{km}^{-1} f_j^m(r). \quad (68)$$

4.2 Iterative Approach to Solve a System of Coupled Equations

The algorithm described above for accurate solution of coupled-channels system is quick, but is still rather time consuming, as we need to get N independent solutions first to get one solution with a necessary asymptotic behavior. "Sequential iteration method for coupled equations" - ECIS, developed

by J. Raynal[39] is also realized in OPTMAN code. It is quicker, but faces iteration convergence problem for some specific scattering cases. We modernized this algorithm improving its convergence.

Let us rewrite Eq. (59), presenting coupling in line j of system of coupled equations as inhomogeneous term of homogeneous uncoupled equation:

$$\frac{d^2 f_j(r)}{dr^2} = V_{jj}(r) f_j(r) + \sum_{k \neq j} V_{jk}(r) f_k(r). \quad (69)$$

If we have some n -order iteration solution $f_j^n(r)$ of Eq. (69) we can find next iteration $f_j^{n+1}(r)$ solution by integrating step-by-step by radius the following inhomogeneous equations:

$$\frac{d^2 f_j^{n+1}(r)}{dr^2} = V_{jj}(r) f_j^{n+1}(r) + W_j(r) \quad (70)$$

with $W_j(r) = \sum_{k \neq j} V_{jk}(r) f_k^n(r)$. To solve the scattering problem, derived solution $f_j^{n+1}(r)$ must have the right asymptotic physical behavior at the infinity - a plane incoming wave with a unit current for initial channels, otherwise no incoming plane wave plus a spherical outgoing wave.

First we match non-normalized derived solution $f_j^{n+1}(r)$, that gives:

$$f_j^{n+1}(r) = A F_{l_j}(r) + B (F_{l_j}(r) + G_{l_j}(r)). \quad (71)$$

To get the normalized $f_j^{n+1}(r)$ with the right asymptotic form Eq. (60), let us recollect that we can add any homogeneous solution to inhomogeneous ones, and it will be still the solution of inhomogeneous one. If normalized homogeneous solution $f_j^H(r)$ has the following asymptotic form:

$$f_j^H(r) = F_{l_j}(r) + C (F_{l_j}(r) + G_{l_j}(r)), \quad (72)$$

normalized function should be

$$f_j^{n+1} = f_j^{n+1}(r) - (A - \delta_{ij}) f_j^H(r), \quad (73)$$

where i means wave functions with scattering through ground state. It is easy to see that normalizing Eq. (73) determines C_{ij} -matrix to be: $C_{ij} = B - C(A - \delta_{ij})$.

Modified Numerov method[40] is applied to integrate inhomogeneous equation (70). For inhomogeneous equation:

$$f''(r) = V(r)f(r) + W(r), \quad (74)$$

the integration algorithm is:

$$\xi(r+h) = 2\xi(r) - \xi(r-h) + u(r) + [W(r+h) + 10W(r) + W(r-h)]/12$$

with $u(r) = (h^2 V(r) + h^4 V^2(r)/12)\xi(r)$ and $f(r) = \xi(r) + u(r)/12$.

Original ECIS code [39] uses homogeneous solutions of Eq. (70) as zeroth order iteration approximation $f_j^0(r)\delta_{ij}$. To improve iterations convergence imaginary part of the diagonal potential $V_{jj}(r)$ for such

zeroth order iteration approximation solutions must be enlarged by a factor $(1 + \beta_2)$. This can be easily understood if one recollects that predictions of inelastic scattering by spherical optical model need such enlargement of the central imaginary potential to give results similar to coupled-channels predictions. Number of arithmetic operations necessary for such coupled-channels solution is $N^2 \times M \times K \times I$; here N , M and K are defined before, while I is the number of iterations necessary for convergence, it is usually not high (~ 10) and decreases as the incident energy increases or coupling decreases (conditions for the DWBA approach to become reliable, which corresponds to the first iteration). Number of arithmetic operations necessary to solve a system of coupled equations for fixed spin J^π using this algorithm is almost the same as the accurate solution algorithm described before with simultaneous independent solutions integration, if number of iterations $L \sim 10$. But for the systems with high spin J^π one iteration is usually enough for solution, as absolute contribution of such states is small, so that high relative solution errors for states with such J^π are acceptable, that makes iteration algorithm much more effective. Nevertheless there are many special cases in which iteration procedure using homogeneous solutions of Eq. (70) as zeroth order iteration approximation do not converge. In this case we suggest to use wave functions from accurate coupled-channels solutions Eq. (68) for coupled system with truncated rank to be used as zeroth order approximations. For such functions, found with coupling of only several levels that are mostly strong coupled, number of coupled equations is small, allowing a quick solution. These solutions describe ground and first excited states wave functions much more accurately than simple homogeneous solutions, as now ground state wave functions used as zeroth order approximation already account existence of coupling with the most strongly coupled excited levels and thus can be used as starting approximations, allowing converging the problems that do not converge in simple approach.

4.3 Asymptotic Wave Functions Used to be Matched with Numerical Solutions

Numerical solutions should be matched with Coulomb wave functions $F_l(kr)$ and $G_l(kr)$, that are solutions of Eq. (56) in the outer region where nuclear potential vanishes and system becomes uncoupled. Coulomb functions are the solutions of the following equation:

$$u_l''(\rho) - [l(l+1)/\rho^2 + 2\eta/\rho \mp 1] u_l(\rho) = 0, \quad (75)$$

sign \mp is for the channels with positive and negative (opened and closed) channels, $\rho = kr$ and $\eta = \frac{Z'Ze^2\mu}{\hbar^2 k}$. For positive energies $F_l(kr)$ and $G_l(kr)$ are two Coulomb functions[32], regular and irregular at $\rho = 0$, respectively. In case of $\eta = 0$ they are reduced to spherical Bessel and Neuman functions multiplied by ρ :

$$\begin{aligned} F_l(\rho) &= (\frac{\pi\rho}{2})^{1/2} J_{l+1/2}(\rho) = \rho j_l(\rho) \\ G_l(\rho) &= (-1)^l (\frac{\pi\rho}{2})^{1/2} J_{-(l+1/2)}(\rho) = (-1)^l \rho j_{-l}(\rho) = -\rho \eta_l(\rho), \end{aligned} \quad (76)$$

that can be easily calculated by recurrence[41].

For closed channels and $\eta > 0$ the only solution allowed from physical point of view is the Whittaker function, which is exponentially decreasing:

$$u_l(\rho) = W(-\eta, l + 1/2, 2\rho). \quad (77)$$

However, we need also linearly-independent exponentially increasing solution for matching procedures of accurate solutions of Eq. (65) and iteration ones of Eq. (71). Both these functions are not easily calculated with high accuracy for the set of appearing l , ρ and η values. On the other hand, values of decreasing and increasing functions may differ by too many orders of magnitude, that can make numerical matching inaccurate. To get the Coulomb functions for closed channels with necessary accuracy it was decided to consider them to be unity at $R - h$ matching point and get their values at $R + h$ point by several step numerical integration of Eqs. (75). Such integration gives correct relative function values with very high accuracy, as integration is done on a very short variable interval of $2h$. The accuracy of the calculated functions is checked using Wronskian relationship:

$$F_l(\rho)G'_l(\rho) - G_l(\rho)F'_l(\rho) = \text{const}, \quad (78)$$

so that Wronskian for calculated $F_l(\rho)$ and $G_l(\rho)$ functions is checked to be the same at $k(R - h)$ and $k(R + h)$ matching points

It is quite clear that such a definition gives functions with arbitrary normalization, but for closed channels we are not interested in absolute value of appropriate C -matrix element of Eq. (60) as there is no current of scattered particles through these channels.

5 C-matrix and Coupled-channels Optical Model Predictions

Using the C -matrix, all optical model cross-sections can be calculated.

Differential nucleon scattering cross-section with excitation of n -th level averaged over projections of incoming particle spin s and nuclear target spin I_1 (scattering of unpolarized nucleon with unpolarized target) can be calculated as:

$$\begin{aligned} \frac{d\sigma_n}{d\Omega} = & \frac{(-1)^{I_1 - I_n}}{2k_1^2(2I_1 + 1)} \sum_{\substack{j_1 j_2 j_1 j_2 l_1 l_2 \\ j'_1 j'_2 l'_1 l'_2}} \exp [i(\sigma_{l'_1} - \sigma_{l'_2})] C_{1l_1 j_1, nl'_1 j'_1}^{J_1} C_{1l_2 j_2, nl'_2 j'_2}^{*J_2} \widehat{J}_1^2 \widehat{J}_2^2 \widehat{j}_1 \widehat{j}_2 \widehat{j}'_1 \widehat{j}'_2 \\ & \times \sum_{L=|l'_2 - l'_1|}^{l'_2 + l'_1} P_L(\cos \theta) \frac{1}{4} [1 + (-1)^{l_1 + l_2 - L}] [1 + (-1)^{l'_1 + l'_2 - L}] \\ & \times (j_1 j_2 1/2 - 1/2 |L0) (j'_1 j'_2 1/2 - 1/2 |L0) W(J_1 j_1 J_2 j_2; I_1 L) W(J_1 j'_1 J_2 j'_2; I_1 L) \\ & + \delta_{1n} \left\{ \frac{1}{k_1(2I_1 + 1)} \sum_{J_1 l_1} (2J_1 + 1) \operatorname{Re} [\exp(i\sigma_{l_1}) f_c^*(\theta) C_{1l_1 j_1, nl_1 j_1}^{J_1}] P_{l_1}(\cos \theta) + |f_c(\theta)|^2 \right\}, \end{aligned} \quad (79)$$

where σ_{l_n} and $\eta_n = \mu Z' Ze^2 / \hbar^2 k_n$ are the corresponding Coulomb phase shift and Sommerfeld parameter accordingly. $f_c(\theta) = -\frac{\eta_1}{2k_1 \sin^2 \theta/2} \exp 2i [\sigma_{l_1} - \eta_1 \ln \sin \theta/2]$ is the Coulomb amplitude, which vanishes in case of neutron scattering.

Integrated scattering cross-sections σ_n can be derived from Eq. (79). Note, that due to Coulomb discontinuity at zero angle, such integration is impossible for elastic proton scattering:

$$\sigma_n = \frac{4\pi}{k_1^2(2I_1+1)(2s+1)} \sum_{Jlj'l'j'} (2J+1) |C_{1ljnl'j'}^J|^2. \quad (80)$$

Total neutron cross section σ_{nT} is determined by optical theorem[41]:

$$\sigma_{nT} = \frac{4\pi}{k_1^2(2I_1+1)(2s+1)} \sum_{Jlj} (2J+1) \operatorname{Im} C_{1lj1lj}^J, \quad (81)$$

and compound formation cross section is:

$$\sigma_c = \sigma_{nT} - \sum_n \sigma_n = \frac{4\pi}{k_1^2(2I_1+1)(2s+1)} \sum_{Jlj} (2J+1) \left(\operatorname{Im} C_{1lj1lj}^J - \sum_{nl'j'} |C_{1ljnl'j'}^J|^2 \right). \quad (82)$$

Generalized transmission coefficients are determined by Eq. (82):

$$T_{lj}^J = 4 \left(\operatorname{Im} C_{1lj1lj}^J - \sum_{nl'j'} |C_{1ljnl'j'}^J|^2 \right). \quad (83)$$

5.1 Legendre Polynomial Expansion of Angular Distributions of Scattered Particles

Formula (79) allows to calculate angular distributions of scattered nucleons to be compared with experimentally measured. On the other hand, OPTMAN code intends to present such angular distributions as Legendre polynomial expansion giving coefficients of such expansion to be used in evaluated nuclear data files.

According to ENDF-6 Formats Manual[42], angular distributions for neutrons (File 4, LTT=1), which is also applicable to inelastically scattered protons (File 6, LAW=2), may be presented as :

$$\frac{d\sigma_n}{d\Omega} = \frac{\sigma_n}{2\pi} \sum_{L=0}^{NL} \frac{2L+1}{2} a_L(E) P_L(\cos \theta). \quad (84)$$

One can see from formula (79) that $a_L(E)$ are real numbers and can be presented (please note, that term with Coulomb amplitude vanishes for neutrons and inelastic proton scattering) as:

$$\begin{aligned} a_L(E) &= \frac{2\pi(-1)^{I_1-I_2}}{\sigma_n k_1^2(2L+1)(2I_1+1)} \sum_{\substack{j_1 j_2 j_1 j_2 l_1 l_2 \\ j'_1 j'_2 l'_1 l'_2}} \exp [i(\sigma_{l'_1} - \sigma_{l'_2})] C_{1lj_1, nl'_1 j'_1}^{J_1} C_{1lj_2, nl'_2 j'_2}^{* J_2} \widehat{J}_1^2 \widehat{J}_2^2 \widehat{j}_1 \widehat{j}_2 \widehat{j}'_1 \widehat{j}'_2 \\ &\times \frac{1}{4} [1 + (-1)^{l_1+l_2-L}] [1 + (-1)^{l'_1+l'_2-L}] \\ &\times (j_1 j_2 1/2 - 1/2 |L0) (j'_1 j'_2 1/2 - 1/2 |L0) W(J_1 j_1 J_2 j_2; I_1 L) W(J_1 j'_1 J_2 j'_2; I_1 L), \end{aligned} \quad (85)$$

with maximum L number $NL = \max(l'_2 + l'_1)$.

In case of elastically scattered protons presence of Coulomb amplitude must be taken into account. According to ENDF-6 Formats Manual[42] angular distributions for protons (File 6, LAW=5) may be presented as:

$$\begin{aligned} \frac{d\sigma_n}{d\Omega} &= \frac{\eta_1^2}{4k_1^2 \sin^4 \theta/2} - \frac{\eta_1}{\sin^2 \theta/2} \operatorname{Re} \left\{ \exp [i\eta \ln (\sin^2 \theta/2)] \sum_{L=0}^{ML} \frac{2L+1}{2} a_L(E) P_L(\cos \theta) \right\} \\ &+ \sum_{L=0}^{NL} \frac{2L+1}{2} b_L(E) P_L(\cos \theta). \end{aligned} \quad (86)$$

Comparing ENDF-6 format formula with (79) gives $a_L(E)$:

$$a_L(E) = \frac{1}{k_1^2 (2L+1)(2I_1+1)} \sum_{J_1 j_1} (2J_1 + 1) C_{1l_1 j_1, L j_1}^{J_1}, \quad (87)$$

with maximum L number $ML = \max(l_1)$. These $a_L(E)$ have complex values, while $b_L(E)$ are real and similar to $a_L(E)$ for neutrons:

$$\begin{aligned} b_L(E) &= \frac{(-1)^{I_1 - I_n}}{k_1^2 (2L+1)(2I_1+1)} \sum_{\substack{j_1 j_2 j_1 j_2 l_1 l_2 \\ j'_1 j'_2 l'_1 l'_2}} \exp [i(\sigma_{l'_1} - \sigma_{l'_2})] C_{1l_1 j_1, n l'_1 j'_1}^{J_1} C_{1l_2 j_2, n l'_2 j'_2}^{* J_2} \widehat{J}_1^2 \widehat{J}_2^2 \widehat{j}_1 \widehat{j}_2 \widehat{j}'_1 \widehat{j}'_2 \\ &\times \frac{1}{4} [1 + (-1)^{l_1 + l_2 - L}] [1 + (-1)^{l'_1 + l'_2 - L}] \\ &\times (j_1 j_2 1/2 - 1/2 | L 0) (j'_1 j'_2 1/2 - 1/2 | L 0) W(J_1 j_1 J_2 j_2; I_1 L) W(J_1 j'_1 J_2 j'_2; I_1 L), \end{aligned} \quad (88)$$

with the only difference that $b_L(E)$ coefficients are not scaled by $\sigma_n/2\pi$ value.

6 Energy Dependence of Optical Potential Parameters

Options of OPTMAN code on the energy dependence of optical potential parameters allow different possibilities. The reason is that there is significant difference for optical potentials used in spherical and CC calculations. In spherical case, optical model calculations for a certain incident energy request the knowledge of the potential only for a specified incident energy, while CC calculations request inherent optical potential energy dependence due to account of energy losses for different coupled channels. As we intend to allow OPTMAN CC code to analyze data in a wide energy region (at least up to 200 MeV incident energies) both for neutrons and protons simultaneously, we keep a global form of optical potential which incorporates the energy dependence of potential, that is derived by considering the dispersion relationship as proposed by Delaroche *et al.*[43], and the high-energy saturation behavior consistent with the Dirac phenomenology. The imaginary components of this potential form vanish at Fermi energy (property stemming from nuclear matter theory). Such an energy dependence allows data analysis without unphysical discontinuities in the whole energy range of interest both for neutrons and protons (constant potential terms, allowing simple potential linear dependencies, shown by bold

characters below for imaginary surface, volume and spin-orbit potentials, can be also used, but please note that being non-zero, they do not vanish at Fermi energies):

$$V_R = (V_R^0 + V_R^1 E^* + V_R^2 E^{*2} + V_R^3 E^{*3} + V_R^{DISP} e^{-\lambda_R E^*}) \left[1 + \frac{1}{V_R^0 + V_R^{DISP}} (-1)^{Z'+1} C_{viso} \frac{A - 2Z}{A} \right] \\ + C_{coul} \frac{ZZ'}{A^{1/3}} \varphi_{coul}(E^*), \quad (89)$$

$$W_D = \left[W_D^{DISP} + (-1)^{Z'+1} C_{wiso} \frac{A - 2Z}{A} \right] e^{-\lambda_D E^*} \frac{E^{*S}}{E^{*S} + WID_D^S} + W_D^0 + W_D^1 E^*, \quad (90)$$

$$W_V = W_V^{DISP} \frac{E^{*S}}{E^{*S} + WID_V^S} + W_V^0 + W_V^1 E^*, \quad (91)$$

$$V_{SO} = V_{SO}^0 e^{-\lambda_{so} E^*}, \quad (92)$$

$$W_{SO} = W_{SO}^{DISP} \frac{E^{*S}}{E^{*S} + WID_{SO}^S} + W_{SO}^0 + W_{SO}^1 E^*. \quad (93)$$

Here, $E^* = (E_p - E_{fm})$, with E_p - energy of the projectile and E_{fm} - the Fermi energy, determined as $E_{fm}(Z, A) = -\frac{1}{2} [S_n(Z, A) + S_n(Z, A + 1)]$ for neutrons and $E_{fm}(Z, A) = -\frac{1}{2} [S_p(Z, A) + S_p(Z + 1, A + 1)]$ for protons, where $S_i(Z, A)$ denotes the separation energy of nucleon i from a nucleus labeled by Z and A , while Z' , Z and A are charges of incident particle, nucleus and nucleus mass number, respectively. As we intend to analyze neutron and proton scattering data simultaneously, we want to have unique optical potential for nucleons with form suggested by Ref. [43] plus a term $C_{coul} ZZ'/A^{1/3} \varphi_{coul}(E^*)$ describing the Coulomb correction to the real optical potential and isospin terms $(-1)^{Z'+1} C_{viso}(A - 2Z)/A \varphi_{viso}(E^*)$ and $(-1)^{Z'+1} C_{wiso}(A - 2Z)/A \cdot \varphi_{wiso}(E^*)$. We assumed that energy dependences of $\varphi_{viso}(E^*)$ and $\varphi_{wiso}(E^*)$ are the same as those of real and imaginary surface potentials (see Eq. (89,90)), while $\varphi_{coul}(E^*)$ can be constant (just unity) or considered to be the minus derivative of Eq. (89), so that

$$\varphi_{coul}(E_p) = (\lambda_R V_R^{DISP} e^{-\lambda_R E^*} - V_R^1 - 2V_R^2 E^* - 3V_R^3 E^{*2}) \left[1 + \frac{1}{V_R^0 + V_R^{DISP}} (-1)^{Z'+1} C_{viso} \frac{A - 2Z}{A} \right]. \quad (94)$$

The parameters WID_D , WID_V , W_D^{DISP} , W_V^{DISP} , W_{SO}^{DISP} , λ_D and λ_R were taken to be equal for neutrons and protons. We assume that Lane model[44] works, therefore the difference of the suggested potential for incident neutron and proton stems from the isospin terms, the Coulomb correction terms and difference of the Fermi energies for neutron and proton.

Real r_R and Coulomb r_C potential radii can be considered to be energy dependent as experimental data analyses [8, 43] indicate dispersion-like energy dependence:

$$r_R(E^*) = r_R^0 \left[1 - \frac{C_R E^{*S}}{E^{*S} + WID_R^S} \right] \quad (95)$$

$$r_C(E^*) = r_C^0 \left[1 - \frac{C_C E^{*S}}{E^{*S} + WID_C^S} \right] \quad (96)$$

Potential diffusenesses a_i can be energy dependent, reflecting that they may grow or decrease with nuclear excitation energy:

$$a_i = a_i^0 + a_i^1 E^* \quad (97)$$

with a_D^1 is assumed to be zero above an energy E_{bound} .

If energy losses due to collective levels excitation as compared to the nucleon incident energies involved in the analysis are noticeable, the dependence of the local optical potential for different channels can be taken into account as:

$$V_{if} = V \left(E_p - \frac{E_i + E_f}{2} \right),$$

where i and f denote initial and final channels, while E_i and E_f the corresponding level energies.

7 Relativistic Generalization of Non-Relativistic Schrödinger Equation

Upper boundary of incident energy of the OPTMAN code is supposed to be about 200 MeV, so our non-relativistic Schrödinger formalism involved relativistic generalization suggested by Elton[18]. The nucleon wave number k was taken in the relativistic form:

$$(\hbar k)^2 = [E^2 - (M_p c^2)^2]/c^2 \quad (98)$$

where E denotes the total energy of projectile, M_p the projectile rest mass, and c the light velocity. To allow non-relativistic motion of the target with rest mass M_T , incident particle mass M_p was replaced with the relativistic projectile energy E in reduced mass formulae, so that the quantity k^2 and optical potential values were multiplied by a coefficient:

$$\frac{1}{1 + E/(M_T c^2)} \quad (99)$$

Following Elton's[18] suggestions, we multiply optical potential strengths except for the spin-orbit and Coulomb terms by a factor $K(E)$, as a relativistic optical potential generalization. Elton[18] suggests it to be $E/(M_p c^2)$. Therefore, the factor increases without limit as the projectile energy E increases. We use this factor as suggested by Madland[19], $K(E) = 2E/(E + M_p c^2)$, which saturates at 2 as incident energy grows, as it looks more physical and allows easier fitting of experimental data. Of course, optical potential can be in any case fitted to the experimental data without such multiplier, so that such relativistic correction can be included while fitting. However, we agree with Elton[18] that "it is advantageous to separate out known relativistic factor in the central potential", as this may allow successful extrapolation of optical potential from low incident projectile energy region to higher and *vice versa*. One can see that for low energies all these relativistic generalization factors have non-relativistic kinematic limit.

8 Potential Adjustment

The best fit optical potential parameters can be found by automatic minimization of χ^2 value:

$$\begin{aligned}
\chi^2 = & \frac{1}{N + M + L + 3} \left[\sum_{i=1}^N \frac{1}{K_i} \sum_{j=1}^{K_i} \left(\frac{d\sigma_{ij}/d\Omega_{calc} - d\sigma_{ij}/d\Omega_{exp}}{\Delta\sigma_{ij}/d\Omega_{exp}} \right)^2 + \sum_{i=1}^M \left(\frac{\sigma_{tot_{cal_i}} - \sigma_{tot_{eval_i}}}{\Delta\sigma_{tot_{eval_i}}} \right)^2 \right] \\
& + \sum_{i=1}^L \left(\frac{\sigma_{reac_{cal_i}} - \sigma_{reac_{eval_i}}}{\Delta\sigma_{reac_{eval_i}}} \right)^2 + \left(\frac{S_{cal}^0 - S_{eval}^0}{\Delta S_{eval}^0} \right)^2 + \left(\frac{S_{cal}^1 - S_{eval}^1}{\Delta S_{eval}^1} \right)^2 + \left(\frac{R'_{cal} - R'_{eval}}{\Delta R'_{eval}} \right)^2,
\end{aligned} \tag{100}$$

where K_i is the number of angles for which angular distribution is measured for incident energy i , and the number of such energies is N , while number of total and reaction cross-sections measurements is M and L accordingly. The symbols S^0 , S^1 and R' denote s-, p-wave strength functions and scattering radius, respectively. All the other optical observable, if any, can be also included in χ^2 search criteria.

9 Analysis of B(E2) Data

The γ -transition probability $B(E\lambda)$ of soft-rotator model can also be calculated. For instance $B(E2)$ calculated in homogeneously charged deformed ellipsoid approximation accounting linear terms of inner $b_{2\mu}$ dynamic variables (higher terms can be taken into consideration, see [30]) is

$$\begin{aligned}
B(E2; I\tau n_\gamma n_{\beta_3} n_{\beta_2} \rightarrow I'\tau' n'_\gamma n'_{\beta_3} n'_{\beta_2}) = & \frac{5Q_0^2}{16\pi} \left\{ \sum_{K,K' \geq 0} \frac{A_{IK}^T A_{I'K'}^{T'}}{[(1+\delta_{0K})(1+\delta_{0K'})]^{1/2}} \right. \\
& \times \left[\langle n_\gamma | \cos \gamma | n'_\gamma \rangle \left[(I'2K'0|IK) + (-1)^{I'} (I'2 - K0|IK) \delta_{K0} \right] \delta_{KK'} \right. \\
& + \sqrt{1/2} \langle n_\gamma | \sin \gamma | n'_\gamma \rangle [(I'2K'2|IK) \delta_{K,K'+2} + (I'2K' - 2|IK) \delta_{K,K'-2} \\
& \left. \left. + (-1)^{I'} (I'2 - K'2|IK) \delta_{K,2-K'} \right] \right\}^2 \left[J_{I\tau n_\gamma n_{\beta_3} n_{\beta_2} \atop I'\tau' n'_\gamma n'_{\beta_3} n'_{\beta_2}} [y] \right]^2,
\end{aligned} \tag{101}$$

where $J_{I\tau n_\gamma n_{\beta_3} n_{\beta_2} \atop I'\tau' n'_\gamma n'_{\beta_3} n'_{\beta_2}} [y]$ is the enhancement factor due to nuclei softness determined by Eq.(41).

10 Program OPTMAN

10.1 Program Description

The present code consists of the main program **ROTAT**, 44 subroutines, 2 functions and a block-data. Brief description of the subroutines, functions, block-data and the main program is given in this chapter, ordered in a natural sequence that follows their calls while code is executing. The block-scheme of the OPTMAN code is given on Figs. 1 - 3.

- **ROTAT** - is the main program. It starts opening files that will be used, and then switches determining program options, such as the nuclear model, method of coupled equation solution, potential expansion and so on. In **ROTAT** one can choose from the two main options: 1 - optical model calculations without optical potential parameters adjustment; 2 - potential parameters adjustment

using experimental optical data. If the first option is chosen **ROTAT** calls subroutine **ABCT**, if the second option is activated subroutine **DATET** is called by **ROTAT**.

- **ABCT** - is a subroutine, organizing optical model calculations without optical parameter adjustment. Subroutines **PREQU**, **RIPAT**, **ASFUT**, **KNCOE** and **QUANT** are called from **ABCT**. Subroutines **PREQU** and **KNCOE** with all thier sequences are called if non-axiality of nuclei is taken into account. If angular distributions of scattered particles are to be calculated, subroutine **DISCA** are also called and results are written into output files. This is repeated for all incident energies specified by the input data.
- **PREQU** - is a subroutine, that prepares necessary averages over dynamic variables: quadrupole deformation β_2 , non-axiality γ and octupole deformation β_3 , which determine enhancement of coupling strength between channels as comparing with rigid non-axial model [4]. If nuclear model with rigid β_2 , γ or β_3 is used, the averages are equal to rigid values. **PREQU** calls subroutines **SHEM**, **OVLAO**, **OVLAB**, **OVLAGE**.
- **SHEM** - is a subroutine, that determines energies of collective excited states determined by Eq. (29,40), indices of rotational and vibrational wave functions (Eq. (32,36)). The last are needed to average β_2 , γ or β_3 over initial $|i\rangle$ and final $|f\rangle$ collective states wave functions (Eq. (37)). **SHEM** calls **ANUDF**, **OVLAB**, **ANDETO**, **OVLAG**, **INERMO**, **MATAM**, **EIT12** and function **ERFC(XX)**.
- **ERFC(XX)** - is a function that calculates the error function $erfc(x)$.
- **ANUDF** and **ANDETO** - are subroutines that find indices of β_2 , γ and β_3 oscillator functions satisfying boundary conditions (Eq. (32,36)); it is equal to quantizing energies. **ANUDF** uses function **DGAMMA(XX)** and rational approximation with coefficients stored in **BLOCK DATA**, common **/SENU/**. **ANDETO** calls subroutine **DETX12**.
- **DGAMMA(XX)** - is a function to calculate gamma function of real argument $\Gamma(x)$
- **DETX12** - is a subroutine that calculates the determinant of a matrix built on independent oscillator functions with two boundary conditions. It calls subroutine **FUDNU**.
- **OVLAG** - is a subroutine making some necessary averages over γ oscillation functions. It calls subroutine **FUDNU**.
- **FUDNU** - is a subroutine that calculates Weber - $D_\nu(y)$ and linearly independent $V_\nu(y)$ functions. **FUDNU** uses function **DGAMMA(XX)** and is called by all the subroutines averaging dynamic variables.
- **OVLAB**, **OVLAGE**, **OVLAO** - are subroutines making some necessary averages over β_2 , γ and β_3 oscillation functions respectively. They all call subroutine **FUDNU**.
- **INERMO** - is a subroutine giving principal moments of inertia for a non-axial rigid nucleus (Eq. (7) with deformations in the minima of the potential energy of the quadrupole and octupole vibrations, *i.e.* β_{20} , γ_0 and β_{30}).

- **MATAM** - is a subroutine that creates matrix determining coupling of rotational functions with different K for one I^π and calls **VECNO**.
- **VECNO** - is a subroutine that diagonalizes the coupling matrix, thus solving the problem of rotational energies $\varepsilon_{I\tau}^\pm$ for a rigid non-axial rotator. Necessary weights A_{IK}^τ for rotational functions (see Eq. (27)) are prepared in this program too.
- **EIT12** - is a subroutine calculating collective excited states energy corrections due to γ_0 vibrations (see Eq. (40)). It calls subroutine **INERMO**.
- **RIPAT** - is a subroutine preparing matching radius, mesh for integrating systems of coupled equations, potential expansion in all mesh points and wave numbers of scattered particles in different channels. In accordance with previously chosen option, potential expansion appears as a result of integration of deformed optical potential with spherical functions $Y_{l0}(\theta)$ (rotational model, deformed axial nuclei, $R(\theta) = R_0 \{1 + \sum_\lambda \beta_{\lambda 0} Y_{\lambda 0}(\theta)\}$) or expanding deformed optical potential by derivatives (rigid and soft non-axial nuclei). Potential expansion is calculated in mesh points necessary for both exact and iteration solutions of coupled equation systems. **RIPAT** activates **POTVOL** and **SPHEPOT**, if optical potential expansion appears as a result of integration of deformed optical potential with spherical functions $Y_{l0}(\theta)$ subroutine **POTET** is called. Coulomb potential multipoles are also calculated for both axial and non-axial nuclear shape options.
- **POTVOL** - is a subroutine which calculates volume-integrals of optical potentials and their three derivatives considering the potentials to be spherical. In case nuclear conservation option is activated while calculations, subroutine prepares necessary C_β constant, using Eq. (52) from calculated spherical real potential derivatives.
- **SPHEPOT** - is a subroutine, that calculates Coulomb potential of charged sphere with surface diffuseness of charge density and uses subroutine **SPHER**.
- **SPHER** - is a subroutine, that calculates charge within a sphere with surface diffuseness of charge density.
- **POTET** - is a subroutine giving optical potential as a function of $R(\theta)$ so that integration with $Y_{l0}(\theta)$ in **RIPAT** can be done.
- **ASFUT** - is a subroutine that determines the maximum value of scattered particle angular momentum l_{max} used in calculations and the Coulomb parameter. It calls **COPHA** for calculation of Coulomb phases, if calculations are carried out for charged particle scattering. Then it calls subroutine **BENEC** and **BESIM** for opened and closed channels, respectively.
- **COPHA** - is a subroutine which calculates Coulomb phases σ_{l_n} for angular momenta up to l_{max} and all excited scattering channels considered (n is a number of channel).

- **BENEC** and **BESIM** - are subroutines which evaluates regular and irregular solutions at matching radius for opened and closed channels, respectively. In case of charged particle scattering **BENEC** calls subroutine **RCWF** for opened channels, and for closed **BESIM** calls **BESIMC**.
- **BESIMC** - is a subroutine evaluating two independent Coulomb equation solutions in two matching points by integration of Coulomb equation from low matching point to high (see Eq. (75)) and explanations below.
- **RCWF** - is a subroutine that calculates Coulomb functions at matching radius. This subroutine originates from well known spherical optical code **SCAT2** with algorithm and modifications presented in Ref.[45] .
- **KNCOE** - is a subroutine that calculates coefficients $\langle I\tau n_\gamma || Q_{\nu\mu}^{(tm\cdots n\lambda'\lambda''\cdots\lambda''')}^* || I'\tau' n'_\gamma \rangle$ in Eq. (57). It calls subroutine **KLEGO**.
- **KLEGO** - is a subroutine that calculates Clebsch-Gordan coefficients, uses data from **BLOCK DATA**.
- **BLOCK DATA** - data stored in common /SENU/ are coefficients of rational approximation used by subroutine **ANUDF**; data stored in common /LOFAC/ are logarithms of factorials used for calculations of Clebsch-Gordan and Racah coefficients used by **KLEGO**.
- **QUANT** - is a subroutine that for a certain incident energy generates coupled channels systems for certain spin and parity J^π , and determines all the necessary quantum numbers of scattered particles by calling **LOGMO** . Number of coupled channels must not exceed 200, so if number of possible coupled channels exceed this number or the one specified in input, other are truncated. Subroutine can choose between truncation of high excitation level channels or channels with higher angular momentum. This subroutine calls **CMATC** and the C-matrix elements given by **CMATC** for growing J^π are checked to add no less than 1.0×10^{-4} barn to optical cross sections. When two systems with the same J and different parities obey this limit, systems with higher J are ignored. Subroutine **QUANT** prepares cross sections, transmission coefficients in formats used by **GNASH**[46] and **STAPRE** [47] statistical codes and strength functions S_0 , S_1 and S_2 .
- **LOGMO** - is a subroutine that generates possible angular momenta of outgoing waves with chosen J^π of compound nucleus and residual excited state.
- **CMATC** - is a subroutine that allows different options for coupled channels solution. Four options can be chosen: 1- standard exact solution (see Chapter 4.1 for description), 2 - standard exact solution for small systems and solution using iterations (see Chapter 4.2 for description) for large systems; 3 - iterations for all systems, with non-coupled scheme as zero approximation; 4 - iterations with zero approximation taken from exact solution with few equations coupled. Number of such coupled equations solutions used as zero approximation must not exceed 20. **CMATC** calls subroutines **KNDIT**, **SOSIT**, **MASCT** or **ECISS**.

- **KNDIT** - is a subroutine that determines coupling strength of different equations in a system of coupled channels for certain J^π . For non-axial nuclei case calculations such coupling is determined by Eq. (57), subroutine uses elements $\langle I\tau n_\gamma || Q_{\nu\mu}^{(tm..n\lambda'\lambda''..\lambda''')} * || I'\tau' n'_\gamma \rangle$ calculated preliminary by **KNCOE**. Coupling strength for rigid axial rotator case calculations formulae is described [2]. **KLEGO** and **RACAH** subroutines are called by the subroutine.
- **RACAH** - is a subroutine calculating Racah coefficients.
- **SOSIT** - is a subroutine integrating system of coupled equations and giving independent solutions in mesh points up to matching radius. The integration method is described in Chapter 4.1, it utilizes suggestions of Ref. [38].
- **MASCT** - is a subroutine that matches the solutions with desired asymptotic behavior and gives C-matrix elements. It calls subroutine **INMAT**.
- **INMAT** - is a subroutine inverting complex matrix C, presented as $C=A+iB$ with A and B real. It calls subroutine **INVER**.
- **INVER** - is a subroutine inverting a real matrix. The quality of inversion is checked by multiplying initial matrix by inverted one to be the unity one. If non-diagonal elements of the resulting matrix and difference of diagonal from unity are greater than 10^{-7} iterations to improve matrix conversion are started. If after two iterations converting is not improved, subroutine prints warning and uses the last result.
- **ECKISS** - is a subroutine, that integrates a coupled system using iterations. The integration method uses the idea of Ref.[39] and is described in Chapter 4.2. Two options for iterations are possible: 1 - with spherical non-coupled optical solutions used as zero approximation; 2 - standard solution for a small number of coupled equations used as zero approximation. **ECKISS** calls subroutines **MATCH** and **PADE**. Iterations are finished when all C-matrix elements for n and n+1 iterations coincide with accuracy leading to accuracy better than 10^{-4} in cross sections. Maximum number of iterations is 20. If iterations do not converge or number of iterations exceeds 20, standard solution method is activated.
- **MATCH** - is a subroutine matching solution in a chosen channel, considering it is described by inhomogeneous Eq. (70), and giving C-matrix element.
- **PADE** - is a subroutine applying Pade approximation[48] for C-matrix elements determinations, this highly improves the iterations convergence, calls subroutine **MATIN**.
- **MATIN** - is a subroutine inverting a real matrix using standard procedure.
- **DISCA** - is a subroutine that calculates angular distributions for particles with $s = 1/2$, both for neutrons and protons, for using analytical formulas and C-matrix elements, calls **PLEGA**, **KLEGO**

and **RACAH** subroutines. **DISCA** prepares Legendre coefficients of angular distributions of scattered particles: real for neutrons (Eq. (85)) and in proton scattering case -real for nuclear part of scattering amplitude (Eq. (88)) and coefficients presenting expansion of nuclear and Coulomb interference term (Eq. (87)) necessary for presenting proton elastic scattering only.

- **PLEGA** - is a subroutine that calculates Legendre polynomials at given angles using recurrence.
- **DATET** - is a subroutine in which all the input data for optical model calculations with optical potential parameters adjustment are organized. First starting, optical model parameters are read, then experimental optical data base is inputted. Switches are also read determining which of the optical parameter must be adjusted and its desired accuracies. **DATET** calls subroutine **PREQU** (see **ABCT** for details) for non-axial nuclear model and subroutine **SEART**.
- **SEART** - is a subroutine that minimizes χ^2 -function. It utilizes gradient method and calls **XISQT** and **DEFGT**.
- **XISQT** - is a subroutine calculating χ^2 (Eq. (100)) built in a standard manner, being the average of the sum of squares of the differences between results of optical calculations and experimental ones divided by square of the appropriate experimental errors . It calls subroutines **PREQU**, **RIPAT**, **ASFUT**, **KNCOE**, **QUANT**, and **DISCA** for each energy point used to evaluate χ^2 . This sequence of subroutine calls leads to optical cross sections calculations and is the same as in **ABCT** and is described above.
- **DEFGT** - is a subroutine, that calculates gradient of χ^2 as a function of adjusted optical parameters, it calls subroutine **XISQT**.

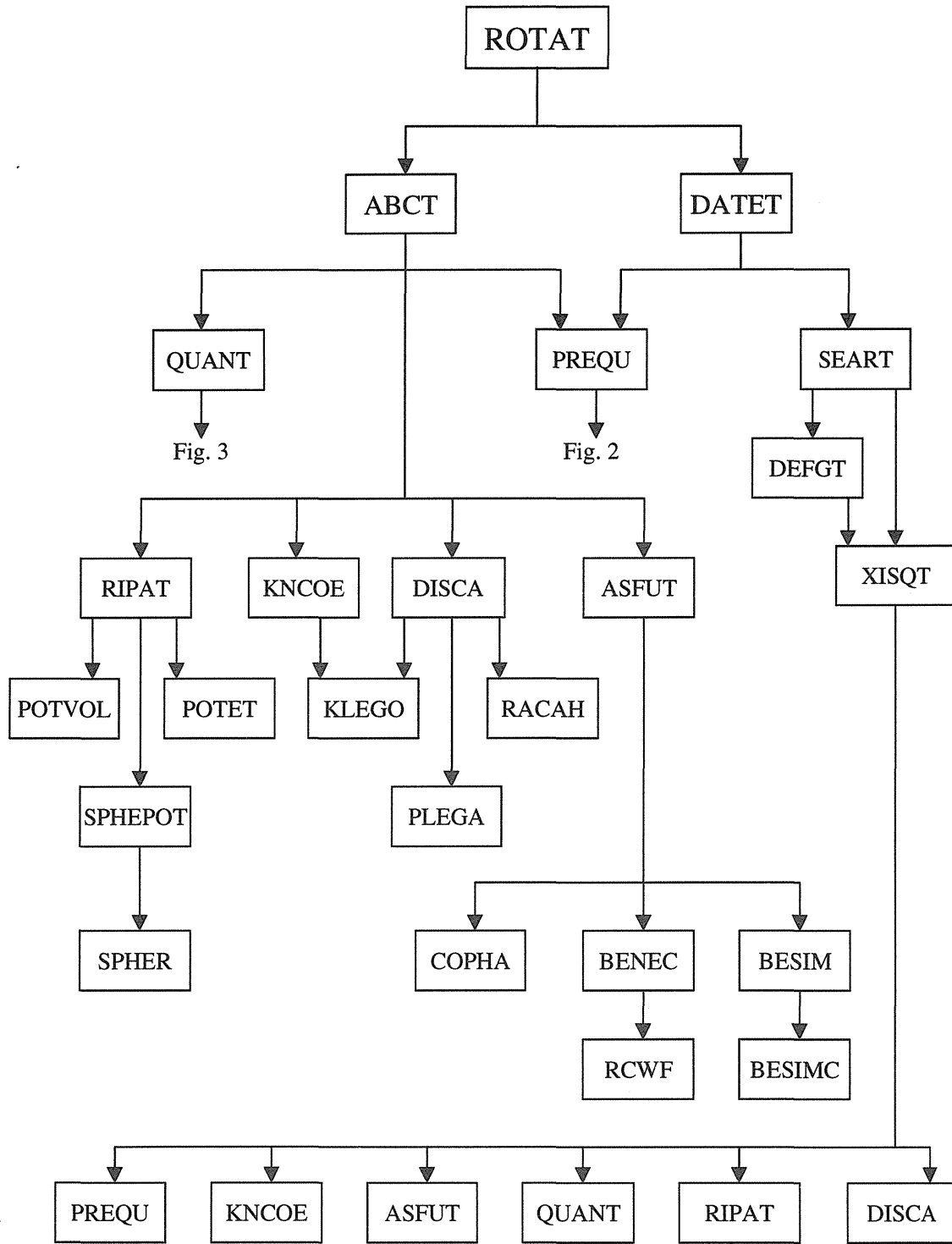


Fig. 1: Block scheme of OPTMAN code - the main chain of subroutine calls.

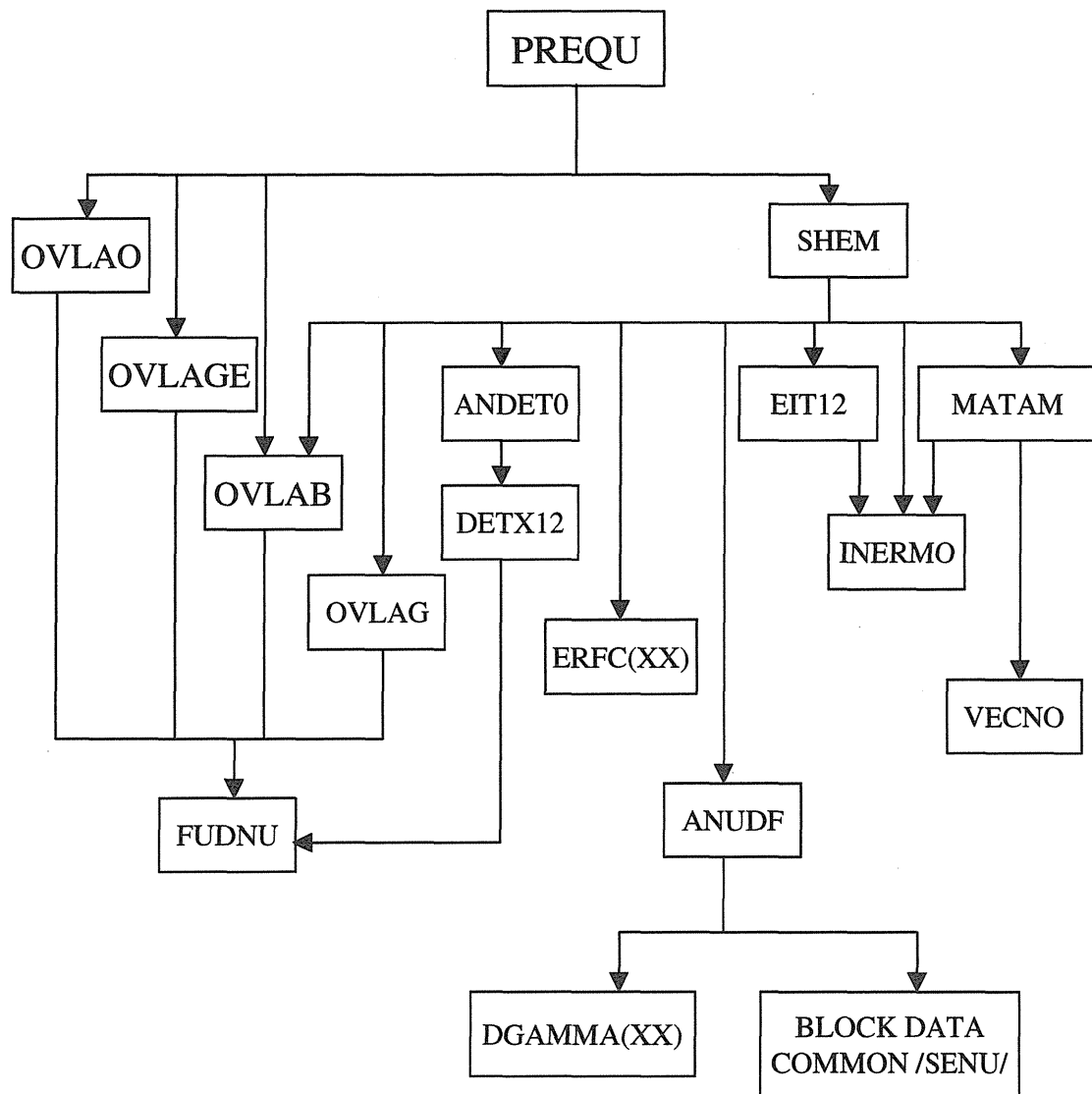


Fig. 2: Block scheme of OPTMAN code - the chain of subroutine calls starting from PREQU.

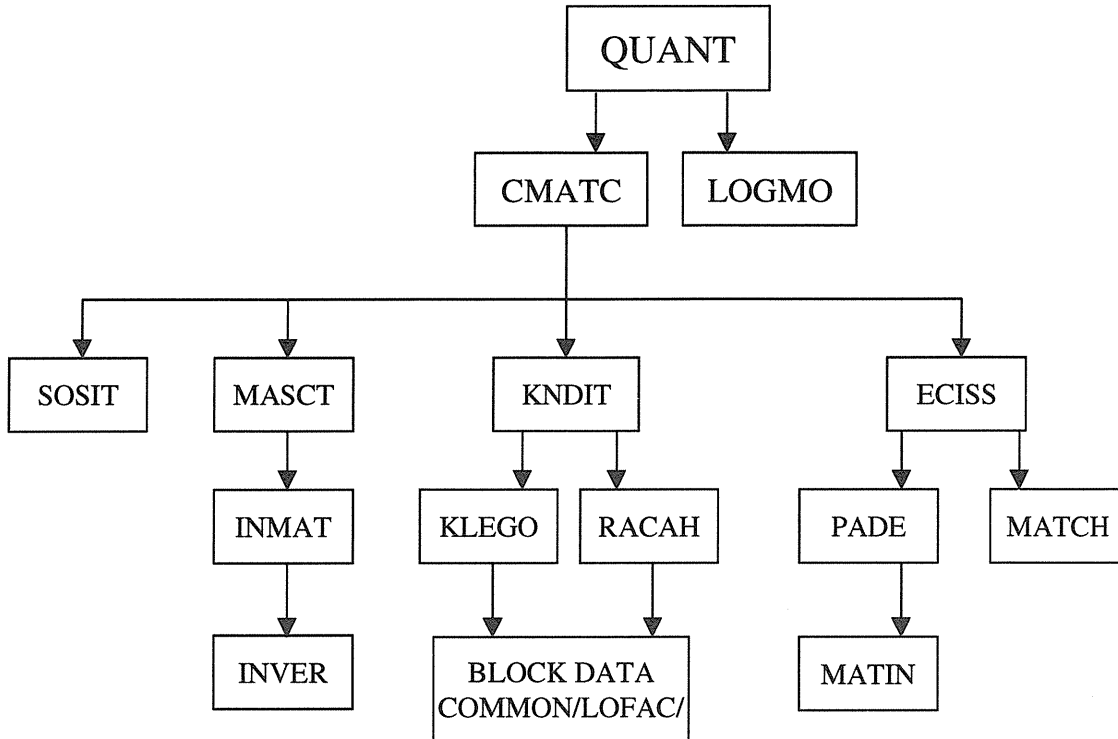


Fig. 3: Block scheme of OPTMAN code - the chain of subroutines starting from QUANT.

10.2 Input Data

Input data of code OPTMAN is described in this section. Data have the card image form. Units of the data are MeV, fm, barn and amu (Carbon units).

- Record 1 - FORMAT(20A4)

Any text information that identifies current calculation. They will be printed in the head of output.

- Record 2 - FORMAT(14I2)

MEJOB, MEPOT, MEHAM, MEPRI, MESOL, MESHA, MESHO, MEHAO, MEAPP, MEVOL, MEREL, MECUL, MERZZ, MERRR

Switches options describing the model.

- MEJOB = 1 - calculations without parameter adjustment, = 2 adjustment of optical potential parameters;
- MEPOT = 1 -rotational model potential, =2 - potential expanded by derivatives;

- **MEHAM** = 1 - rigid-rotational model, = 2 - not in use yet, = 3 - Davydov-Chaban model, = 4 - Davydov-Fillipov model, = 5 - soft-rotator model with account of γ softness [5, 6] , = 6,7 - not in use yet;
 - **MEPRI** = 0 - short output, additional output as **MEPRI** is growing :
 - **MESOL** = 1 - code will choose which method of coupled channels system solution for a certain J^π should be used to reduce time of calculations, = 2 - exact solution, =3 - solution using iterations, with spherical solutions as zero approximation, >3 - solution using iterations, with exact couple channels solution with number of coupled states equal **MESOL** as zero approximation, **MESOL** must be less than or equal to 20;
 - **MESHA** = 1 - rigid hexadecapole deformations are not taken into account, = 2 - with account of axial rigid hexadecapole deformations. = 3 - rigid hexadecapole deformations with non-axial parameters $\gamma_4 = \gamma$ and $\delta_4 = \cos^{-1} \left(\sqrt{\frac{7}{12}} \cos 3\gamma \right)$ (Ref.[49]), = 4 - rigid hexadecapole deformations in the most general case [49] where γ_4 and δ_4 are independent and chosen freely;
 - **MESHO** = 0 - nuclear shape without octupole deformations, = 1 -nuclear shape with axial octupole deformations, = 2 - nuclear shape with non-axial octupole deformations;
 - **MEHAO** = 0 - nucleus is rigid to octupole deformations, = 1 - nucleus is soft to non symmetric octupole, = 2 - nucleus is soft to symmetric octupole deformations scaled by β_2 [4] , = 3 - nucleus is soft to symmetric octupole deformations not scaled by β_2 ;
 - **MEAPP** = 0 - solution with the potential dependency on level energy losses in the channel, =1 - quick solution without potential dependency on level energy losses, can be used when energies of levels are much less than particle incident energy;
 - **MEVOL** = 0 - solution without account of volume conservation, =1 - account of volume conservation in uniform nuclear density approximation[30] , =2 - common case[36] , presenting nuclear density distribution by real potential form factor;
 - **MEREL** = 0 - calculations using non-relativistic Schrödinger formalism, =1 -account of relativistic kinematics and potential dependence, =2 - account of relativistic kinematic only, =3 - account of relativistic kinematics and real potential dependence;
 - **MECUL** = 0 - solution with Coulomb correction potential proportional to derivative of real potential dependence (Eq. (94)), = 1 - Coulomb correction is energy independent;
 - **MERZZ** = 0 - charge radius is considered to be constant, = 1 - charge radius is considered to be energy dependent (Eq. (96));
 - **MERRR** = 0 - real potential radius is considered to be constant, = 1 - charge radius is considered energy dependent (Eq. (95)) .
- Record 3 - FORMAT(6E12.7), cards - 3a, 3b, 3c

Parameters of non-axial nuclear Hamiltonian. These cards are read if **MEHAM** > 1. In details this parameters are described elsewhere[4, 10, 49] .

HW, AMBO, AMGO, GAMO, BETO, BET4 - card 3a

- **HW** - energy scale factor $\hbar\omega_0$;
- **AMBO** - nuclear softness $\mu_{\beta_{20}}$;
- **AMGO** - nuclear softness μ_{γ_0} ,
- **GAMO** - equilibrium non-axiality $0 < \gamma_0 < \pi/3$ in radians;
- **BETO** - equilibrium deformation β_{20} , for non-axial Hamiltonian;
- **BET4** - rigid deformation β_4 , for non-axial Hamiltonian.

BB42, GAMG, DELG, BET3, ETO, AMUO - card 3b

- **BB42** - $a_{42} = B_4/B_2(\beta_4/\beta_{20})^2$, where B_λ - are mass parameters;
- **GAMG** - parameter of β_4 non-axiality, γ_4 ;
- **DELG** - parameter of β_4 non-axiality, δ_4 ;
- **BET3** - if **MEHAO** = 2 - **BET3**= ϵ_0 and $\beta_{30} = \beta_{20}\epsilon_0 = \text{BET3} * \text{BETO}$, if **MEHAO** = 3 - **BET3**= equilibrium deformation $\beta_{30} = \epsilon_0 = \text{BET3}$;
- **ETO** - non-axiality of octupole β_3 deformation η ;
- **AMUO** - nuclear softness μ_ϵ .

HWO, BB32, GAMDE, DPAR, GSHPA - card 3c

- **HWO** - energy scale for octupole oscillations $\hbar\omega_\epsilon$, used if **MEHAO** = 1;
- **BB32** - $a_{32} = B_3/B_2(\beta_{30}/\beta_{20})^2$;
- **GAMDE** - yet not in use;
- **DPAR** - splitting of energy for the states with different parity in symmetric potential well for octupole oscillations equal δ_n ;
- **GSHPA** - parameter allowing negative β_2 deformations so that $\cos(\gamma_0 + \text{GSHAPE})$ is negative.

• Record 4 - FORMAT(9I3)

Switches for details of calculations

NUR, NST, NPD, LAS, MTET, LLMA, NCMA, NSMA, KODMA

- **NUR** - number of coupled levels in optical model calculations (**NUR** ≤ 20);
- **NST** - number of energy points for which optical model calculations will be carried out if **MEJOB**=1; if **MEJOB** = 2, number of energy points with experimental data that will be used for optical parameters adjustment; (**NST** ≤ 50);

- **NPD** - the highest multipole Y_{l0} in deformed radii expansion, $l_{max} = \text{NPD}$ for rotational model (**MEPOT** = **MEHAM** = 1), **NPD** ≤ 8 . For non-axial nuclear Hamiltonian models (**MEPOT** = 2, **MEHAM** > 2), not in use;
 - **LAS** - the highest multipole Y_{l0} in deformed potential expansion, $l_{max} = \text{LAS}$ for rotational model (**MEPOT** = **MEHAM** = 1), **LAS** ≤ 8 . For non-axial nuclear Hamiltonian models (**MEPOT** = 2, **MEHAM** > 2), number of potential derivatives for deformed potential expansion, must be no more than 4;
 - **MTET** - number of angles (in c.m.) for which angular distributions of scattered nucleons will be calculated (used only for **MEJOB** = 1, for **MEJOB** = 2 it is not used, put any value), if **MTET** = 0 angular distributions are not calculated, **MTET** must be no more than 150;
 - **LLMA** = maximum angular momentum of scattered nucleons that is taken into account; higher are rejected. **LLMA** < 90;
 - **NCMA** - maximum number of coupled equation for certain J^π ; **NCMA** ≤ 200 ;
 - **NSMA** - maximum number of J^π states for which coupled channels systems are solved; **NSMA** ≤ 180 ;
 - **KODMA** - = 0 - coupled equations are ordered one by one, first for the first level, then for the second, etc., = 1 - coupled equations are ordered one by one by growing angular momentum of scattered nucleons, the total number of coupled equations $\leq \text{NCMA}$.
- Record 5 - FORMAT(6E12.7)
 - MEJOB** = 1 - energies (**EE(I)**) in which optical model cross sections are calculated, **MEJOB** = 2 - energies for experimental points which will be used for potential adjustment; **NST** ≤ 50
 - (**EE(I)**, **I**=1,**NST**) - cards 5a, 5b, ...
 - Record 6 - FORMAT(36I2)
 - Flags determining charge (in units of electron charge) of the incident particles Z' for which calculations for energy **EE(I)** will be carried out.
 - (**MCHAE(I)**, **I**=1,**NST**) - card 6a and for **NST** > 36 - card 6b.
 - Record 7 - FORMAT(6E12.7)
 - Angles at which angular distributions will be calculated. If **MTET** = 0 or **MEJOB** = 2 these cards are not read, **MTET** must be no more than 150;
 - (**TET(I)**, **I**=1,**MTET**) - Cards 7a, 7b,
 - Record 8 - FORMAT(E12.7,3I2) for **MEHAM** = 1, FORMAT(E12.7,6I2) for **MEHAM** > 1
 - Characteristics of nuclear levels

(**EL(I)**, **J0(I)**, **NPO(I)**, **KO(I)**, **I=1,NUR**) - Cards 8a, 8b, .. for **MEHAM =1**
 (**EL(I)**, **J0(I)**, **NPO(I)**, **NTU(I)**, **NNB(I)**, **NNG(I)**, **NNO(I)**, **I=1,NUR**) - Cards 8a, 8b, .. for **MEHAM > 1**

- **EL(I)** -energy of the I^{th} level;
- **J0(I)** - spin of the level multiplied by two;
- **NPO(I)** - parity of the level = +1 - for positive, = -1 - for negative;
- **KO(I)** - K of the levels band multiplied by two;
- **NTU(I)** - the number of rotational energy solution τ ;
- **NNB(I)** - the number of β_2 oscillation function solution n_{β_2} ;
- **NNG(I)** - the number or γ oscillation function solution n_γ ;
- **NNO(I)** - the number of β_3 oscillation function solution n_{β_3} .

• Record 9 - FORMAT(6E12.7)

Characteristics of interacting incident particle and nuclei

ANEU, **ASP**, **AT**, **ZNUC**, **EFERMN**, **EFERMP**

- **ANEU** - incident particle mass (in amu);
- **ASP** - incident particle spin;
- **AT** - target nuclear mass (in amu);
- **ZNUC** - target nuclear charge Z ;
- **EFERMN** - Fermi energy for neutrons;
- **EFERMP** - Fermi energy for protons.

• Record 10 - FORMAT(6E12.7)

Optical potential parameters, for details see Chapter 6.

VRO, **VR1**, **VR2**, **VR3**, **VRLA**, **ALAVR** - card 10a

- **VRO** - real optical potential V_R constant term V_R^0 ;
- **VR1** - real optical potential V_R linear term V_R^1 ;
- **VR2** - real optical potential V_R square term V_R^2 ;
- **VR3** - real optical potential V_R cubic term V_R^3 ;
- **VRLA** - real optical potential V_R exponential term V_R^{DISP} ;
- **ALAVR** - real optical potential V_R exponential constant λ_R .

WDO, **WD1**, **WDA1**, **WDBW**, **WDWID**, **ALAWD** - card 10b

- WDO - imaginary surface potential W_D constant term W_D^0 ;
- WD1 - imaginary surface potential W_D linear term W_D^1 ;
- WDA1 - imaginary surface potential W_D linear term W_D^1 for the projectile energies above E_{change} ;
- WDBW - imaginary surface potential W_D term W_D^{DISP} ;
- WDWID - imaginary surface potential W_D dispersion width WID_D ;
- ALAWD - imaginary surface potential W_D exponential constant λ_D .

WCO, WC1, WCA1, WCBW, WCWID, BNDC - card 10c

- WCO - imaginary volume potential W_V constant term W_V^0 ;
- WC1 - imaginary volume potential W_V linear term W_V^1 ;
- WCA1 - imaginary volume potential W_V linear term W_V^1 for the projectile energies above E_{change} ;
- WCBW - imaginary volume potential W_V term W_V^{DISP} ;
- WCWID - imaginary volume potential W_V dispersion width WID_V ;
- BNDC - boundary energy where linear potential slopes change E_{change} .

VS, ALASO, WSO, WS1, WSBW, WSWID - card 10d

- VS - real spin orbit potential V_{SO}^0 ;
- ALASO - real spin orbit potential V_{SO} exponential constant λ_{so} ;
- WSO - imaginary spin orbit potential W_{SO} constant term W_{SO}^0 ;
- WS1 - imaginary spin orbit potential W_{SO} linear term W_{SO}^1 ;
- WSBW - imaginary spin orbit potential W_{SO} term W_{SO}^{DISP} ;
- WSWID - imaginary spin orbit potential W_{SO} dispersion width WID_{SO} .

RR, RRBWC, RRWID, PDIS, ARO, AR1 - card 10e

- RR - real potential radius R_R ;
- RRBWC - real potential radius R_R dispersion constant C_R ;
- RRWID - real potential radius R_R dispersion width WID_R ;
- PDIS - dispersion power constant S ;
- ARO - real potential diffuseness a_R constant term a_R^0 ;
- AR1 - real potential diffuseness a_R linear term a_R^1 .

RD, ADO, AD1, RC, ACO, AC1 - card 10f

- RD - imaginary surface potential radius R_D ;
- ADO -imaginary surface potential diffuseness a_D constant term a_D^0 ;
- AD1 - imaginary surface potential diffuseness a_D linear term a_D^1 ;
- RC - imaginary volume potential radius R_V ;
- ACO - imaginary volume potential diffuseness a_V constant term a_V^0 ;
- AC1 - imaginary volume potential diffuseness a_V linear term a_V^1 .

RW, AWO, AW1, RS, AS0, AS1 - card 10g

- RW - imaginary Gaussian potential radius R_W ;
- AWO - imaginary Gaussian potential diffuseness a_W constant term a_W^0 ;
- AW1 - imaginary Gaussian potential diffuseness a_W linear term a_W^1 ;
- RS - spin orbit potential radius R_{SO} ;
- AS0 - spin orbit potential diffuseness a_{SO} constant term a_{SO}^0 ;
- AS1 - spin orbit potential diffuseness a_{SO} linear term a_{SO}^1 .

RZ, RZBWC, RZWID, AZ, CCOUL, ALF - card 10h

- RZ - equivalent charged ellipsoid radius R_C ;
- RZBWC - equivalent charged ellipsoid radius R_C dispersion constant C_C ;
- RZWID - equivalent charged ellipsoid radius R_C dispersion width WID_C ;
- AZ - charged ellipsoid radius diffuseness a_Z ;
- CCOUL - Coulomb correction constant C_{Coul} ;
- ALF- mixture coefficient for imaginary volume and Gaussian potentials α .

CISO, WCISO - card 10i

- CISO - constant for real potential isospin term C_{viso} ;
- WCISO - constant for imaginary surface potential isospin term C_{wiso} .

• Record 11 - FORMAT(6E12.7)

Input of even axial coefficients of radii deformations $\beta_{\lambda 0}$ from β_{20} to $\beta_{\lambda 0}$, $\lambda=NPD$. This Record is read only for axial rotator model (**MEHAM** = 1). Note that λ is even and no more than 8.

(**BET(I), I=2,NPD,2**)

It is the last card of input for optical model calculations (**MEJOB** = 1), the following cards are used when potential parameters adjustment is desired.

- Record 12 - FORMAT(6I2)

Input of flags that determine which parameters will be adjusted; if $\text{NPJ}(I) = 1$ the chosen parameter will be adjusted. Number of parameters to be adjusted must not exceed 20. Please note, that up to $\text{NPJ}(50)$ for users convenience sequence of inputted flags follows sequence of potential parameters.

$(\text{NPJ}(I), I=1,58)$ cards 12a,...12j

- $\text{NPJ}(1)$ - flag for real optical potential V_R constant term adjustment **VR0**;
- $\text{NPJ}(2)$ - flag for real optical potential V_R linear term adjustment **VR1**;
- $\text{NPJ}(3)$ - flag for real optical potential V_R square term adjustment **VR2**;
- $\text{NPJ}(4)$ - flag for real optical potential V_R cubic term adjustment **VR3**;
- $\text{NPJ}(5)$ - flag for real optical potential V_R exponential term V_R^{DISP} adjustment **VRLA**;
- $\text{NPJ}(6)$ - flag for real optical potential V_R exponential constant λ_R adjustment **ALAVR**;
- $\text{NPJ}(7)$ - flag for constant term, W_D^0 , of imaginary surface potential adjustment **WD0**;
- $\text{NPJ}(8)$ - flag for linear term, W_D^1 , of imaginary surface potential adjustment **WD1**;
- $\text{NPJ}(9)$ - flag for imaginary surface potential W_D linear term W_D^1 for particle incident energies above $\text{BNDC} = E_{change}$ adjustment **WDA1**;
- $\text{NPJ}(10)$ - flag for imaginary surface potential W_D dispersion term W_D^{DISP} adjustment **WDBW**;
- $\text{NPJ}(11)$ - flag for imaginary surface potential W_D dispersion width term WID_D adjustment **WDWID**;
- $\text{NPJ}(12)$ - flag for imaginary surface potential W_D exponential constant λ_D adjustment **ALAWD**;
- $\text{NPJ}(13)$ - flag for imaginary volume potential W_V constant term linear term W_V^0 adjustment **WCO**;
- $\text{NPJ}(14)$ - flag for imaginary volume potential W_V linear term W_V^1 adjustment **WC1**;
- $\text{NPJ}(15)$ - flag for imaginary volume potential W_V linear term W_V^1 for particle incident energies above $\text{BNDC} = E_{change}$ adjustment **WCA1**;
- $\text{NPJ}(16)$ - flag for imaginary surface potential W_V dispersion term W_V^{DISP} adjustment **WCBW**;
- $\text{NPJ}(17)$ - flag for imaginary surface potential W_V dispersion width term WID_V adjustment **WCWID**;
- $\text{NPJ}(18)$ - flag for energy where linear potential slopes change E_{change} adjustment **BNDC**;
- $\text{NPJ}(19)$ - flag for real spin-orbit potential V_{SO} adjustment **VS**;
- $\text{NPJ}(20)$ - flag for real spin-orbit potential V_{SO} exponential constant λ_{so} adjustment **ALASO**;
- $\text{NPJ}(21)$ - flag for imaginary spin-orbit potential W_{SO} constant term W_{SO}^0 adjustment **WSO**;

- NPJ(22) - flag for imaginary spin-orbit potential W_{SO} linear term W_{SO}^1 adjustment WS1;
- NPJ(23) - flag for imaginary spin-orbit potential W_{SO} dispersion term W_{SO}^{DISP} adjustment WSBW;
- NPJ(24) - flag for imaginary spin-orbit potential W_{SO} dispersion width WID_{SO} adjustment WSWID;
- NPJ(25) - flag for real potential radius R_R adjustment RR;
- NPJ(26) - flag for real potential radius R_R dispersion constant C_R adjustment RRBWC;
- NPJ(27) - flag for real potential radius R_R dispersion dispersion width WID_R adjustment RRWID;
- NPJ(28) - flag for dispersion power constant S adjustment PDIS;
- NPJ(29) - flag for real potential diffuseness a_R constant term adjustment ARO;
- NPJ(30) - flag for real potential diffuseness a_R linear term a_R^1 adjustment AR1;
- NPJ(31) - flag for imaginary surface potential radius R_D adjustment RD;
- NPJ(32) - flag for imaginary surface potential diffuseness a_D constant term adjustment ADO;
- NPJ(33) - flag for imaginary surface potential diffuseness a_D linear term a_D^1 adjustment AD1;
- NPJ(34) - flag for imaginary volume potential radius R_V adjustment RC;
- NPJ(35) - flag for imaginary volume potential diffuseness a_V constant term adjustment ACO;
- NPJ(36) - flag for imaginary volume potential diffuseness a_V linear term a_V^1 adjustment AC1;
- NPJ(37) - flag for Gaussian potential radius R_W adjustment RW;
- NPJ(38) - flag for Gaussian potential radius diffuseness a_W constant term adjustment AWO;
- NPJ(39) - flag for Gaussian potential radius diffuseness a_W linear term a_W^1 adjustment AW1;
- NPJ(40) - flag for spin-orbit potential radius R_{SO} adjustment RS;
- NPJ(41) - flag for spin-orbit potential diffuseness a_{SO} constant term adjustment ASO;
- NPJ(42) - flag for spin-orbit potential diffuseness a_{SO} linear term a_{SO}^1 adjustment AS1;
- NPJ(43) - flag for equivalent charged ellipsoid radius R_C adjustment RZ;
- NPJ(44) - flag for equivalent charged ellipsoid radius R_C dispersion constant C_C adjustment RZBWC;
- NPJ(45) - flag for equivalent charged ellipsoid radius R_C dispersion width WID_C adjustment RZWID;
- NPJ(46) - flag for equivalent charged ellipsoid radius R_C diffuseness a_Z adjustment AZ;
- NPJ(47) - flag for Coulomb correction constant adjustment CCOUL;
- NPJ(48) - flag for mixture coefficient α for imaginary volume and Gaussian potentials adjustment ALF;

- NPJ(49) - flag for real potential isospin constant C_{viso} adjustment CIS0;
- NPJ(50) - flag for imaginary surface potential isospin constant C_{wiso} adjustment WCISO;
- NPJ(51) - flag for equilibrium deformation β_{20} for non-axial Hamiltonian model adjustment BETO;
- NPJ(52) - flag for equilibrium deformation β_{30} for non-axial Hamiltonian adjustment BET3;
- NPJ(53) - flag for rigid deformation β_4 for non-axial Hamiltonian model adjustment BET4;
- NPJ(54) - flag for rotational model axial rigid deformation β_{20} adjustment BET(2);
- NPJ(55) - flag for rotational model axial rigid deformation β_{40} adjustment BET(4);
- NPJ(56) - flag for rotational model axial rigid deformation β_{60} adjustment BET(6);
- NPJ(57) - flag for nuclear softness $\mu_{\beta_3} = \mu_\epsilon$ adjustment AMU0;
- NPJ(58) - flag for nuclear softness μ_{γ_0} adjustment AMGO.

Next block of cards will be read for each energy point EE(I), that means NST blocks.

- Record 13 - FORMAT(6I2)

Input of flags determining which experimental data will be used in parameters adjustment (flag = 1 means used in adjustment) for the current energy EE(I).

NT(I), NR(I), NGN(I), NGD(I), NSF1(I), NSF2(I)

- NT(I) - flag of total cross section;
- NR(I) - flag of reaction cross section;
- NGN(I) - flag of integral excitation cross section of a group of levels, number of such groups, NGN(I) must be no more than 5;
- NGD(I) - flag of angular distributions of scattered nucleons with excitation of a group of levels, number of such groups, NGD(I) must be no more than 5;
- NSF1(I) - flag of S_0 strength function;
- NSF2(I) - flag of S_1 strength function.

- Record 14 - FORMAT(4E12.7)

Experimental data for total and reaction cross sections for current energy, if flag = 0 may be blank.

STE(I), DST(I), SRE(I), DSR(I)

- STE(I) - experimental total cross section;

- **DST(I)** - experimental total cross section error;
 - **SRE(I)** - experimental reaction cross section;
 - **DSR(I)** - experimental reaction cross section error.
- Record 15 - FORMAT(4E12.7)
- Experimental data for strength functions, if **NSF1(I) = 0** this Record is not read.
- SE1(I), DS1(I), SE2(I), DS2(I)**
- **SE1(I)** - experimental S_0 strength function;
 - **DS1(I)** - experimental S_0 strength function error;
 - **SE2(I)** - experimental S_1 strength function;
 - **DS2(I)** - experimental S_1 strength function error.
- Record 16 - FORMAT(2E12.7,2I2), cards 16a, 16b, ...
- Experimental data for integral excitation of groups of levels for current energy, each card is read for the group of excited levels, that means **NGN(I)** times, if **NGN(I) = 0** - these cards are not read. Number of groups must not exceed 5.
- (SNE(I,K), DSN(I,K), NIN(I,K), NFN(I,K), K=1,NGN(I))**
- **SNE(I,K)** - experimental integral cross section of a group of levels;
 - **DSN(I,K)** - experimental integral cross section error of a group of levels;
 - **NIN(I,K)** - the number of the first excited level in a group as specified in Record 8;
 - **NFN(I,K)** - the number of the last excited level in a group as specified in Record 8.
- Record 17 - FORMAT(15I2)
- Description of experimental data for angular distributions of scattered nucleons with excitation of a group of levels, if **NGD(I) = 0**, this Record is not read. Number of groups must not exceed 5.
- (NID(I,K), NFD(I,K), MTD(I,K), K =1,NGD(I))**
- **NID(I,K)** - the number of the first excited level in a group as specified in Record 8;
 - **NFD(I,K)** - the number of the last excited level in a group as specified in Record 8;
 - **MTD(I,K)** - number of angles in which experimental angular distributions with excitation of a group of levels exist.
- Record 18 - FORMAT(6E12.7), cards 18a, 18b, ...
- Experimental angular distribution with excitation of a group of levels, this block of cards is read **NGD(I)** times, if **NGD(I)=0**, this Record is not read.
- (TED(I,K,L), SNGD(I,K,L), DSD(I,K,L), L=1,MTD(I,K))** Cards 18a, 18b,...

- **TED(I,K,L)** - center-of-mass angles for angular distribution in degrees;
 - **SNGD(I,K,L)** - experimental differential cross section in b/sr;
 - **DSD(I,K,L)** - experimental differential cross section error in b/sr.
 - Record 19 - FORMAT(6E12.7), cards 19a, 19b,...
- Estimated accuracy of parameter adjustment
 $(EP(I), I= 1, NV)$
- **EP(I)** - absolute accuracy for a parameter with i^{th} flag=1, NV is equal to a number of flags=1.
 Number of flags =1 must not exceed 20.
 - Record 20 - FORMAT(E12.7)

Initial value of χ^2 . if equal 0.000000E+00 - will start calculating of initial value χ^2 .

This is the last card in input.

10.3 Examples of Input Files

Here we are going to present two inputs. Both inputs are for optical model parameters adjustment calculations. The first one deals with the rigid-rotator model, and the second one activates the non-axial soft-rotator model. As it is described in previous chapters one who needs to get the input data set for optical model calculations without parameter adjustment must do the following simple changes in these inputs:

1. change value of variable **MEJOB** from 2 to 1 in the 2nd Record of input;
2. define variable **MTET** in Record 4;
3. if **MTET > 0** is chosen, add cards describing angles (Record 7).

10.3.1 Input for the Rigid-rotator Model

Here one can find description of actual input file, that was used for adjustment of ^{238}U optical model parameters, which is attached below.

- Card 1 - some text information.
- Card 2 - defines that a run with adjustment of optical potential parameters (**MEJOB=2**) for rigid-rotator CC-model (**MEPOT=1**) will be organized; rotational model nuclear Hamiltonian will be used to determine coupling (**MEHAM=1**); output will be the shortest (**MEPRI=0**); code will choose optimal method for coupled equations system solution (**MESOL=1**); switches **MESHA**, **MESHO**, **MEHAO** are set zero, but will be ignored as **MEPOT=1**; energy dependence of optical potential in different channels

caused by energy losses due to levels excitation is ignored in this run (**MEAPP=1**); **MEVOL** is set zero, but will be ignored as **MEPOT=1**; relativistic generalization will be taken into account (**MEREL=1**); Coulomb correction will be taken proportional to real potential derivative (**MECUL=0**); Coulomb and real potential radii will be considered energy independent (**MERZZ= MERRR=0**).

- Card 3 - defines that five levels are coupled (**NUR=5**); potential will be adjusted using experimental data at five energy points simultaneously (**NST=5**); the highest order L for radius deformation expansion is chosen to be 6 (**NPD=6**); resulting optical potential will be expanded up to Y_{80} spherical harmonic (**LAS=8**); **MTET** is set to zero, but will be ignored as **MEJOB=2**, waves with angular momentum greater than 89 will be ignored (**LLMA=89**); coupling of no more than 150 equations will be taken into account, other ignored (**NCMA=150**); no more than 180 J^π states ordered by increasing J will be taken into consideration (**NSMA=180**); coupled equations will be ordered one by one, starting with the first level, then the second and so on (**KODMA=0**).
- Card 4 - five energies, as it was stated in Card 3 (**NST=5**), in which adjustment of optical potential to experimental data will be organized in the code.
- Card 5 - five **MCHAE(I)** flags (**NST=5** in Card 3), in our case four equal to 0 (experimental data for incident neutrons) and fifth equal to 1 defining that fifth experimental data set is for incident protons.
- Cards 6-10 - excitation energies and quantum numbers of the five levels (**NUR=5** in Card 3) that should be coupled.
- Card 11 - quantities of incident particle and interacting nucleus.
- Cards 12-20 - starting set of optical potential parameters, even in case some values of the potential are equal to zero their radii and diffusenesses must be set non-zero.
- Card 21 - β_2 , β_4 and β_6 as defined by **NPD=6** on Card 3.
- Cards 22 -31 - **NPJ(I)** values; in our case only **NPJ(1)** and **NPJ(5)** are equal 1: constant and pre exponential real potential terms are to be adjusted in this run.

Next cards 32-35 apply to the experimental data used for adjustment at the first energy point.

- Card 32 - information about experimental data at the first experimental energy point ($E_n=3.0$ keV), that will be used in optical parameters adjustment; total cross section is not used in adjustment at this energy point (**NT(1)=0**); reaction cross section is not used in adjustment at this energy (**NR(1)=0**); one experimental integral scattering cross section with excitation of a group of levels will be used for adjustment (**NGN(1)=1**) and no angular distributions (**NGD(1)=0**); strength functions S_0 and S_1 will be adjusted at this energy (**NSF1(1)=NSF2(1)=1**).

- Card 33 - total and reaction cross sections and their errors at first energy; as **NT(1)** and **NR(1)** are equal to zero this card is blank.
- Card 34 - experimental S_0 and S_1 values with their errors.
- Card 35 - experimental integral scattering cross section and its error for excitation of a group of levels and **NIN(1,1)**, **NFM(1,1)** numbers of the first and last excited level in a group, in our case both equal to 1, that means experimental elastic scattering cross section is inputted for adjustment.

Next cards 36, 37 apply to the experimental data used for adjustment at the second energy point.

- Card 36 - information about experimental data at second energy point ($E_n=50.0$ keV) used for adjustment; only total cross section will be adjusted at this energy point (**NT(2)=1**), other switches are equal to zero.
- Card 37 - experimental total cross section and its error at second point, reaction cross section is blank.

Next cards 38-65 apply to the experimental data used for adjustment at the third energy point.

- Card 38 - information about experimental cross sections used for adjustment at third energy point ($E_n=3.4$ MeV); at this energy point total cross section (**NT(3)=1**) and three angular distributions with excitation of groups of levels (**NGD(3)=3**) will be adjusted.
- Card 39 - experimental total cross section with its error, reaction cross section is blank.
- Card 40 - information about experimental angular distributions: initial and final excited levels of the group and number of experimental angles (**NID(3,K)**, **NFD(3,K)**, **MTD(3,K)**, **K=1,3**); in our case **NID** and **NFD** coincide, it means that experimental angular distributions present excitations of resolved levels: first, second and third.
- Cards 41-65 - experimental angular distributions for the third energy point as angle, data, data error. Cards 41- 49 excitation of the first level, Cards 50 - 57 - second, Cards 58 - 65 - third.
- Cards 66 - 88 - description of experimental data used for adjustment of optical potential at fourth energy point ($E_n=10.0$ MeV); structure of this block of input is the same as described above with one exception: initial (**NID(4,1)=1**) and final excited levels (**NFD(4,1)=4**), so for this incident energy code will adjust results to angular distributions of neutrons scattered with excitation of the first four levels.

- Cards 89- 121 - description of experimental data used for adjustment of optical potential at the fifth energy point ($E_p=35.0$ MeV); structure of this block of input is the same as described for the third point, but with experimental data for protons (**MCHAE(5)=1** on Card 5); due to zero angle infinity of Coulomb cross-section there is no experimental total cross section data.
- Card 122 - two values of absolute accuracies for adjusted parameters as defined by **NPJ(I)** on Cards 22-31.
- Card 123 - zero (initial χ^2 is unknown).

Actual rigid-rotator input file for adjustment of ^{238}U optical model parameters

```

1 U-238      TEST      RIGID ROTATOR
2 0201010001000000010001000000
3 005005006008000089150180000
4 .3000000-02 .5000000-01 .3400000+01 .1000000+02 .3500000+02
5 0000000001
6 .0000000-0000+100
7 .4490000-0104+100
8 .1484000-0008+100
9 .3074000-0012+100
10 .5174000-0016+100
11 1.00866520 .5000000-00 .2380000+03 .9200000+02-.5479130+01-.6454370+01
12 -.4842000+02-.0000000-00 .0003381+00 .0000000+00 .9989000+02 .3752000-02
13 .0000000+01-.0000000-00 .0000000+01 .1975000+02 .1179000+02 .1758000-01
14 .0000000+01-.0000000-00 .0000000+01 .1660000+02 .9341000+02 .0000000+01
15 .6160000+01 .0030000000 .0000000+01-.0000000-00 -3.100      160.
16 .1243900+01 .0          .1000000+01 2.          .6640000-00 .3000000-03
17 .1209400+01 .5910000-00 .0000000-02 .1245700+01 .5850000+00 .0000000-02
18 .1000000+01 .1000000+01 .0000000-00 .1081300+01 .5900000-00-.0000000-02
19 .1264300+01 .00          .1000000+01 .327          0.9000      .1000000+01
20 .1300000+02 .3000000+02
21 .2220000+00 .5600000-01-.8000000-02
22 010000000100
23 000000000000
24 000000000000
25 000000000000
26 000000000000
27 000000000000
28 000000000000

```

```

29  0000000000000
30  0000000000000
31  00000000
32  000001000101
33  .0000000-00 .0000000-00 .0000000-00 .0000000-00
34  .1080000-03 .8700000-05 .2000000-03 .5000000-04
35  .1134000+02 .6000000-00 1 1
36  010000000000
37  .1315000+02 .2500000-00 .0000000-00 .0000000-00
38  010000030000
39  .8040000+01 .8000000-01 .0000000-00 .0000000-00
40  010118020216030315
41  .2010000+02 .2866800+01 .1749000-00 .3010000+02 .1540100+01 .9580000-01
42  .4020000+02 .3096000-00 .2390000-01 .4520000+02 .1443000-00 .1170000-01
43  .5020000+02 .2730000-01 .3400000-02 .6020000+02 .3670000-01 .5400000-02
44  .6520000+02 .8420000-01 .8200000-02 .8020000+02 .1135000-00 .1220000-01
45  .8520000+02 .1052000-00 .9800000-02 .9020000+02 .8700000-01 .8700000-02
46  .1002000+03 .3300000-01 .4200000-02 .1052000+03 .2660000-01 .3600000-02
47  .1102000+03 .1030000-01 .1900000-02 .1202000+03 .2100000-02 .7000000-03
48  .1302000+03 .5400000-02 .1500000-02 .1402000+03 .1410000-01 .2700000-02
49  .1501000+03 .2420000-01 .3700000-02 .1601000+03 .3350000-01 .4400000-02
50  .4020000+02 .8160000-01 .9700000-02 .4520000+02 .6130000-01 .6600000-02
51  .5020000+02 .4530000-01 .6200000-02 .6020000+02 .3590000-01 .5900000-02
52  .6520000+02 .4330000-01 .5100000-02 .8020000+02 .5070000-01 .7400000-02
53  .8520000+02 .4970000-01 .5800000-02 .9020000+02 .5230000-01 .5800000-02
54  .1002000+03 .3010000-01 .4100000-02 .1052000+03 .1980000-01 .3100000-02
55  .1102000+03 .1660000-01 .2800000-02 .1202000+03 .9800000-02 .2100000-02
56  .1302000+03 .3400000-01 .4600000-02 .1402000+03 .4240000-01 .5200000-02
57  .1501000+03 .2780000-01 .3900000-02 .1601000+03 .1930000-01 .3100000-02
58  .4020000+02 .2190000-01 .4500000-02 .4520000+02 .2220000-01 .3500000-02
59  .5020000+02 .1580000-01 .3500000-02 .6020000+02 .1220000-01 .3300000-02
60  .6520000+02 .9900000-02 .2100000-02 .8020000+02 .9000000-02 .2800000-02
61  .8520000+02 .9900000-02 .2200000-02 .9020000+02 .1010000-01 .2600000-02
62  .1052000+03 .9700000-02 .2200000-02 .1102000+03 .8400000-02 .2000000-02
63  .1202000+03 .6800000-02 .1800000-02 .1302000+03 .6600000-02 .1700000-02
64  .1402000+03 .4800000-02 .1500000-02 .1501000+03 .3900000-02 .1300000-02
65  .1601000+03 .3100000-02 .1100000-02
66  010100010000
67  .5870000+01 .1000000-00 .2800000+01 .1500000-00
68  010440
69  .1786000E+02.2061000E+01.8244000E-01.2181000E+02.8312000E+00.3324800E-01

```

```

70 .2578000E+02.3177000E+00.1270800E-01.2776000E+02.2454000E+00.9816000E-02
71 .2865000E+02.1943000E+00.7772000E-02.3194000E+02.2153000E+00.8611999E-02
72 .3592000E+02.2857000E+00.1142800E-01.3871000E+02.3030000E+00.1212000E-01
73 .4369000E+02.2352000E+00.9408000E-02.4718000E+02.1562000E+00.6248000E-02
74 .5117000E+02.9487000E-01.3794800E-02.5416000E+02.5911000E-01.2364400E-02
75 .5915000E+02.6205000E-01.2482000E-02.6264000E+02.8345000E-01.3338000E-02
76 .6664000E+02.1043000E+00.4172000E-02.6963000E+02.1132000E+00.4528000E-02
77 .7562000E+02.9620000E-01.3848000E-02.7862000E+02.7150000E-01.2860000E-02
78 .8261000E+02.4671000E-01.1868400E-02.8561000E+02.3355000E-01.1500021E-02
79 .9110000E+02.2740000E-01.1499876E-02.9409000E+02.2678000E-01.1499948E-02
80 .9809000E+02.3055000E-01.1500005E-02.1011000E+03.3392000E-01.1499942E-02
81 .1066000E+03.3063000E-01.1499951E-02.1096000E+03.2543000E-01.1500116E-02
82 .1136000E+03.2277000E-01.1500088E-02.1166000E+03.1894000E-01.1500048E-02
83 .1225000E+03.1651000E-01.1499934E-02.1255000E+03.1301000E-01.1500053E-02
84 .1290000E+03.9657000E-02.1499732E-02.1320000E+03.9843000E-02.1500073E-02
85 .1385000E+03.9784000E-02.1499887E-02.1415000E+03.1301000E-01.1500053E-02
86 .1445000E+03.1380000E-01.1500060E-02.1475000E+03.1735000E-01.1500081E-02
87 .1485000E+03.1414000E-01.1500254E-02.1514000E+03.1517000E-01.1500009E-02
88 .1544000E+03.1167000E-01.1499595E-02.1574000E+03.1087000E-01.1500060E-02
89 000000030000
90 .5950000+01 .1000000-00 .0000000-00 .0000000-00
91 020221030320040418
92 .2200000E+02.7000000E-01.1120000E-01.2690000E+02.2750000E-01.4400000E-02
93 .3040000E+02.1620000E-01.1620000E-02.3650000E+02.2360000E-01.2360000E-02
94 .4190000E+02.1660000E-01.1660000E-02.4700000E+02.7500000E-02.8250000E-03
95 .5210000E+02.7600000E-02.6840000E-03.5650000E+02.7700000E-02.6930000E-03
96 .6020000E+02.4000000E-02.4000000E-03.6700000E+02.2340000E-02.2340000E-03
97 .7000000E+02.3090000E-02.3090000E-03.7640000E+02.2710000E-02.2710000E-03
98 .8330000E+02.1420000E-02.1420000E-03.8680000E+02.9600000E-03.8640000E-04
99 .9000000E+02.9700001E-03.8730000E-04.9630000E+02.9800000E-03.8820000E-04
100 .9980000E+02.6300000E-03.6300000E-04.1034000E+03.3900000E-03.3900000E-04
101 .1099000E+03.3500000E-03.3150000E-04.1162000E+03.3900000E-03.3900000E-04
102 .1196000E+03.2700000E-03.2700000E-04
103 .2570000E+02.1810000E-02.3801000E-03.3090000E+02.1490000E-02.2235000E-03
104 .3600000E+02.6800001E-03.1088000E-03.3930000E+02.6100000E-03.6100000E-04
105 .4550000E+02.7600000E-03.6840000E-04.4890000E+02.5400000E-03.4860000E-04
106 .5580000E+02.2860000E-03.2860000E-04.6070000E+02.3700000E-03.4070000E-04
107 .6510000E+02.4300000E-03.3870000E-04.7010000E+02.2960000E-03.2960000E-04
108 .7530000E+02.1770000E-03.1770000E-04.8160000E+02.1950000E-03.1950000E-04
109 .8800000E+02.2080000E-03.2080000E-04.9130000E+02.1610000E-03.1610000E-04
110 .9500000E+02.9100000E-04.9100000E-05.1001000E+03.9300001E-04.9300001E-05

```

```

111 .1045000E+03.9900000E-04.9900000E-05.1109000E+03.1000000E-03.1000000E-04
112 .1144000E+03.6500000E-04.5850000E-05.1177000E+03.5300000E-04.4770000E-05
113 .3430000E+02.8600001E-04.1118000E-04.4060000E+02.1030000E-03.1648000E-04
114 .4540000E+02.1000000E-03.2300000E-04.5020000E+02.9200000E-04.1380000E-04
115 .5570000E+02.5300000E-04.4770000E-05.6060000E+02.3200000E-04.4160001E-05
116 .6670000E+02.4600000E-04.5060000E-05.6970000E+02.5500000E-04.4950000E-05
117 .7610000E+02.5600000E-04.5040000E-05.7970000E+02.3300000E-04.2970000E-05
118 .8630000E+02.2550000E-04.4080000E-05.9260000E+02.2580000E-04.2580000E-05
119 .9570000E+02.2960000E-04.2960000E-05.9920000E+02.2000000E-04.2200000E-05
120 .1044000E+03.1760000E-04.2816000E-05.1090000E+03.1490000E-04.1937000E-05
121 .1141000E+03.1560000E-04.2496000E-05.1185000E+03.1580000E-04.1422000E-05
122 .5000000E-02.5000000E-02.
123 0.0

```

10.3.2 Input for the Soft-rotator Model

Input for the soft-rotator model is similar to that for the rigid-rotator model. So we have no need to repeat all the details that can be found by reading the input description for the rigid-rotator model. All the changes are found in the first 21 cards of the input shown below. So we describe them here, although most of them have the same meanings for both models.

- Card 1 - some text information.
- Card 2 - defines that a run with adjustment of optical potential parameters (**MEJOB=2**) for soft-rotator CC-model (**MEPOT=2**) will be organized, nuclear non-axial Hamiltonian with account of β and γ softness will be used to determine coupling (**MEHAM=5**); output will be the shortest (**MEPRI=0**); iteration method with wave functions from spherical calculations as zero approximation for coupled equations system solution will be used (**MESOL=3**); rigid hexadecapole deformations will be taken into account in the most common way (**MESHA=4**), with non-axial octupole deformations (**MESH0=2**) which are soft, symmetric and scaled by β_2 (**MEHA0=2**); energy dependence of optical potential in different channels caused by energy losses due to levels excitation will be taken into account in this run (**MEAPP=0**); nuclear volume conservation is not taken into account (**MEVOL=0**); relativistic generalization will be taken into account (**MEREL=1**); Coulomb correction will be taken proportional to real potential derivative (**MECUL=0**); Coulomb and real potential radii will be considered energy independent (**MERZZ= MERRR=1**).
- Cards 3-5 - (**Attention! These Cards do not present in input for rigid-rotator**) parameters of nuclear Hamiltonian as described in Chapter IV
- Card 6 - defines that five levels (**NUR=5**) will be coupled; potential will be adjusted using experimental data at two energy points simultaneously (**NST=2**); **NPD=4** is not in use for this case; deformed

optical potential will be expanded by derivatives up to the fourth power (**LAS=4**); **MTET=0** is not in use for this case; waves with angular momentum greater than 50 will be ignored (**LLMA=50**); coupling of no more than 100 equations will be taken into account, other ignored (**NCMA=100**); no more than 100 J^π states ordered by increasing J will be taken into consideration (**NSMA=100**); coupled equations will be ordered one by one, by increasing angular momentum, total number no more than **NCMA=100** (**KODMA=1**).

- Card 7 - two energy points, as it was stated in Card 6 (**NST=2**), in which adjustment of optical potential to experimental data will be organized in the code.
- Card 8 - two **MCHAE(I)** flags (**NST=2**, in Card 3), in our case one flag equal to 0 and one flag - to 1 that means experimental data for incident neutrons in the first energy point and for protons in the second point will be used for adjustment.
- Cards 9-13 - energies and quantum numbers of the five levels (**NUR=5** in Card 6) that should be coupled.
- Card 14 - quantities of incident particle and interacting nucleus.
- Cards 15-23 - starting set of optical potential parameters, even in case some values of the potential are equal to zero their radii and diffusenesses must be set non-zero.

Attention

As comparing with rigid-rotator input, the card related with rigid radius deformations (Record 11) is not needed in this input (deformations are already determined in nuclear Hamiltonian parameter part of input).

- Cards 24 -... - input of **NPJ(I)**, experimental data, accuracy of adjusted parameters and initial χ^2 are as explained in rigid-rotator input.

Soft-rotator model input for adjustment of ^{12}C optical model parameters

```

1 C-12 OCTUPOLE CALCULATION bet3=ksi*bet2
2 0202050003040202000001000101
3 0.42825E+01 0.27943E+01 0.11860E+00 0.32107E+00 0.16400E+00 0.12600E+00
4 0.14694E+00 0.21419E-03 0.52045E+00 0.24200E+00 0.21005E-01 0.83263E+00
5 0.35000E+00 0.22130E+00 0.00000E+00 0.17221E+01 0.00000E+00
6 005002004004000050100100001
7 .2090000+02 .3970000+02
8 0001
9 .0000000-0000+101000000
10 .4440000+0104+101000000

```

```

11 .9640000+0106-101000001
12 .7650000+0100+101010000
13 .1780000+0204+102000000
14 1.00866520 .5000000-00 .1200000+02 .6000000+01-.1183500+02-.8950000+01
15 -.3094000+02-.0000000-00 .0002381+00 .3000000-06 .8630000+02 .4532000-02
16 .0000000+01-.0000000-00 .0000000+01 .9530000+01 .1533000+02 .1755000-01
17 .0000000+01-.0000000-00 .0000000+01 .1909000+02 .9429000+02 .0000000+01
18 .7840000+01 .0030000000 .0000000+01-.0000000-00 -3.100 160.
19 .1150000+01 .10 .5000000+02 2. .5190000-00 .2600000-02
20 .1072600+01 .4460000-00 .0000000-02 .1039700+01 .4570000+00 .0000000-02
21 .1000000+01 .1000000+01 .0000000-00 .1086300+01 .6050000-00-.0000000-02
22 .1145300+01 .00 .1000000+01 .680 1.1000 .1000000+01
23 .1300000+02 .3000000+02
24 0000000000000
25 0000000000000
26 0000000000000
27 0000000000000
28 0001000000000
29 0000000000000
30 0000000000000
31 0000000000000
32 0000000000000
33 0000000000000
34 010000030000
35 .1450000+01 .5000000-01 .0000000-00 .0000000-00
36 010134040432030332
37 0.10827E+02 0.10147E+01 0.87000E-02 0.13542E+02 0.90149E+00 0.70600E-02
38 0.16240E+02 0.80964E+00 0.65300E-02 0.18933E+02 0.71743E+00 0.60400E-02
39 0.21627E+02 0.62305E+00 0.55300E-02 0.27013E+02 0.44466E+00 0.40300E-02
40 0.32382E+02 0.29082E+00 0.31600E-02 0.37740E+02 0.17096E+00 0.23500E-02
41 0.43072E+02 0.96560E-01 0.15800E-02 0.48371E+02 0.50840E-01 0.95000E-03
42 0.53658E+02 0.28660E-01 0.85000E-03 0.58909E+02 0.19560E-01 0.70000E-03
43 0.64132E+02 0.20350E-01 0.67000E-03 0.69329E+02 0.20790E-01 0.66000E-03
44 0.74484E+02 0.23150E-01 0.67000E-03 0.79613E+02 0.23510E-01 0.66000E-03
45 0.84704E+02 0.21420E-01 0.64000E-03 0.89759E+02 0.18060E-01 0.49000E-03
46 0.94778E+02 0.13980E-01 0.44000E-03 0.99759E+02 0.11060E-01 0.42000E-03
47 0.10470E+03 0.83900E-02 0.37000E-03 0.10962E+03 0.65800E-02 0.24000E-03
48 0.11449E+03 0.50900E-02 0.23000E-03 0.11933E+03 0.40400E-02 0.19000E-03
49 0.12413E+03 0.30700E-02 0.19000E-03 0.12891E+03 0.25000E-02 0.17000E-03
50 0.13365E+03 0.20000E-02 0.18000E-03 0.13837E+03 0.21400E-02 0.18000E-03
51 0.14306E+03 0.15000E-02 0.20000E-03 0.14774E+03 0.10900E-02 0.19000E-03

```

52 0.15239E+03 0.95000E-03 0.26000E-03 0.15701E+03 0.61000E-03 0.31000E-03
 53 0.16164E+03 0.39000E-03 0.25000E-03 0.16164E+03 0.39000E-03 0.25000E-03
 54 0.13842E+02 0.29590E-02 0.47900E-03 0.16605E+02 0.23700E-02 0.42900E-03
 55 0.19365E+02 0.14010E-02 0.41100E-03 0.22121E+02 0.15670E-02 0.30700E-03
 56 0.27621E+02 0.12020E-02 0.22400E-03 0.33102E+02 0.64200E-03 0.27400E-03
 57 0.38559E+02 0.63200E-03 0.22500E-03 0.43989E+02 0.70800E-03 0.21300E-03
 58 0.49388E+02 0.60200E-03 0.15300E-03 0.54755E+02 0.10990E-02 0.20400E-03
 59 0.60086E+02 0.80300E-03 0.18700E-03 0.65377E+02 0.46700E-03 0.18000E-03
 60 0.70628E+02 0.45100E-03 0.17000E-03 0.75836E+02 0.38700E-03 0.17800E-03
 61 0.81000E+02 0.31000E-03 0.15200E-03 0.86118E+02 0.12600E-03 0.15700E-03
 62 0.91189E+02 0.25700E-03 0.11400E-03 0.96212E+02 0.20400E-03 0.12500E-03
 63 0.10119E+03 0.12100E-03 0.11300E-03 0.10612E+03 0.18600E-03 0.12900E-03
 64 0.11100E+03 0.23100E-03 0.92000E-04 0.11584E+03 0.31000E-03 0.10500E-03
 65 0.12063E+03 0.17800E-03 0.75000E-04 0.12538E+03 0.27600E-03 0.82000E-04
 66 0.13009E+03 0.34700E-03 0.72000E-04 0.13475E+03 0.13900E-03 0.75000E-04
 67 0.13939E+03 0.13800E-03 0.73000E-04 0.14399E+03 0.21900E-03 0.78000E-04
 68 0.14856E+03 0.15000E-03 0.65000E-04 0.15310E+03 0.65000E-04 0.65000E-04
 69 0.15762E+03 0.12600E-03 0.86000E-04 0.16212E+03 0.71000E-04 0.82000E-04
 70 0.13974E+02 0.36200E-02 0.48200E-03 0.16762E+02 0.30630E-02 0.44900E-03
 71 0.19548E+02 0.27490E-02 0.43600E-03 0.22329E+02 0.29090E-02 0.31600E-03
 72 0.27879E+02 0.28430E-02 0.26000E-03 0.33406E+02 0.28360E-02 0.32000E-03
 73 0.38908E+02 0.29460E-02 0.28800E-03 0.44381E+02 0.30690E-02 0.26800E-03
 74 0.49820E+02 0.28310E-02 0.20000E-03 0.55223E+02 0.29870E-02 0.25400E-03
 75 0.60586E+02 0.29870E-02 0.24000E-03 0.65907E+02 0.28150E-02 0.24700E-03
 76 0.71182E+02 0.27230E-02 0.24100E-03 0.76411E+02 0.25810E-02 0.24700E-03
 77 0.81591E+02 0.31060E-02 0.23100E-03 0.86720E+02 0.27670E-02 0.23700E-03
 78 0.91798E+02 0.30100E-02 0.18700E-03 0.96825E+02 0.30220E-02 0.19600E-03
 79 0.10180E+03 0.27050E-02 0.18500E-03 0.10672E+03 0.22630E-02 0.18800E-03
 80 0.11159E+03 0.21140E-02 0.13100E-03 0.11641E+03 0.21620E-02 0.13600E-03
 81 0.12118E+03 0.17140E-02 0.11200E-03 0.12591E+03 0.17950E-02 0.11800E-03
 82 0.13059E+03 0.16680E-02 0.10900E-03 0.13522E+03 0.15900E-02 0.11100E-03
 83 0.13982E+03 0.11750E-02 0.10800E-03 0.14438E+03 0.11300E-02 0.10500E-03
 84 0.14891E+03 0.10670E-02 0.86000E-04 0.15341E+03 0.10600E-02 0.87000E-04
 85 0.15788E+03 0.10160E-02 0.10100E-03 0.16233E+03 0.89100E-03 0.98000E-04
 86 000000030000
 87 .1350000+01 .5000000-01 .0000000-00 .0000000-00
 88 020209040407030306
 89 .5774566E+01.1879471E-01.1879471E-02.6972687E+01.2377528E-01.2139775E-02
 90 .9912569E+01.2059393E-01.1853454E-02.1567775E+02.1823039E-01.1640735E-02
 91 .2143210E+02.1585695E-01.1427126E-02.2727986E+02.1539024E-01.1385121E-02
 92 .3300065E+02.1416826E-01.1416826E-02.4330416E+02.1139910E-01.1367892E-02

```

93 .5467881E+02.6200595E-02.1240119E-02
94 .1137750E+02.3348969E-02.6697937E-03.1574669E+02.1584991E-02.3169983E-03
95 .2152556E+02.7339561E-03.1467912E-03.2739751E+02.5179655E-03.1087728E-03
96 .3314104E+02.5194567E-03.1090859E-03.3778394E+02.5724197E-03.1202081E-03
97 .4348261E+02.6105253E-03.1282103E-03
98 .1579547E+02.1139016E-02.1366819E-03.2159170E+02.2071540E-02.2485848E-03
99 .2748077E+02.2372577E-02.2847093E-03.3324040E+02.2757822E-02.3309386E-03
100 .3789575E+02.3156208E-02.3787449E-03.4360892E+02.3189772E-02.3827726E-03
101 .500000-02 .500000-03 .500000-03 .500000-03 .500000-03 .500000-03
102 0.0

```

10.4 User-friendly Input Interface

In previous subsection we gave complete instructions for organizing OPTMAN code's input. Running code BEGIN, which is written as a user-friendly input interface for OPTMAN code, may be much more convenient when one organises input. After running BEGIN, the user will get OPTMAN code input file checked to be free of inconsistencies and format errors. It will also add some useful head-line comments, helping to understand the input, to each Record (except to Records 1 and 18) of initial input file in position beyond occupied by input format. If initial file has some comments in free positions beyond format - they will be also saved in modernized one, when typed in figure brackets and having no more than 80 symbols, otherwise the comment will be missed and warning !WRONG COMMENT! will be added to that line (except for any comments in Record 18, which are always saved).

Attention

One should put symbol * to run BEGIN code, for the purposes of analysing the input file against consistency check with OPTMAN code's input format, at the second column after the last requested by data input format in the last card of the each input record.

Starting, this code will ask the user to choose between two possible options:

- EXPERT - this option is to be used, when you already organized OPTMAN code input, which has some problems while running. If this option is activated input file will be checked for selfconsistency and give recommendations for corrections if necessary. You will be suggested to make corrections in input file and continue checking. After EXPERT input interface checking options finished code organizes modernized input file - `optman.inp`, which includes corrections.
 - BEGINNER - this option will help to organize OPTMAN code input while interactive dialog. If this option is activated one must follow on screen instructions choosing OPTMAN code options from suggestions, having preliminary prepared files with:
1. nuclear Hamiltonian parameters (in case of non-axial nuclei) - Record 3;

2. energies in which optical model calculations will be carried out - Record 5;
3. flags determining charge of incident particles for determined energies - Record 6;
4. angles in which angular distributions of scattered particles will be calculated (necessary for **MEJOB=1, MTET>0** case) - Record 7;
5. characteristics of nuclear levels (FORMAT according with **MEHAM** value) - Record 8;
6. characteristics of interacting incident particle and nuclei - Record 9;
7. optical potential parameters - Record 10;
8. deformations $\beta_{\lambda 0}$ from β_{20} to $\beta_{\lambda 0}$, $\lambda=NPD$. This file is necessary for axial rotator model (**MEHAM = 1**) case - Record 11;
9. flags for model parameters adjustment - Record 12;
10. experimental data used for parameters adjustment - Records 13-18;
11. absolute accuracy of parameters adjustment - Record 19.

Note that Records 1, 2, 4, 20 are created using on screen interactive dialog and necessary symbol * will be added by the code.

All these files will be checked to be consistent with the chosen codes option keys and input formats and you will be suggested possible changes for corrections if necessary. After corrections, code check them and continue corrections. After the **BEGINNER** input building option interface run is finished, code organizes input file - **optman.inp** including corrections made.

For both options code will also create protocol file - **inform.out** describing details of calculations with organized input.

Below we show an example of the input file, prepared to be checked, using **EXPERT** option of user-friendly interface. To prepare such a file by using an input file for the soft-rotator model, we added * at the second column after the last data in the last card of each record (see previous screen comment), and added some comments in positions beyond occupied by record format (to demonstrate how it works with comments). Input file after checking - **optman.inp** and protocol file - **inform.out** are also shown.

Input file for checking

```

1 C-12 OCTUPOLE CALCULATION bet3=ksi*bet2
2 2 2 5 0 1 4 2 2 0 0 1 0 1 1 *
3 4.282500+00 2.794300+00 1.186000-01 3.210700-01 1.640000-01 1.260000-01 parameters of non-axial
4 1.469400-01 2.141900-04 5.204500-01 2.420000-01 2.100500-02 8.326300-01 nuclear Hamiltonian
5 3.500000-01 2.213000-01 0.000000+00 1.722100+00 0.000000+00 *
6 5 2 0 4 0 50100100 1 *
7 2.090000+01 3.970000+01 *

```

```

8   0 1 *
9   0.000000+00 0 1 1 0 0 0                                { 5 LEVELS }
10  4.440000+00 4 1 1 0 0 0
11  9.640000+00 6-1 1 0 0 1
12  7.650000+00 0 1 1 1 0 0
13  1.780000+01 4 1 2 0 0 0 *
14  1.008665+00 5.000000-01 1.200000+01 6.000000+00-1.183500+01-8.950000+00 *
15  -3.094000+01 0.000000+00 2.381000-04 3.000000-07 8.630000+01 4.532000-03
16  0.000000+00 0.000000+00 0.000000+00 9.530000+00 1.533000+01 1.755000-02
17  0.000000+00 0.000000+00 0.000000+00 1.909000+01 9.429000+01 0.000000+00
18  7.840000+00 3.000000-03 0.000000+00 0.000000+00-3.100000+00 1.600000+02
19  1.150000+00 1.000000-01 5.000000+01 2.000000+00 5.190000-01 2.600000-03
20  1.072600+00 4.460000-01 0.000000+00 1.039700+00 4.570000-01 0.000000+00
21  1.000000+00 1.000000+00 0.000000+00 1.086300+00 6.050000-01 0.000000+00
22  1.145300+00 0.000000+00 1.000000+00 6.800000-01 1.100000+00 1.000000+00
23  1.300000+01 3.000000+01 *
24  0 0 0 0 0 0
25  0 0 0 0 0 0
26  0 0 0 0 0 0
27  0 0 0 0 0 0
28  0 1 0 0 0 0          NPJ(26) adjusted          { RRBWC adjustment  }
29  0 0 0 0 0 0
30  0 0 0 0 0 0
31  0 0 0 0 0 0
32  0 0 0 0 0 0
33  0 0 0 0 *
34  1 0 0 3 0 0 *
35  1.450000+00 5.000000-02 0.000000+00 0.000000+00 *
36  1 134 4 432 3 332 *
37  1.082700+01 1.014700+00 8.700000-03 1.354200+01 9.014900-01 7.060000-03
38  1.624000+01 8.096400-01 6.530000-03 1.893300+01 7.174300-01 6.040000-03
39  2.162700+01 6.230500-01 5.530000-03 2.701300+01 4.446600-01 4.030000-03
40  3.238200+01 2.908200-01 3.160000-03 3.774000+01 1.709600-01 2.350000-03      neutron angular 0+
41  4.307200+01 9.656000-02 1.580000-03 4.837100+01 5.084000-02 9.500000-04
42  5.365800+01 2.866000-02 8.500000-04 5.890900+01 1.956000-02 7.000000-04
43  6.413200+01 2.035000-02 6.700000-04 6.932900+01 2.079000-02 6.600000-04
44  7.448400+01 2.315000-02 6.700000-04 7.961300+01 2.351000-02 6.600000-04
45  8.470400+01 2.142000-02 6.400000-04 8.975900+01 1.806000-02 4.900000-04
46  9.477800+01 1.398000-02 4.400000-04 9.975900+01 1.106000-02 4.200000-04
47  1.047000+02 8.390000-03 3.700000-04 1.096200+02 6.580000-03 2.400000-04
48  1.144900+02 5.090000-03 2.300000-04 1.193300+02 4.040000-03 1.900000-04

```

```

49  1.241300+02 3.070000-03 1.900000-04 1.289100+02 2.500000-03 1.700000-04
50  1.336500+02 2.000000-03 1.800000-04 1.383700+02 2.140000-03 1.800000-04
51  1.430600+02 1.500000-03 2.000000-04 1.477400+02 1.090000-03 1.900000-04
52  1.523900+02 9.500000-04 2.600000-04 1.570100+02 6.100000-04 3.100000-04
53  1.616400+02 3.900000-04 2.500000-04 1.616400+02 3.900000-04 2.500000-04 *
54  1.384200+01 2.959000-03 4.790000-04 1.660500+01 2.370000-03 4.290000-04      neutron angular second 0+
55  1.936500+01 1.401000-03 4.110000-04 2.212100+01 1.567000-03 3.070000-04
56  2.762100+01 1.202000-03 2.240000-04 3.310200+01 6.420000-04 2.740000-04
57  3.855900+01 6.320000-04 2.250000-04 4.398900+01 7.080000-04 2.130000-04
58  4.938800+01 6.020000-04 1.530000-04 5.475500+01 1.099000-03 2.040000-04
59  6.008600+01 8.030000-04 1.870000-04 6.537700+01 4.670000-04 1.800000-04
60  7.062800+01 4.510000-04 1.700000-04 7.583600+01 3.870000-04 1.780000-04
61  8.100000+01 3.100000-04 1.520000-04 8.611800+01 1.260000-04 1.570000-04
62  9.118900+01 2.570000-04 1.140000-04 9.621200+01 2.040000-04 1.250000-04
63  1.011900+02 1.210000-04 1.130000-04 1.061200+02 1.860000-04 1.290000-04
64  1.110000+02 2.310000-04 9.200000-05 1.158400+02 3.100000-04 1.050000-04
65  1.206300+02 1.780000-04 7.500000-05 1.253800+02 2.760000-04 8.200000-05
66  1.300900+02 3.470000-04 7.200000-05 1.347500+02 1.390000-04 7.500000-05
67  1.393900+02 1.380000-04 7.300000-05 1.439900+02 2.190000-04 7.800000-05
68  1.485600+02 1.500000-04 6.500000-05 1.531000+02 6.500000-05 6.500000-05
69  1.576200+02 1.260000-04 8.600000-05 1.621200+02 7.100000-05 8.200000-05 *
70  1.397400+01 3.620000-03 4.820000-04 1.676200+01 3.063000-03 4.490000-04 neutron angular 3-
71  1.954800+01 2.749000-03 4.360000-04 2.232900+01 2.909000-03 3.160000-04
72  2.787900+01 2.843000-03 2.600000-04 3.340600+01 2.836000-03 3.200000-04
73  3.890800+01 2.946000-03 2.880000-04 4.438100+01 3.069000-03 2.680000-04
74  4.982000+01 2.831000-03 2.000000-04 5.522300+01 2.987000-03 2.540000-04
75  6.058600+01 2.987000-03 2.400000-04 6.590700+01 2.815000-03 2.470000-04
76  7.118200+01 2.723000-03 2.410000-04 7.641100+01 2.581000-03 2.470000-04
77  8.159100+01 3.106000-03 2.310000-04 8.672000+01 2.767000-03 2.370000-04
78  9.179800+01 3.010000-03 1.870000-04 9.682500+01 3.022000-03 1.960000-04
79  1.018000+02 2.705000-03 1.850000-04 1.067200+02 2.263000-03 1.880000-04
80  1.115900+02 2.114000-03 1.310000-04 1.164100+02 2.162000-03 1.360000-04
81  1.211800+02 1.714000-03 1.120000-04 1.259100+02 1.795000-03 1.180000-04
82  1.305900+02 1.668000-03 1.090000-04 1.352200+02 1.590000-03 1.110000-04
83  1.398200+02 1.175000-03 1.080000-04 1.443800+02 1.130000-03 1.050000-04
84  1.489100+02 1.067000-03 8.600000-05 1.534100+02 1.060000-03 8.700000-05
85  1.578800+02 1.016000-03 1.010000-04 1.623300+02 8.910000-04 9.800000-05 *
86  0 0 0 3 0 0 *
87  1.350000+00 5.000000-02 0.000000+00 0.000000+00 *
88  2 2 9 4 4 7 3 3 6 *
89  5.774566+00 1.879471-02 1.879471-03 6.972687+00 2.377528-02 2.139775-03      proton angular 2+

```

```

90  9.912569+00 2.059393-02 1.853454-03 1.567775+01 1.823039-02 1.640735-03
91  2.143210+01 1.585695-02 1.427126-03 2.727986+01 1.539024-02 1.385121-03
92  3.300065+01 1.416826-02 1.416826-03 4.330416+01 1.139910-02 1.367892-03
93  5.467881+01 6.200595-03 1.240119-03 *
94  1.137750+01 3.348969-03 6.697937-04 1.574669+01 1.584991-03 3.169983-04
95  2.152556+01 7.339561-04 1.467912-04 2.739751+01 5.179655-04 1.087728-04
96  3.314104+01 5.194567-04 1.090859-04 3.778394+01 5.724197-04 1.202081-04
97  4.348261+01 6.105253-04 1.282103-04 *
98  1.579547+01 1.139016-03 1.366819-04 2.159170+01 2.071540-03 2.485848-04 proton angular 3-
99  2.748077+01 2.372577-03 2.847093-04 3.324040+01 2.757822-03 3.309386-04
100 3.789575+01 3.156208-03 3.787449-04 4.360892+01 3.189772-03 3.827726-04 *
101 5.000000-03 *
102 0.000000+00 *

```

Input file after checking

```

1 C-12 OCTUPOLE CALCULATION bet3=ksi*bet2
2 2 2 5 0 1 4 2 2 0 0 1 0 1 1 *
3 4.282500+00 2.794300+00 1.186000-01 3.210700-01 1.640000-01 1.260000-01 / HE(JOB,POT,MAH,PEI,SOL,SHA,SHO,HAO,APP,VOL,REL,CUL,EZZ,EEB) /
4 1.469400-01 2.141900-04 5.204500-01 2.420000-01 2.100500-02 8.326300-01 / nucl. Nam. param: NW,AHBO,ANG0,GAHO,BETO,BET4 / ! WRONG CORRECTION !
5 3.500000-01 2.213000-01 0.000000+00 1.722100+00 0.000000+00 * / nucl. Nam. param: NW0,BB32,GARDE,DPAE,GSHAPE /
6 5 2 0 4 0 50100100 1 * / NW,E,BST,PPD,LAS,HTET,LLHA,WCHA,WSHA,KODHA /
7 2.090000+01 3.970000+01 * / energies EE(I),I=1,BST /
8 0 1 * / HCHAE(I),I=1,BST /
9 0.000000+00 0 1 1 0 0 0 / Characteristics of nuclear levels ( HEWAH>1 ) / { 5 LEVELS }
10 4.440000+00 4 1 1 0 0 0
11 9.640000+00 6-1 1 0 0 1
12 7.650000+00 0 1 1 1 0 0
13 1.780000+01 4 1 2 0 0 0 *
14 1.008665+00 5.000000-01 1.200000+01 6.000000+00-1.183500+01-8.950000+00 * / ADE0,ASP,AT,ZBUC,EFEHH,EFEHMP /
15 -3.094000+01 0.000000+00 2.381000-04 3.000000-07 8.630000+01 4.532000-03 / optic. poten. param.: VEO,VE1,VE2,VE3,VELA,ALAVB /
16 0.000000+00 0.000000+00 0.000000+00 9.530000+00 1.533000+01 1.755000-02 / optic. poten. param.: WDO,WD1,WDA1,WDBW,WWDWID,ALAWD /
17 0.000000+00 0.000000+00 0.000000+00 1.909000+01 9.429000+01 0.000000+00 / optic. poten. param.: WCO,WCA1,WCA1,WCBW,WCHID,BBDC /
18 7.840000+00 3.000000-03 0.000000+00 0.000000+00-3.100000+01 1.600000+02 / optic. poten. param.: VS,ALASO,WSD,WS1,WSBW,WSHID /
19 1.150000+00 1.000000-01 5.000000+01 2.000000+00-1.519000-01 2.600000-03 / optic. poten. param.: EZ,EBBWC,EBWID,PDIS,AR0,AR1 /
20 1.072600+00 4.460000-01 0.000000+00 1.039700+00 4.570000-01 0.000000+00 / optic. poten. param.: RD,ADO,AD1,EC,ACO,AC1 /
21 1.000000+00 1.000000+00 0.000000+00 1.086300+00 6.050000-01 0.000000+00 / optic. poten. param.: EW,AHO,AH1,ES,AS0,AS1 /
22 1.145300+00 0.000000+00 1.000000+00 6.800000-01 1.100000+00 1.000000+00 / optic. poten. param.: EZ,EZBWC,EZHID,AZ,CCOUL,ALF /
23 1.300000+01 3.000000+01 * / optic. poten. param.: CIS0,WCI0 /
24 0 0 0 0 0 0 / flags for adjust. param.: VEO,VE1,VE2,VE3,VELA,ALAVB /
25 0 0 0 0 0 0 / flags for adjust. param.: WDO,WD1,WDA1,WDBW,WWDWID /
26 0 0 0 0 0 0 / flags for adjust. param.: WCO,WCA1,WCA1,WCBW,WCHID /
27 0 0 0 0 0 0 / flags for adjust. param.: VS,ALASO,WSD,WS1,WSBW,WSHID /
28 0 1 0 0 0 0 / flags for adjust. param.: EZ,EBBWC,EBWID,PDIS,AR0,AR1 / { EBBWC adjustment } + ! WRONG CORRECTION !
29 0 0 0 0 0 0 / flags for adjust. param.: RD,ADO,AD1,EC,ACO,AC1 /
30 0 0 0 0 0 0 / flags for adjust. param.: EW,AHO,AH1,ES,AS0,AS1 /
31 0 0 0 0 0 0 / flags for adjust. param.: EZ,EZBWC,EZHID,AZ,CCOUL,ALF /
32 0 0 0 0 0 0 / flags for adjust. param.: CIS0,WCI0,BETO,BET3,BET4,BET(2) /
33 0 0 0 0 * / flags for adjust. param.: BET(4),BET(6),AHU0,AHGO /
34 1 0 0 3 0 0 * / I=1 IT(I),IR(I),IGD(I),JSF1(I),JSF2(I) - Neutron data for EE(I)= 20.900 MeV /
35 1.450000+00 5.000000-02 0.000000+00 0.000000+00 * / I=1 STE(I),DST(I),SEE(I),DSE(I) /
36 1 134 4 432 3 332 * / I=1 K=1,3 IID(I,K),IFD(I,K),HTD(I,K) /
37 1.082700+01 1.014700+00 8.700000-03 1.354200+01 9.014900-01 7.060000-03
38 1.624000+01 8.096400-01 6.530000-03 1.893300+01 7.174300-01 6.040000-03
39 2.162700+01 6.230500-01 5.530000-03 2.701300+01 4.446600-01 4.030000-03
40 3.238200+01 2.908200-01 3.160000-03 3.774000+01 1.709600-01 2.350000-03 neutron angular 0+
41 4.307200+01 9.656000-02 1.580000-03 4.837100+01 5.084000-02 9.500000-04
42 5.365800+01 2.866000-02 8.500000-04 5.890900+01 1.956000-02 7.000000-04

```

```

43  6.413200+01 2.035000-02 6.700000-04 6.932900+01 2.079000-02 6.600000-04
44  7.448400+01 2.315000-02 6.700000-04 7.961300+01 2.351000-02 6.600000-04
45  8.470400+01 2.142000-02 6.400000-04 8.975900+01 1.806000-02 4.900000-04
46  9.477800+01 1.398000-02 4.400000-04 9.975900+01 1.106000-02 4.200000-04
47  1.047000+02 8.390000-03 3.700000-04 1.096200+02 6.580000-03 2.400000-04
48  1.144900+02 5.090000-03 2.300000-04 1.193300+02 4.040000-03 1.900000-04
49  1.241300+02 3.070000-03 1.900000-04 1.289100+02 2.500000-03 1.700000-04
50  1.336500+02 2.000000-03 1.800000-04 1.383700+02 2.140000-03 1.800000-04
51  1.430600+02 1.500000-03 2.000000-04 1.477400+02 1.090000-03 1.900000-04
52  1.523900+02 9.500000-04 2.600000-04 1.570100+02 6.100000-04 3.100000-04
53  1.616400+02 3.900000-04 2.500000-04 1.616400+02 3.900000-04 2.500000-04 *
54  1.384200+01 2.959000-03 4.790000-04 1.660500+01 2.370000-03 4.290000-04 neutron angular second 0+
55  1.936500+01 1.401000-03 4.110000-04 2.212100+01 1.567000-03 3.070000-04
56  2.762100+01 1.202000-03 2.240000-04 3.310200+01 6.420000-04 2.740000-04
57  3.855900+01 6.320000-04 2.250000-04 4.398900+01 7.080000-04 2.130000-04
58  4.938800+01 6.020000-04 1.530000-04 5.475500+01 1.090000-03 2.040000-04
59  6.008600+01 8.030000-04 1.870000-04 6.537700+01 4.670000-04 1.800000-04
60  7.062800+01 4.510000-04 1.700000-04 7.583600+01 3.870000-04 1.780000-04
61  8.100000+01 3.100000-04 1.520000-04 8.611800+01 1.260000-04 1.570000-04
62  9.118900+01 2.570000-04 1.140000-04 9.621200+01 2.040000-04 1.250000-04
63  1.011900+02 1.210000-04 1.130000-04 1.061200+02 1.860000-04 1.290000-04
64  1.110000+02 2.310000-04 9.200000-05 1.158400+02 3.100000-04 1.050000-04
65  1.206300+02 1.780000-04 7.500000-05 1.253800+02 2.760000-04 8.200000-05
66  1.300900+02 3.470000-04 7.200000-05 1.347500+02 1.390000-04 7.500000-05
67  1.393900+02 1.380000-04 7.300000-05 1.439900+02 2.190000-04 7.800000-05
68  1.485600+02 1.500000-04 6.500000-05 1.531000+02 6.500000-05 6.500000-05
69  1.576200+02 1.260000-04 8.600000-05 1.621200+02 7.100000-05 8.200000-05 *
70  1.397400+01 3.620000-03 4.820000-04 1.676200+01 3.063000-03 4.490000-04 neutron angular 3-
71  1.954800+01 2.749000-03 4.360000-04 2.232900+01 2.909000-03 3.160000-04
72  2.787900+01 2.843000-03 2.600000-04 3.340600+01 2.836000-03 3.200000-04
73  3.890800+01 2.946000-03 2.880000-04 4.438100+01 3.069000-03 2.680000-04
74  4.982000+01 2.831000-03 2.000000-04 5.522300+01 2.987000-03 2.540000-04
75  6.058600+01 2.987000-03 2.400000-04 6.590700+01 2.815000-03 2.470000-04
76  7.118200+01 2.723000-03 2.410000-04 7.641100+01 2.581000-03 2.470000-04
77  8.159100+01 3.106000-03 2.310000-04 8.672000+01 2.767000-03 2.370000-04
78  9.179800+01 3.010000-03 1.870000-04 9.682500+01 3.022000-03 1.960000-04
79  1.018000+02 2.705000-03 1.850000-04 1.067200+02 2.263000-03 1.880000-04
80  1.115900+02 2.114000-03 1.310000-04 1.164100+02 2.162000-03 1.360000-04
81  1.211800+02 1.714000-03 1.120000-04 1.259100+02 1.795000-03 1.180000-04
82  1.305900+02 1.668000-03 1.090000-04 1.352200+02 1.590000-03 1.110000-04
83  1.398200+02 1.175000-03 1.080000-04 1.443800+02 1.130000-03 1.050000-04
84  1.489100+02 1.067000-03 8.600000-05 1.534100+02 1.060000-03 8.700000-05
85  1.578800+02 1.016000-03 1.010000-04 1.623300+02 8.910000-04 9.800000-05 *

86  0 0 0 3 0 0 *                                / I=2  BT(I),BKE(I),BGN(I),BGD(I),BSP1(I),BSF2(I) - Proton data for EE(I)= 39.700 MeV /
87  1.350000+00 5.000000-02 0.000000+00 0.000000+00 *                                / I=2  STE(I),DST(I),SRE(I),DSK(I) /
88  2 2 9 4 4 7 3 3 6 *                                / I=2 K=1,3  IID(I,K),JFD(I,K),HTD(I,K) /
89  5.774566+00 1.879471-02 1.879471-03 6.972687+00 2.377528-02 2.139775-03 proton angular 2+
90  9.912569+00 2.059393-02 1.853454-03 1.567775+01 1.823039-02 1.640735-03
91  2.143210+01 1.585695-02 1.427126-03 2.727986+01 1.539024-02 1.385121-03
92  3.30065+01 1.416826-02 1.416826-03 4.330416+01 1.139910-02 1.367892-03
93  5.467881+01 6.200595-03 1.240119-03
94  1.137750+01 3.348969-03 6.697937-04 1.574669+01 1.584991-03 3.169983-04
95  2.152556+01 7.339561-04 1.467912-04 2.739751+01 5.179655-04 1.087728-04
96  3.314104+01 5.194567-04 1.090859-04 3.778394+01 5.724197-04 1.202081-04
97  4.348261+01 6.105253-04 1.282103-04
98  1.579547+01 1.139016-03 1.366819-04 2.159170+01 2.071540-03 2.485848-04 proton angular 3-
99  2.748077+01 2.372577-03 2.847093-04 3.324040+01 2.757822-03 3.309386-04
100 3.789575+01 3.156208-03 3.787449-04 4.360892+01 3.189772-03 3.827726-04 *

101 5.000000-03 *                                / estimated accuracy of parameter adjustment /
102 0.000000+00 *                                / value of HI**2 /

```

PROTOCOL file

```

1   Expert
2   Input data file - OC12FORCHECK.IU
3   Variant of job :
4   C-12 OCTUPOLE CALCULATION bet3=ksi*bet2
5   HEJOB = 2 - adjustment of optical potential parameters

```

```

6 HEPOT = 2 - potential expanded by derivatives, requires HENAH = 3 - 5
7 HENAH = 5 - nuclear Hamiltonian with account of gamma softness
8 HEPAI = 0 - short output
9 HESOL = 1 - code will choose which method of coupled channels system solution for a certain J*(pi) should be used to reduce time of calculations
10 HESNA = 4 - rigid hexadecapole deformations in the most general case
11 HESHO = 2 - nuclear shape with non-axial octupole deformations
12 HEWA0 = 2 - nucleus is soft to symmetric octupole deformations scaled by betha2
13 HEAPP = 0 - solution with potential dependency on level energy losses in the channel
14 HEVOL = 0 - standard solution
15 HEREL = 1 - account of relativistic kinematics and potential dependence
16 HECUL = 0 - Coulomb correction proportional to derivative of real potential
17 HERZZ = 1 - charge radius is energy dependent : EZ=EZ0*(1.-EZBHC*(EE-EFERH)**S/((EE-EFERH)**S+LZHID**S))
18 HERRR = 1 - real radius is energy dependent : RR=R0*(1.-RBBHC*(EE-EFERH)**S/((EE-EFERH)**S+LRHID**S))
19
20 ! Switches of the model accepted !
21
22
23 HENAH = 5 ! Parameters of non-axial nuclear Hamiltonian accepted !
24
25 NUR= 5, NST <= 20 - number of coupled levels in optical model calcnlations
26 NST= 2, NST <= 50 - number of energy points with experimental data that will be used for optical parameters adjustment (HEJOB = 2)
27 NPD= 0, NPD = 0 (not in use) - for non-axial nuclear Hamiltonian models (HEPOT = 2, HENAH > 3)
28 LAS= 4, LAS <= 4 - number of potential derivatives for deformed potential expansion for non-axial nuclear Hamiltonian models (HEPOT = 2, HENAH > 2)
29 NTET= 0 value NTET not used for HEJOB = 2
30 LLHA=50, LLHA <= 89 - maximum momentum of scattered neutrons
31 DCMA=100, DCMA <= 200 - maximum number of coupled equations for certain J*(pi)
32 ISHA=100, ISHA <= 180 - maximum number of J*(pi) states for which coupled channels systems are solved
33 KODHA= 1, KODHA > 0 - coupled equations are orded by growing angular momentum of scattered neutrons, the total number of coupled equations <= DCMA
34
35 ! Switches for details of calculations accepted !
36
37
38 HEJOB=2 - (EE(I),I=1,NST) - energies for experimental points which will be used for potential adjustment
39 ! Energies accepted !
40
41 (HCWAE(I),I=1,NST) - flags determining charge of incident particles for which calculations for energy EE(I) will be carried out
42 ! Flags HCWAE accepted !
43
44 ! Characteristics of levels accepted !
45
46 ! Characteristics of interacting incident particle and nucleus accepted !
47
48 ! Optical potential parameters accepted !
49
50 ! Flags that determine adjusted parameters accepted !
51 Number of adjusted parameters - 1
52
53 ! Experimental data for all energy point EE(I) (I=1, 2) accepted !
54
55 ! 1 estimated accuracies of parameter adjustment accepted !
56
57 ! Value of FU = 0.000000E+00 is taken !
58
59
60 ! HEJOB = 2 - INPUT file for adjustment of optical potential parameters passed consistency control !
61
62
63 !!! No mistakes in INPUT file !!!

```

10.5 Running the Code OPTMAN and Description of Output Files

As one runs the code it will first ask the name of the input file and, after it will be read, the code asks to give the name for the output file, in which all the calculated information will be stored. While running, five more files are created by the code: CR-SECT, TRANSME, GNASH, ANG-DIST, ANG-POL. File CR-SECT contains one line for each calculated energy. Line starts with a value of energy, and then

follow total, reaction cross sections and level excitation cross sections ordered by their excitation energies (in case calculations are made for protons, they include contribution of nuclear amplitude only since the total and elastic cross sections are infinity). File TRANSME contains nucleon transmission coefficients for each calculated energy to be used by the code STAPRE [47]. For each calculated energy the first line indicates incident energy and l_{\max} - maximum angular momentum for which nucleon transmission coefficients are available for this energy, and then lines with $l_{\max} + 1$ transmissions follow ordered by growing angular momentum starting with $T_{l=0}$ by six in a line. As the calculated transmission coefficients are intended to be used by the code STAPRE [47] they are averaged over J dependence and depend only on angular momentum l . Many zero-value higher angular momentum transmissions are outputted by code, it is convenient for STAPRE code calculations. File GNASH contains nucleon transmission coefficients for each calculated energy to be used by the code GNASH [46]. For each energy the first line indicates the energy and l_{\max} - maximum angular momentum for which nucleon transmission coefficients are available for this energy, and according with the GNASH format lines with transmissions: first $T_{l=0,j=1/2}$, then pares $T_{l,j=l-1/2}, T_{l,j=1/2}$ follow ordered by growing angular momentum up to l_{\max} by six in a line. File ANGL-DIST contains calculated angular distributions for all excited levels for energies described by Record 5 at angles distinguished by Record 7 of input file. File ANGLE-DIST consists of NST block: the first card of the block indicated incident energy and type of the particle, then follow MTET lines with first angle and then angular distributions for excited levels in order following the order of levels input. File ANGL-POL gives polynomial expansion for angular distributions determined by Eqs. (87) and (88). This file consists of NST blocks. Each block starts with line describing incident energy and numbers of coefficients in expansions $LKK=NL$ and $LCOUL=ML$ (see Eqs. (87) and (88)). Second line of the block gives total, reaction cross sections and level excitation cross sections ordered by their excitation energies, then for each excited level follow NL of $a_L(E)$ coefficients six in line and for elastically scattered protons ML pares of $Reb_L(E)$ and $Imb_L(E)$ coefficients. When one runs optical parameter adjustment files CR-SECT, TRANSME, GNASH, ANGL-DIST and ANGL-POL are organized but are blank. When one runs optical calculations code's option with $MTET=0$ input files ANGL-DIST and ANGL-POL are also blank. Below we present these files for a run in which optical calculations of ^{12}C cross sections are organized, as well as the appropriate input file.

INPUT file

```

1 C-12 OCTUPOLE CALCULATION bet3=ksi*bet2
2 0102050001040202000001000101
3 0.42825E+01 0.27943E+01 0.11860E+00 0.32107E+00 0.16400E+00 0.12600E+00
4 0.14694E+00 0.21419E-03 0.52045E+00 0.24200E+00 0.21005E-01 0.83263E+00
5 0.35000E+00 0.22130E+00 0.00000E+00 0.17221E+01 0.00000E+00
6 005002004004040050100100001

```

```

7   .2090000+02 .3970000+02
8   0001
9   .1000000+01 .5000000+01 .1000000+02 .1500000+02 .1800000+02 .2100000+02
10  .2400000+02 .2700000+02 .3000000+02 .3300000+02 .3600000+02 .3900000+02
11  .4200000+02 .4500000+02 .4800000+02 .5100000+02 .5400000+02 .5600000+02
12  .5900000+02 .6200000+02 .6500000+02 .7000000+02 .7500000+02 .8000000+02
13  .8500000+02 .9000000+02 .9500000+02 .1000000+03 .1050000+03 .1100000+03
14  .1150000+03 .1200000+03 .1250000+03 .1300000+03 .1350000+03 .1400000+03
15  .1500000+03 .1600000+03 .1700000+03 .1800000+03
16  .0000000-0000+101000000
17  .4440000+0104+101000000
18  .9640000+0106-101000001
19  .7650000+0100+101010000
20  .1780000+0204+102000000
21  1.00866520  .5000000-00 .1200000+02 .6000000+01-.1183500+02-.8950000+01
22  -.3094000+02-.0000000-00 .0002381+00 .3000000-06 .8630000+02 .4532000-02
23  .0000000+01-.0000000-00 .0000000+01 .9530000+01 .1533000+02 .1755000-01
24  .0000000+01-.0000000-00 .0000000+01 .1909000+02 .9429000+02 .0000000+01
25  .7840000+01 .0030000000 .0000000+01-.0000000-00 -3.100      160.
26  .1150000+01 .10          .5000000+02 2.          .5190000-00 .2600000-02
27  .1072600+01 .4460000-00 .0000000-02 .1039700+01 .4570000+00 .0000000-02
28  .1000000+01 .1000000+01 .0000000-00 .1086300+01 .6050000-00-.0000000-02
29  .1145300+01 .00          .1000000+01 .680          1.1000      .1000000+01
30  .1300000+02 .3000000+02

```

OUTPUT file

```

1 C-12 OCTUPOLE CALCULATION bet3=ksi*bet2
2           INTERACTION OF PARTICLE HAVING SPIN = 0.50
3           WITH NUCLEI A= 12.0000000
4           COUPLED CHANNELS METHOD
5           RELATIVISTIC KINEMATICS AND POTENTIAL DEPENDENCE
6           COULOMB CORRECTION PROPORTIONAL REAL POTENTIAL DER-VE
7           CHARGE RADIUS IS ENERGY DEPENDENT
8           REAL RADIUS IS ENERGY DEPENDENT
9           WITH AC. NONAXIAL GEXADECAPOLE DEFORMATIONS
10
11           HAMILTONN-A SPAO      POTENTIAL EXPANDED BY      BETO
12           WITH AC. NONAXIAL OCTUPOLE      SOFT      DEFORMATIONS
13
14           NUMBER OF COUPLED LEVELS= 5      NPD = 4
15           NUMBER OF TERMS IN POTENTIAL EXPANSION= 4
16
17

```

18		ENERGY	LEVEL'S	SPIN*2	NTU	NNB	NNG	NNO	NPO
19									
20	1	.0000000E+00		0	1	0	0	0	1
21	2	.4440000E+01		4	1	0	0	0	1
22	3	.9640000E+01		6	1	0	0	1	-1
23	4	.7650000E+01		0	1	1	0	0	1
24	5	.1780000E+02		4	2	0	0	0	1
25									
26									
		PARAMETERS OF HAMILTONIAN							
27	HW=	4.28250	AMBO=	2.79430	AMGO=	0.11860	GAMO=	0.32107	BETO= 0.16400
28	BET4=	0.12600	BB42=	0.14694	GAMG=	0.00021	DELG=	0.52045	
29	BET3=	0.24200	ET0=	0.02100	AMU0=	0.83263	HW0=	0.35000	BB32= 0.22130
30	GAMDE=	0.00000	DPAR=	1.7221	GSHAPE=	0.00000			
31									
32									
33	I01= 1 I02= 1 NNT= 1	FOLAR= 0.000000D+00	ANU1=	0.7043448D+00	ANU2=	0.7043448D+00			
34	I01= 1 I02= 1 NNT= 2	FOLAR= 0.6440039D+01	ANU1=	0.7043448D+00	ANU2=	0.7043448D+00			
35	I01= 1 I02= 2 NNT= 1	FOLAR= 0.2536337D+01	ANU1=	0.7043448D+00	ANU2=	0.2543514D+01			
36	I01= 1 I02= 2 NNT= 2	FOLAR= 0.000000D+00	ANU1=	0.7043448D+00	ANU2=	0.2543514D+01			
37	I01= 2 I02= 2 NNT= 1	FOLAR= 0.000000D+00	ANU1=	0.2543514D+01	ANU2=	0.2543514D+01			
38	I01= 2 I02= 2 NNT= 2	FOLAR= 0.1826384D+02	ANU1=	0.2543514D+01	ANU2=	0.2543514D+01			
39	JU1= 1 JU2= 1 NNT= 1 FOV(JU1,JU2,NNT)=	0.3397700D+01	ANU1=	0.6449750D+00	ANU2=	0.6449750D+00			
40	JU1= 1 JU2= 1 NNT= 2 FOV(JU1,JU2,NNT)=	0.1353617D+02	ANU1=	0.6449750D+00	ANU2=	0.6449750D+00			
41	JU1= 1 JU2= 1 NNT= 3 FOV(JU1,JU2,NNT)=	0.6079694D+02	ANU1=	0.6449750D+00	ANU2=	0.6449750D+00			
42	JU1= 1 JU2= 1 NNT= 4 FOV(JU1,JU2,NNT)=	0.3006270D+03	ANU1=	0.6449750D+00	ANU2=	0.6449750D+00			
43	JU1= 1 JU2= 2 NNT= 1 FOV(JU1,JU2,NNT)=	0.3478151D+01	ANU1=	0.6449750D+00	ANU2=	0.7977824D-01			
44	JU1= 1 JU2= 2 NNT= 2 FOV(JU1,JU2,NNT)=	0.1400784D+02	ANU1=	0.6449750D+00	ANU2=	0.7977824D-01			
45	JU1= 1 JU2= 2 NNT= 3 FOV(JU1,JU2,NNT)=	0.6277322D+02	ANU1=	0.6449750D+00	ANU2=	0.7977824D-01			
46	JU1= 1 JU2= 2 NNT= 4 FOV(JU1,JU2,NNT)=	0.3064995D+03	ANU1=	0.6449750D+00	ANU2=	0.7977824D-01			
47	JU1= 1 JU2= 3 NNT= 1 FOV(JU1,JU2,NNT)=	0.3667907D+01	ANU1=	0.6449750D+00	ANU2=	0.7969259D-02			
48	JU1= 1 JU2= 3 NNT= 2 FOV(JU1,JU2,NNT)=	0.1677113D+02	ANU1=	0.6449750D+00	ANU2=	0.7969259D-02			
49	JU1= 1 JU2= 3 NNT= 3 FOV(JU1,JU2,NNT)=	0.8411341D+02	ANU1=	0.6449750D+00	ANU2=	0.7969259D-02			
50	JU1= 1 JU2= 3 NNT= 4 FOV(JU1,JU2,NNT)=	0.4547311D+03	ANU1=	0.6449750D+00	ANU2=	0.7969259D-02			
51	JU1= 1 JU2= 4 NNT= 1 FOV(JU1,JU2,NNT)=	0.1368376D+01	ANU1=	0.6449750D+00	ANU2=	0.2446976D+01			
52	JU1= 1 JU2= 4 NNT= 2 FOV(JU1,JU2,NNT)=	0.1082197D+02	ANU1=	0.6449750D+00	ANU2=	0.2446976D+01			
53	JU1= 1 JU2= 4 NNT= 3 FOV(JU1,JU2,NNT)=	0.7238643D+02	ANU1=	0.6449750D+00	ANU2=	0.2446976D+01			
54	JU1= 1 JU2= 4 NNT= 4 FOV(JU1,JU2,NNT)=	0.4740800D+03	ANU1=	0.6449750D+00	ANU2=	0.2446976D+01			
55	JU1= 1 JU2= 5 NNT= 1 FOV(JU1,JU2,NNT)=	0.3589556D+01	ANU1=	0.6449750D+00	ANU2=	0.2785297D-02			
56	JU1= 1 JU2= 5 NNT= 2 FOV(JU1,JU2,NNT)=	0.1724151D+02	ANU1=	0.6449750D+00	ANU2=	0.2785297D-02			
57	JU1= 1 JU2= 5 NNT= 3 FOV(JU1,JU2,NNT)=	0.9031816D+02	ANU1=	0.6449750D+00	ANU2=	0.2785297D-02			
58	JU1= 1 JU2= 5 NNT= 4 FOV(JU1,JU2,NNT)=	0.5078508D+03	ANU1=	0.6449750D+00	ANU2=	0.2785297D-02			
59	JU1= 2 JU2= 2 NNT= 1 FOV(JU1,JU2,NNT)=	0.3586025D+01	ANU1=	0.7977824D-01	ANU2=	0.7977824D-01			
60	JU1= 2 JU2= 2 NNT= 2 FOV(JU1,JU2,NNT)=	0.1459821D+02	ANU1=	0.7977824D-01	ANU2=	0.7977824D-01			
61	JU1= 2 JU2= 2 NNT= 3 FOV(JU1,JU2,NNT)=	0.6540952D+02	ANU1=	0.7977824D-01	ANU2=	0.7977824D-01			
62	JU1= 2 JU2= 2 NNT= 4 FOV(JU1,JU2,NNT)=	0.3166611D+03	ANU1=	0.7977824D-01	ANU2=	0.7977824D-01			
63	JU1= 2 JU2= 3 NNT= 1 FOV(JU1,JU2,NNT)=	0.3800098D+01	ANU1=	0.7977824D-01	ANU2=	0.7969259D-02			
64	JU1= 2 JU2= 3 NNT= 2 FOV(JU1,JU2,NNT)=	0.1733502D+02	ANU1=	0.7977824D-01	ANU2=	0.7969259D-02			
65	JU1= 2 JU2= 3 NNT= 3 FOV(JU1,JU2,NNT)=	0.8590071D+02	ANU1=	0.7977824D-01	ANU2=	0.7969259D-02			
66	JU1= 2 JU2= 3 NNT= 4 FOV(JU1,JU2,NNT)=	0.4554697D+03	ANU1=	0.7977824D-01	ANU2=	0.7969259D-02			
67	JU1= 2 JU2= 4 NNT= 1 FOV(JU1,JU2,NNT)=	0.1455094D+01	ANU1=	0.7977824D-01	ANU2=	0.2446976D+01			
68	JU1= 2 JU2= 4 NNT= 2 FOV(JU1,JU2,NNT)=	0.1080186D+02	ANU1=	0.7977824D-01	ANU2=	0.2446976D+01			
69	JU1= 2 JU2= 4 NNT= 3 FOV(JU1,JU2,NNT)=	0.6984171D+02	ANU1=	0.7977824D-01	ANU2=	0.2446976D+01			
70	JU1= 2 JU2= 4 NNT= 4 FOV(JU1,JU2,NNT)=	0.4429782D+03	ANU1=	0.7977824D-01	ANU2=	0.2446976D+01			
71	JU1= 2 JU2= 5 NNT= 1 FOV(JU1,JU2,NNT)=	0.3708943D+01	ANU1=	0.7977824D-01	ANU2=	0.2785297D-02			
72	JU1= 2 JU2= 5 NNT= 2 FOV(JU1,JU2,NNT)=	0.1767531D+02	ANU1=	0.7977824D-01	ANU2=	0.2785297D-02			
73	JU1= 2 JU2= 5 NNT= 3 FOV(JU1,JU2,NNT)=	0.9103598D+02	ANU1=	0.7977824D-01	ANU2=	0.2785297D-02			

```

74  JU1= 2 JU2= 5 NNT= 4 FOV(JU1,JU2,NNT)= 0.4998478D+03 ANU1= 0.7977824D-01 ANU2= 0.2785297D-02
75  JU1= 3 JU2= 3 NNT= 1 FOV(JU1,JU2,NNT)= 0.4650767D+01 ANU1= 0.7969259D-02 ANU2= 0.7969259D-02
76  JU1= 3 JU2= 3 NNT= 2 FOV(JU1,JU2,NNT)= 0.2364654D+02 ANU1= 0.7969259D-02 ANU2= 0.7969259D-02
77  JU1= 3 JU2= 3 NNT= 3 FOV(JU1,JU2,NNT)= 0.1289822D+03 ANU1= 0.7969259D-02 ANU2= 0.7969259D-02
78  JU1= 3 JU2= 3 NNT= 4 FOV(JU1,JU2,NNT)= 0.7459344D+03 ANU1= 0.7969259D-02 ANU2= 0.7969259D-02
79  JU1= 3 JU2= 4 NNT= 1 FOV(JU1,JU2,NNT)= 0.3176693D+01 ANU1= 0.7969259D-02 ANU2= 0.2446976D+01
80  JU1= 3 JU2= 4 NNT= 2 FOV(JU1,JU2,NNT)= 0.2092894D+02 ANU1= 0.7969259D-02 ANU2= 0.2446976D+01
81  JU1= 3 JU2= 4 NNT= 3 FOV(JU1,JU2,NNT)= 0.1356776D+03 ANU1= 0.7969259D-02 ANU2= 0.2446976D+01
82  JU1= 3 JU2= 4 NNT= 4 FOV(JU1,JU2,NNT)= 0.8938593D+03 ANU1= 0.7969259D-02 ANU2= 0.2446976D+01
83  JU1= 3 JU2= 5 NNT= 1 FOV(JU1,JU2,NNT)= 0.4816125D+01 ANU1= 0.7969259D-02 ANU2= 0.2785297D-02
84  JU1= 3 JU2= 5 NNT= 2 FOV(JU1,JU2,NNT)= 0.2551115D+02 ANU1= 0.7969259D-02 ANU2= 0.2785297D-02
85  JU1= 3 JU2= 5 NNT= 3 FOV(JU1,JU2,NNT)= 0.1443104D+03 ANU1= 0.7969259D-02 ANU2= 0.2785297D-02
86  JU1= 3 JU2= 5 NNT= 4 FOV(JU1,JU2,NNT)= 0.8626245D+03 ANU1= 0.7969259D-02 ANU2= 0.2785297D-02
87  JU1= 4 JU2= 4 NNT= 1 FOV(JU1,JU2,NNT)= 0.4940767D+01 ANU1= 0.2446976D+01 ANU2= 0.2446976D+01
88  JU1= 4 JU2= 4 NNT= 2 FOV(JU1,JU2,NNT)= 0.2992855D+02 ANU1= 0.2446976D+01 ANU2= 0.2446976D+01
89  JU1= 4 JU2= 4 NNT= 3 FOV(JU1,JU2,NNT)= 0.1981755D+03 ANU1= 0.2446976D+01 ANU2= 0.2446976D+01
90  JU1= 4 JU2= 4 NNT= 4 FOV(JU1,JU2,NNT)= 0.1380222D+04 ANU1= 0.2446976D+01 ANU2= 0.2446976D+01
91  JU1= 4 JU2= 5 NNT= 1 FOV(JU1,JU2,NNT)= 0.3838257D+01 ANU1= 0.2446976D+01 ANU2= 0.2785297D-02
92  JU1= 4 JU2= 5 NNT= 2 FOV(JU1,JU2,NNT)= 0.2517325D+02 ANU1= 0.2446976D+01 ANU2= 0.2785297D-02
93  JU1= 4 JU2= 5 NNT= 3 FOV(JU1,JU2,NNT)= 0.1655250D+03 ANU1= 0.2446976D+01 ANU2= 0.2785297D-02
94  JU1= 4 JU2= 5 NNT= 4 FOV(JU1,JU2,NNT)= 0.1113186D+04 ANU1= 0.2446976D+01 ANU2= 0.2785297D-02
95  JU1= 5 JU2= 5 NNT= 1 FOV(JU1,JU2,NNT)= 0.5108385D+01 ANU1= 0.2785297D-02 ANU2= 0.2785297D-02
96  JU1= 5 JU2= 5 NNT= 2 FOV(JU1,JU2,NNT)= 0.2815616D+02 ANU1= 0.2785297D-02 ANU2= 0.2785297D-02
97  JU1= 5 JU2= 5 NNT= 3 FOV(JU1,JU2,NNT)= 0.1650190D+03 ANU1= 0.2785297D-02 ANU2= 0.2785297D-02
98  JU1= 5 JU2= 5 NNT= 4 FOV(JU1,JU2,NNT)= 0.1018772D+04 ANU1= 0.2785297D-02 ANU2= 0.2785297D-02
99

100          POTENTIAL      PARAMETERS      V(R)
101
102  VR0=-30.940      VR1= 0.0000      VR2= 0.0002381    RR= 1.1500      ARO= 0.5190      AR1= 0.0026
103  WDO= 0.0000      WD1= 0.0000      VR3= 0.0000003    RD= 1.0726      ADO= 0.4460      AD1= 0.0000
104  WCO= 0.0000      WC1= 0.0000
105
106  VS0= 7.8400
107  ALF= 1.0000      ANEU= 1.0087
108  BNDC= 0.00      WDA1= 0.0000      WCA1= 0.0000      CCOUL= 1.1000      CIS0= 13.000      WCIS0= 30.000
109  WS0= 0.0000      WS1= 0.0000      VRLA=86.3000    ALAVR= 0.00453     WCBW=19.0900     WCWID=94.2900
110  WDBW= 9.5300      WDWID=15.3300    ALAWD= 0.0175      EFERMN=-11.835    EFERMP= -8.950     ALAS0= 0.0030
111  PDIS= 2.0000      WSBW=-3.1000    WSWID= 160.00     RRBWC= 0.10000    RRWID= 50.00      RZBWC= 0.0000
112  RZWID= 1.0000
113
114          NUCLEUS CHARGE = 6.0000
115
116
117          SPHERICAL VOLUME INTEGRALS OF REAL POTENTIAL F-FACTORS AND DERIVATIVES:
118  VIRO= 8.625  VIR1= 20.235  VIR2= 17.490  VIR3= 5.754  CBETO= 1.000
119          SPHERICAL VOLUME INTEGRALS OF IMAGINARY (WC) F-FACTORS AND DERIVATIVES:
120  WICO= 6.132  WIC1= 15.117  WIC2= 13.501  WIC3= 4.471  CBETC= 0.893
121          SPHERICAL VOLUME INTEGRALS OF IMAGINARY (WD) F-FACTORS AND DERIVATIVES:
122  WIDO= 11.922  WID1= 21.532  WID2= 10.714  WID3= 0.080  CBETD= 0.498
123          SPHERICAL VOLUME INTEGRALS OF IMAGINARY (WW) F-FACTORS AND DERIVATIVES:
124  WIWO= 0.000  WIW1= 0.000  WIW2= 0.000  WIW3= 0.000  CBETW= 0.000
125
126          POTENTIAL VALUES FOR INCIDENT ENERGY= 20.900000 MeV:
127
128  VR= 43.727  WC= 2.053  WD= 4.400  VS0= 7.107  WS0= -0.125  RELPOT= 1.011
129

```

130
 131
 132 ORB. MOMENT TRANSITIONS SR SI
 133
 134 0 0.5679855207 -0.2857931776 -0.4224467826
 135 1 0.5331908701 -0.5003147571 -0.2998733949
 136 2 0.6336119417 -0.3663618832 -0.0511858307
 137 3 0.5442170355 0.2428931782 0.3583146897
 138 4 0.1229785502 0.8896431281 0.2195276388
 139 5 0.0156933341 0.9877122891 0.0494384142
 140 6 0.0023144735 0.9984430910 0.0111952050
 141 7 0.0002668717 0.9998552767 0.0023598100
 142 8 0.0000192592 0.4705784743 0.0001313851
 143 9 0.0000000000 0.0000000000 0.0000000000
 144 10 0.0000000000 0.0000000000 0.0000000000
 145 11 0.0000000000 0.0000000000 0.0000000000
 146 12 0.0000000000 0.0000000000 0.0000000000
 147 13 0.0000000000 0.0000000000 0.0000000000
 148 14 0.0000000000 0.0000000000 0.0000000000
 149 15 0.0000000000 0.0000000000 0.0000000000
 150 16 0.0000000000 0.0000000000 0.0000000000
 151 17 0.0000000000 0.0000000000 0.0000000000
 152 18 0.0000000000 0.0000000000 0.0000000000
 153 19 0.0000000000 0.0000000000 0.0000000000
 154 20 0.0000000000 0.0000000000 0.0000000000
 155 21 0.0000000000 0.0000000000 0.0000000000
 156 ANGULAR DISTRIBUTIONS OF SCATTERED PARTICLES
 157
 158 0.100E+01 0.109E+01 0.162E-01 0.233E-02 0.206E-02 0.112E-03
 159 0.500E+01 0.106E+01 0.159E-01 0.233E-02 0.196E-02 0.112E-03
 160 0.100E+02 0.968E+00 0.150E-01 0.234E-02 0.166E-02 0.111E-03
 161 0.150E+02 0.836E+00 0.139E-01 0.234E-02 0.124E-02 0.108E-03
 162 0.180E+02 0.743E+00 0.132E-01 0.234E-02 0.966E-03 0.106E-03
 163 0.210E+02 0.646E+00 0.126E-01 0.235E-02 0.707E-03 0.104E-03
 164 0.240E+02 0.550E+00 0.121E-01 0.235E-02 0.477E-03 0.102E-03
 165 0.270E+02 0.458E+00 0.117E-01 0.236E-02 0.291E-03 0.996E-04
 166 0.300E+02 0.372E+00 0.113E-01 0.238E-02 0.157E-03 0.969E-04
 167 0.330E+02 0.296E+00 0.111E-01 0.240E-02 0.772E-04 0.941E-04
 168 0.360E+02 0.230E+00 0.109E-01 0.243E-02 0.509E-04 0.911E-04
 169 0.390E+02 0.174E+00 0.107E-01 0.246E-02 0.716E-04 0.881E-04
 170 0.420E+02 0.129E+00 0.104E-01 0.250E-02 0.130E-03 0.850E-04
 171 0.450E+02 0.945E-01 0.101E-01 0.255E-02 0.215E-03 0.820E-04
 172 0.480E+02 0.682E-01 0.971E-02 0.260E-02 0.315E-03 0.790E-04
 173 0.510E+02 0.492E-01 0.921E-02 0.265E-02 0.419E-03 0.761E-04
 174 0.540E+02 0.362E-01 0.862E-02 0.269E-02 0.516E-03 0.733E-04
 175 0.560E+02 0.301E-01 0.819E-02 0.272E-02 0.573E-03 0.716E-04
 176 0.590E+02 0.241E-01 0.750E-02 0.275E-02 0.642E-03 0.692E-04
 177 0.620E+02 0.207E-01 0.679E-02 0.277E-02 0.689E-03 0.670E-04
 178 0.650E+02 0.191E-01 0.607E-02 0.278E-02 0.711E-03 0.651E-04
 179 0.700E+02 0.183E-01 0.495E-02 0.276E-02 0.694E-03 0.626E-04
 180 0.750E+02 0.180E-01 0.401E-02 0.270E-02 0.621E-03 0.611E-04
 181 0.800E+02 0.172E-01 0.330E-02 0.260E-02 0.512E-03 0.606E-04
 182 0.850E+02 0.156E-01 0.283E-02 0.247E-02 0.388E-03 0.611E-04
 183 0.900E+02 0.134E-01 0.256E-02 0.232E-02 0.272E-03 0.627E-04
 184 0.950E+02 0.108E-01 0.246E-02 0.217E-02 0.181E-03 0.651E-04
 185 0.100E+03 0.829E-02 0.245E-02 0.202E-02 0.125E-03 0.684E-04

```

186    0.105E+03    0.613E-02    0.249E-02    0.187E-02    0.106E-03    0.724E-04
187    0.110E+03    0.446E-02    0.253E-02    0.172E-02    0.120E-03    0.769E-04
188    0.115E+03    0.329E-02    0.254E-02    0.159E-02    0.157E-03    0.818E-04
189    0.120E+03    0.257E-02    0.252E-02    0.145E-02    0.207E-03    0.869E-04
190    0.125E+03    0.219E-02    0.244E-02    0.133E-02    0.257E-03    0.921E-04
191    0.130E+03    0.205E-02    0.233E-02    0.120E-02    0.300E-03    0.972E-04
192    0.135E+03    0.204E-02    0.219E-02    0.108E-02    0.329E-03    0.102E-03
193    0.140E+03    0.211E-02    0.202E-02    0.963E-03    0.347E-03    0.107E-03
194    0.150E+03    0.239E-02    0.165E-02    0.749E-03    0.362E-03    0.115E-03
195    0.160E+03    0.282E-02    0.132E-02    0.577E-03    0.382E-03    0.122E-03
196    0.170E+03    0.328E-02    0.109E-02    0.465E-03    0.413E-03    0.126E-03
197    0.180E+03    0.348E-02    0.101E-02    0.426E-03    0.429E-03    0.127E-03
198
199 NEUTRON ENERGY = 20.900000
200 TOTAL CR-SECT.= 1.385445
201 REACTION CR-SECT. = 0.379940
202
203      NMAX          CR-SECT. OF LEVEL EXCITATION
204      1              0.914067
205      2              0.060535
206      3              0.025181
207      4              0.004689
208      5              0.001033
209
210          STRENGTH FUNCTIONS
211 SFO= 0.1977353E-04      SF1= 0.2020374E-04      SF2= 0.2946288E-04
212
213 SPHERICAL VOLUME INTEGRALS OF REAL POTENTIAL F-FACTORS AND DERIVATIVES:
214 VIRO= 8.637 VIR1= 19.405 VIR2= 16.282 VIR3= 5.314 CBETO= 1.000
215 SPHERICAL VOLUME INTEGRALS OF IMAGINARY (WC) F-FACTORS AND DERIVATIVES:
216 WICO= 6.132 WIC1= 15.117 WIC2= 13.501 WIC3= 4.471 CBETC= 0.893
217 SPHERICAL VOLUME INTEGRALS OF IMAGINARY (WD) F-FACTORS AND DERIVATIVES:
218 WIDO= 11.922 WID1= 21.532 WID2= 10.714 WID3= 0.080 CBETD= 0.498
219 SPHERICAL VOLUME INTEGRALS OF IMAGINARY (WW) F-FACTORS AND DERIVATIVES:
220 WIWO= 0.000 WIW1= 0.000 WIW2= 0.000 WIW3= 0.000 CBETW= 0.000
221
222 POTENTIAL VALUES FOR INCIDENT ENERGY= 39.700000 MeV:
223
224 VR= 39.714 WC= 4.014 WD= 3.691 VS0= 6.775 WS0= -0.262 RELPOT= 1.021
225
226
227
228 ORB. MOMENT          TRANSITIONS          SR          SI
229
230      0              0.5805468936    -0.5306541597    -0.2360303736
231      1              0.5802486293    -0.5717369989    0.0653369985
232      2              0.6019798371    -0.4199247125    0.2805230575
233      3              0.5687316331    -0.0303323005    0.4317270279
234      4              0.3414767943    0.5280184923    0.4666962137
235      5              0.1034497385    0.8917564142    0.2467789328
236      6              0.0240418145    0.9793434440    0.0911588566
237      7              0.0054580339    0.9960256767    0.0316681426
238      8              0.0011489898    0.9993014787    0.0106888903
239      9              0.0002389284    0.9998702360    0.0035057561
240     10              0.0000501210    0.9999737528    0.0010910045
241     11              0.0000103491    0.9999946188    0.0003104894

```

242	12	0.0000020402	0.9999989510	0.0000789919		
243	13	0.0000004113	0.9999997917	0.0000179140		
244	14	0.0000000759	0.9999999619	0.0000036620		
245	15	0.0000000125	0.9999999938	0.0000006855		
246	16	0.0000000018	0.4848484839	0.0000000421		
247	17	0.0000000000	0.0000000000	0.0000000000		
248	18	0.0000000000	0.0000000000	0.0000000000		
249	19	0.0000000000	0.0000000000	0.0000000000		
250	20	0.0000000000	0.0000000000	0.0000000000		
251	21	0.0000000000	0.0000000000	0.0000000000		
252	22	0.0000000000	0.0000000000	0.0000000000		
253	23	0.0000000000	0.0000000000	0.0000000000		
254	24	0.0000000000	0.0000000000	0.0000000000		
255	25	0.0000000000	0.0000000000	0.0000000000		
256		ANGULAR DISTRIBUTIONS OF SCATTERED PARTICLES				
257						
258	0.100E+01	0.556E+04	0.785E-02	0.892E-03	0.315E-02	0.434E-03
259	0.500E+01	0.501E+01	0.766E-02	0.922E-03	0.286E-02	0.432E-03
260	0.100E+02	0.738E+00	0.727E-02	0.101E-02	0.211E-02	0.428E-03
261	0.150E+02	0.722E+00	0.713E-02	0.115E-02	0.123E-02	0.423E-03
262	0.180E+02	0.645E+00	0.732E-02	0.127E-02	0.771E-03	0.422E-03
263	0.210E+02	0.540E+00	0.773E-02	0.142E-02	0.429E-03	0.421E-03
264	0.240E+02	0.428E+00	0.831E-02	0.161E-02	0.222E-03	0.421E-03
265	0.270E+02	0.324E+00	0.892E-02	0.184E-02	0.142E-03	0.420E-03
266	0.300E+02	0.235E+00	0.943E-02	0.209E-02	0.163E-03	0.418E-03
267	0.330E+02	0.163E+00	0.969E-02	0.237E-02	0.247E-03	0.413E-03
268	0.360E+02	0.109E+00	0.963E-02	0.263E-02	0.356E-03	0.404E-03
269	0.390E+02	0.705E-01	0.920E-02	0.287E-02	0.459E-03	0.391E-03
270	0.420E+02	0.443E-01	0.844E-02	0.304E-02	0.531E-03	0.374E-03
271	0.450E+02	0.278E-01	0.745E-02	0.314E-02	0.563E-03	0.352E-03
272	0.480E+02	0.180E-01	0.632E-02	0.315E-02	0.553E-03	0.327E-03
273	0.510E+02	0.127E-01	0.519E-02	0.307E-02	0.507E-03	0.299E-03
274	0.540E+02	0.100E-01	0.414E-02	0.291E-02	0.437E-03	0.270E-03
275	0.560E+02	0.915E-02	0.351E-02	0.276E-02	0.383E-03	0.251E-03
276	0.590E+02	0.846E-02	0.272E-02	0.249E-02	0.299E-03	0.222E-03
277	0.620E+02	0.803E-02	0.210E-02	0.219E-02	0.221E-03	0.194E-03
278	0.650E+02	0.757E-02	0.165E-02	0.188E-02	0.156E-03	0.169E-03
279	0.700E+02	0.645E-02	0.120E-02	0.138E-02	0.846E-04	0.134E-03
280	0.750E+02	0.499E-02	0.997E-03	0.968E-03	0.581E-04	0.107E-03
281	0.800E+02	0.352E-02	0.913E-03	0.657E-03	0.629E-04	0.888E-04
282	0.850E+02	0.229E-02	0.855E-03	0.450E-03	0.809E-04	0.768E-04
283	0.900E+02	0.141E-02	0.775E-03	0.325E-03	0.967E-04	0.694E-04
284	0.950E+02	0.878E-03	0.664E-03	0.258E-03	0.102E-03	0.647E-04
285	0.100E+03	0.602E-03	0.533E-03	0.223E-03	0.937E-04	0.612E-04
286	0.105E+03	0.483E-03	0.402E-03	0.202E-03	0.759E-04	0.580E-04
287	0.110E+03	0.438E-03	0.288E-03	0.184E-03	0.541E-04	0.546E-04
288	0.115E+03	0.410E-03	0.201E-03	0.163E-03	0.341E-04	0.507E-04
289	0.120E+03	0.372E-03	0.142E-03	0.139E-03	0.201E-04	0.463E-04
290	0.125E+03	0.318E-03	0.109E-03	0.113E-03	0.137E-04	0.416E-04
291	0.130E+03	0.252E-03	0.975E-04	0.877E-04	0.143E-04	0.367E-04
292	0.135E+03	0.185E-03	0.997E-04	0.662E-04	0.201E-04	0.320E-04
293	0.140E+03	0.127E-03	0.110E-03	0.497E-04	0.288E-04	0.277E-04
294	0.150E+03	0.640E-04	0.131E-03	0.325E-04	0.490E-04	0.212E-04
295	0.160E+03	0.812E-04	0.138E-03	0.302E-04	0.692E-04	0.184E-04
296	0.170E+03	0.137E-03	0.131E-03	0.329E-04	0.866E-04	0.184E-04
297	0.180E+03	0.167E-03	0.126E-03	0.343E-04	0.940E-04	0.187E-04

```

298
299  PROTON ENERGY = 39.700000
300  TOTAL CR-SECT.= 1.000653
301  REACTION CR-SECT. = 0.264859
302
303      NMAX          CR-SECT. OF LEVEL EXCITATION
304      1              0.692410
305      2              0.027280
306      3              0.012021
307      4              0.002326
308      5              0.001758
309
310          STRENGTH FUNCTIONS
311  SF0= 0.1466433E-04    SF1= 0.1533456E-04    SF2= 0.1760779E-04

```

CR-SECT file

```

1  2.09000E+01 1.38545E+00 3.79940E-01 9.14067E-01 6.05351E-02 2.51807E-02 4.68860E-03 1.03309E-03
2  3.97000E+01 1.00065E+00 2.64859E-01 6.92410E-01 2.72795E-02 1.20206E-02 2.32602E-03 1.75777E-03

```

TRANSME file

```

1  0.209000E+02 21
2  0.56798552 0.53319087 0.63361194 0.54421704 0.12297855 0.01569333
3  0.00231447 0.00026687 0.00001926 0.00000000 0.00000000 0.00000000
4  0.00000000 0.00000000 0.00000000 0.00000000 0.00000000 0.00000000
5  0.00000000 0.00000000 0.00000000 0.00000000
6  0.397000E+02 25
7  0.58054689 0.58024863 0.60197984 0.56873163 0.34147679 0.10344974
8  0.02404181 0.00545803 0.00114899 0.00023893 0.00005012 0.00001035
9  0.00000204 0.00000041 0.00000008 0.00000001 0.00000000 0.00000000
10 0.00000000 0.00000000 0.00000000 0.00000000 0.00000000 0.00000000
11 0.00000000 0.00000000

```

GNASH file

```

1  0.209000E+02 50
2  0.5680E+00 0.5656E+00 0.7078E+00 0.5170E+00 0.5842E+00 0.3946E+00
3  0.8497E-01 0.6565E+00 0.1534E+00 0.1412E-01 0.2221E-02 0.1700E-01
4  0.2394E-02 0.2906E-03 0.4093E-04 0.2461E-03 0.0000E+00 0.0000E+00
5  0.0000E+00 0.0000E+00 0.0000E+00 0.0000E+00 0.0000E+00 0.0000E+00

```

```

6   0.0000E+00 0.0000E+00 0.0000E+00 0.0000E+00 0.0000E+00 0.0000E+00
7   0.0000E+00 0.0000E+00 0.0000E+00 0.0000E+00 0.0000E+00 0.0000E+00
8   0.0000E+00 0.0000E+00 0.0000E+00 0.0000E+00 0.0000E+00 0.0000E+00
9   0.0000E+00 0.0000E+00 0.0000E+00 0.0000E+00 0.0000E+00 0.0000E+00
10  0.0000E+00 0.0000E+00 0.0000E+00 0.0000E+00 0.0000E+00 0.0000E+00
11  0.0000E+00 0.0000E+00 0.0000E+00 0.0000E+00 0.0000E+00 0.0000E+00
12  0.0000E+00 0.0000E+00 0.0000E+00 0.0000E+00 0.0000E+00 0.0000E+00
13  0.0000E+00 0.0000E+00 0.0000E+00 0.0000E+00 0.0000E+00 0.0000E+00
14  0.0000E+00 0.0000E+00 0.0000E+00 0.0000E+00 0.0000E+00 0.0000E+00
15  0.0000E+00 0.0000E+00 0.0000E+00 0.0000E+00 0.0000E+00 0.0000E+00
16  0.0000E+00 0.0000E+00 0.0000E+00 0.0000E+00 0.0000E+00 0.0000E+00
17  0.0000E+00 0.0000E+00 0.0000E+00 0.0000E+00 0.0000E+00 0.0000E+00
18  0.0000E+00 0.0000E+00 0.0000E+00 0.0000E+00 0.0000E+00 0.0000E+00
19  0.397000E+02 50
20  0.5805E+00 0.6021E+00 0.6613E+00 0.5693E+00 0.5624E+00 0.5437E+00
21  0.2676E+00 0.5875E+00 0.4006E+00 0.8819E-01 0.2423E-01 0.1162E+00
22  0.2388E-01 0.6114E-02 0.1432E-02 0.4884E-02 0.8974E-03 0.3360E-03
23  0.7998E-04 0.1516E-03 0.2298E-04 0.1877E-04 0.4178E-05 0.2632E-05
24  0.6723E-07 0.8543E-06 0.1572E-06-0.5349E-16 0.1129E-15 0.2579E-07
25  0.3758E-08-0.4354E-16 0.0000E+00 0.0000E+00 0.0000E+00 0.0000E+00
26  0.0000E+00 0.0000E+00 0.0000E+00 0.0000E+00 0.0000E+00 0.0000E+00
27  0.0000E+00 0.0000E+00 0.0000E+00 0.0000E+00 0.0000E+00 0.0000E+00
28  0.0000E+00 0.0000E+00 0.0000E+00 0.0000E+00 0.0000E+00 0.0000E+00
29  0.0000E+00 0.0000E+00 0.0000E+00 0.0000E+00 0.0000E+00 0.0000E+00
30  0.0000E+00 0.0000E+00 0.0000E+00 0.0000E+00 0.0000E+00 0.0000E+00
31  0.0000E+00 0.0000E+00 0.0000E+00 0.0000E+00 0.0000E+00 0.0000E+00
32  0.0000E+00 0.0000E+00 0.0000E+00 0.0000E+00 0.0000E+00 0.0000E+00
33  0.0000E+00 0.0000E+00 0.0000E+00 0.0000E+00 0.0000E+00 0.0000E+00
34  0.0000E+00 0.0000E+00 0.0000E+00 0.0000E+00 0.0000E+00 0.0000E+00
35  0.0000E+00 0.0000E+00 0.0000E+00 0.0000E+00 0.0000E+00 0.0000E+00
36  0.0000E+00 0.0000E+00 0.0000E+00 0.0000E+00 0.0000E+00 0.0000E+00

```

ANG-DIST file

```

1
2
3  NEUTRON ENERGY = 20.900000
4      0.100E+01    0.109E+01  0.162E-01  0.233E-02  0.206E-02  0.112E-03
5      0.500E+01    0.106E+01  0.159E-01  0.233E-02  0.196E-02  0.112E-03

```

6	0.100E+02	0.968E+00	0.150E-01	0.234E-02	0.166E-02	0.111E-03
7	0.150E+02	0.836E+00	0.139E-01	0.234E-02	0.124E-02	0.108E-03
8	0.180E+02	0.743E+00	0.132E-01	0.234E-02	0.966E-03	0.106E-03
9	0.210E+02	0.646E+00	0.126E-01	0.235E-02	0.707E-03	0.104E-03
10	0.240E+02	0.550E+00	0.121E-01	0.235E-02	0.477E-03	0.102E-03
11	0.270E+02	0.458E+00	0.117E-01	0.236E-02	0.291E-03	0.996E-04
12	0.300E+02	0.372E+00	0.113E-01	0.238E-02	0.157E-03	0.969E-04
13	0.330E+02	0.296E+00	0.111E-01	0.240E-02	0.772E-04	0.941E-04
14	0.360E+02	0.230E+00	0.109E-01	0.243E-02	0.509E-04	0.911E-04
15	0.390E+02	0.174E+00	0.107E-01	0.246E-02	0.716E-04	0.881E-04
16	0.420E+02	0.129E+00	0.104E-01	0.250E-02	0.130E-03	0.850E-04
17	0.450E+02	0.945E-01	0.101E-01	0.255E-02	0.215E-03	0.820E-04
18	0.480E+02	0.682E-01	0.971E-02	0.260E-02	0.315E-03	0.790E-04
19	0.510E+02	0.492E-01	0.921E-02	0.265E-02	0.419E-03	0.761E-04
20	0.540E+02	0.362E-01	0.862E-02	0.269E-02	0.516E-03	0.733E-04
21	0.560E+02	0.301E-01	0.819E-02	0.272E-02	0.573E-03	0.716E-04
22	0.590E+02	0.241E-01	0.750E-02	0.275E-02	0.642E-03	0.692E-04
23	0.620E+02	0.207E-01	0.679E-02	0.277E-02	0.689E-03	0.670E-04
24	0.650E+02	0.191E-01	0.607E-02	0.278E-02	0.711E-03	0.651E-04
25	0.700E+02	0.183E-01	0.495E-02	0.276E-02	0.694E-03	0.626E-04
26	0.750E+02	0.180E-01	0.401E-02	0.270E-02	0.621E-03	0.611E-04
27	0.800E+02	0.172E-01	0.330E-02	0.260E-02	0.512E-03	0.606E-04
28	0.850E+02	0.156E-01	0.283E-02	0.247E-02	0.388E-03	0.611E-04
29	0.900E+02	0.134E-01	0.256E-02	0.232E-02	0.272E-03	0.627E-04
30	0.950E+02	0.108E-01	0.246E-02	0.217E-02	0.181E-03	0.651E-04
31	0.100E+03	0.829E-02	0.245E-02	0.202E-02	0.125E-03	0.684E-04
32	0.105E+03	0.613E-02	0.249E-02	0.187E-02	0.106E-03	0.724E-04
33	0.110E+03	0.446E-02	0.253E-02	0.172E-02	0.120E-03	0.769E-04
34	0.115E+03	0.329E-02	0.254E-02	0.159E-02	0.157E-03	0.818E-04
35	0.120E+03	0.257E-02	0.252E-02	0.145E-02	0.207E-03	0.869E-04
36	0.125E+03	0.219E-02	0.244E-02	0.133E-02	0.257E-03	0.921E-04
37	0.130E+03	0.205E-02	0.233E-02	0.120E-02	0.300E-03	0.972E-04
38	0.135E+03	0.204E-02	0.219E-02	0.108E-02	0.329E-03	0.102E-03
39	0.140E+03	0.211E-02	0.202E-02	0.963E-03	0.347E-03	0.107E-03
40	0.150E+03	0.239E-02	0.165E-02	0.749E-03	0.362E-03	0.115E-03
41	0.160E+03	0.282E-02	0.132E-02	0.577E-03	0.382E-03	0.122E-03
42	0.170E+03	0.328E-02	0.109E-02	0.465E-03	0.413E-03	0.126E-03
43	0.180E+03	0.348E-02	0.101E-02	0.426E-03	0.429E-03	0.127E-03
44						
45						
46						

47 PROTON ENERGY = 39.700000

48	0.100E+01	0.556E+04	0.785E-02	0.892E-03	0.315E-02	0.434E-03
49	0.500E+01	0.501E+01	0.766E-02	0.922E-03	0.286E-02	0.432E-03
50	0.100E+02	0.738E+00	0.727E-02	0.101E-02	0.211E-02	0.428E-03
51	0.150E+02	0.722E+00	0.713E-02	0.115E-02	0.123E-02	0.423E-03
52	0.180E+02	0.645E+00	0.732E-02	0.127E-02	0.771E-03	0.422E-03
53	0.210E+02	0.540E+00	0.773E-02	0.142E-02	0.429E-03	0.421E-03
54	0.240E+02	0.428E+00	0.831E-02	0.161E-02	0.222E-03	0.421E-03
55	0.270E+02	0.324E+00	0.892E-02	0.184E-02	0.142E-03	0.420E-03
56	0.300E+02	0.235E+00	0.943E-02	0.209E-02	0.163E-03	0.418E-03
57	0.330E+02	0.163E+00	0.969E-02	0.237E-02	0.247E-03	0.413E-03
58	0.360E+02	0.109E+00	0.963E-02	0.263E-02	0.356E-03	0.404E-03
59	0.390E+02	0.705E-01	0.920E-02	0.287E-02	0.459E-03	0.391E-03
60	0.420E+02	0.443E-01	0.844E-02	0.304E-02	0.531E-03	0.374E-03
61	0.450E+02	0.278E-01	0.745E-02	0.314E-02	0.563E-03	0.352E-03
62	0.480E+02	0.180E-01	0.632E-02	0.315E-02	0.553E-03	0.327E-03
63	0.510E+02	0.127E-01	0.519E-02	0.307E-02	0.507E-03	0.299E-03
64	0.540E+02	0.100E-01	0.414E-02	0.291E-02	0.437E-03	0.270E-03
65	0.560E+02	0.915E-02	0.351E-02	0.276E-02	0.383E-03	0.251E-03
66	0.590E+02	0.846E-02	0.272E-02	0.249E-02	0.299E-03	0.222E-03
67	0.620E+02	0.803E-02	0.210E-02	0.219E-02	0.221E-03	0.194E-03
68	0.650E+02	0.757E-02	0.165E-02	0.188E-02	0.156E-03	0.169E-03
69	0.700E+02	0.645E-02	0.120E-02	0.138E-02	0.846E-04	0.134E-03
70	0.750E+02	0.499E-02	0.997E-03	0.968E-03	0.581E-04	0.107E-03
71	0.800E+02	0.352E-02	0.913E-03	0.657E-03	0.629E-04	0.888E-04
72	0.850E+02	0.229E-02	0.855E-03	0.450E-03	0.809E-04	0.768E-04
73	0.900E+02	0.141E-02	0.775E-03	0.325E-03	0.967E-04	0.694E-04
74	0.950E+02	0.878E-03	0.664E-03	0.258E-03	0.102E-03	0.647E-04
75	0.100E+03	0.602E-03	0.533E-03	0.223E-03	0.937E-04	0.612E-04
76	0.105E+03	0.483E-03	0.402E-03	0.202E-03	0.759E-04	0.580E-04
77	0.110E+03	0.438E-03	0.288E-03	0.184E-03	0.541E-04	0.546E-04
78	0.115E+03	0.410E-03	0.201E-03	0.163E-03	0.341E-04	0.507E-04
79	0.120E+03	0.372E-03	0.142E-03	0.139E-03	0.201E-04	0.463E-04
80	0.125E+03	0.318E-03	0.109E-03	0.113E-03	0.137E-04	0.416E-04
81	0.130E+03	0.252E-03	0.975E-04	0.877E-04	0.143E-04	0.367E-04
82	0.135E+03	0.185E-03	0.997E-04	0.662E-04	0.201E-04	0.320E-04
83	0.140E+03	0.127E-03	0.110E-03	0.497E-04	0.288E-04	0.277E-04
84	0.150E+03	0.640E-04	0.131E-03	0.325E-04	0.490E-04	0.212E-04
85	0.160E+03	0.812E-04	0.138E-03	0.302E-04	0.692E-04	0.184E-04
86	0.170E+03	0.137E-03	0.131E-03	0.329E-04	0.866E-04	0.184E-04
87	0.180E+03	0.167E-03	0.126E-03	0.343E-04	0.940E-04	0.187E-04

ANG-POL file

1 EN= 20.900 LKK= 16 LCoul= 0
 2 2.09000E+01 1.38545E+00 3.79940E-01 9.14067E-01 6.05351E-02 2.51807E-02 4.68860E-03 1.03309E-03
 3
 4 LEGENDR. COEFFICIENTS FOR SCATTERED NUCLEONS
 5 ANGULAR DISTRIBUTIONS - NUCLEAR AMPLITUDE
 6 0.7273915E-01 0.5898448E-01 0.4390528E-01 0.3077654E-01 0.2000609E-01 0.1092628E-01
 7 0.4836791E-02 0.1777011E-02 0.5940243E-03 0.1795478E-03 0.5006882E-04 0.1215770E-04
 8 0.2469515E-05 0.4116757E-06 0.5821751E-07 0.5745959E-08
 9
 10 LEGENDR. COEFFICIENTS FOR SCATTERED NUCLEONS
 11 ANGULAR DISTRIBUTIONS - NUCLEAR AMPLITUDE
 12 0.4817228E-02 0.1848747E-02 0.6925918E-03 0.1671676E-03 -0.1167548E-03 -0.2017821E-04
 13 0.6002816E-04 0.5633421E-04 0.2904394E-04 0.1113681E-04 0.3735483E-05 0.1044271E-05
 14 0.2531019E-06 0.4616125E-07 0.6739197E-08 0.6387672E-09
 15
 16 LEGENDR. COEFFICIENTS FOR SCATTERED NUCLEONS
 17 ANGULAR DISTRIBUTIONS - NUCLEAR AMPLITUDE
 18 0.2003816E-02 0.3550142E-03 -0.1354394E-03 -0.3502169E-04 0.1373164E-05 0.1409758E-04
 19 0.4758183E-05 -0.8137583E-06 -0.1089153E-05 -0.4855418E-06 -0.1935467E-06 -0.5276595E-07
 20 -0.1149961E-07 -0.1935349E-08 -0.2541339E-09 -0.2070934E-10
 21
 22 LEGENDR. COEFFICIENTS FOR SCATTERED NUCLEONS
 23 ANGULAR DISTRIBUTIONS - NUCLEAR AMPLITUDE
 24 0.3731065E-03 0.5591280E-04 0.2433522E-04 -0.1947962E-04 0.2411375E-04 0.5483680E-04
 25 0.3466208E-04 0.1054768E-04 0.4555719E-05 0.1271215E-05 0.3495058E-06 0.8173112E-07
 26 0.1660130E-07 0.2365169E-08 0.2804025E-09 0.2310940E-10
 27
 28 LEGENDR. COEFFICIENTS FOR SCATTERED NUCLEONS
 29 ANGULAR DISTRIBUTIONS - NUCLEAR AMPLITUDE
 30 0.8221064E-04 -0.4358407E-05 0.7687309E-05 0.8635448E-06 -0.8584820E-07 -0.4253553E-07
 31 0.5103806E-08 0.6306504E-09 0.1028740E-09 0.9863331E-11 0.9145143E-12 0.7514261E-13
 32 0.4705348E-14 0.2251600E-15 0.9656394E-17 0.2954612E-18
 33
 34 EN= 39.700 LKK= 32 LCoul= 17
 35 3.97000E+01 1.00065E+00 2.64859E-01 6.92410E-01 2.72795E-02 1.20206E-02 2.32602E-03 1.75777E-03
 36
 37 LEGENDR. COEFFICIENTS FOR SCATTERED NUCLEONS
 38 ANGULAR DISTRIBUTIONS - NUCLEAR AMPLITUDE
 39 0.5510026E-01 0.5001478E-01 0.4225945E-01 0.3380929E-01 0.2559971E-01 0.1796658E-01
 40 0.1146576E-01 0.6588372E-02 0.3442153E-02 0.1665099E-02 0.7598520E-03 0.3308341E-03
 41 0.1382521E-03 0.5551628E-04 0.2136753E-04 0.7856113E-05 0.2754915E-05 0.9224075E-06
 42 0.2955555E-06 0.9079054E-07 0.2672562E-07 0.7523182E-08 0.2022715E-08 0.5179501E-09
 43 0.1255245E-09 0.2855019E-10 0.6028901E-11 0.1166925E-11 0.2038538E-12 0.3138475E-13
 44 0.4039403E-14 0.3655144E-15
 45
 46 LEGENDR. COEFFICIENTS FOR SCATTERED PROTONS
 47 ANGULAR DISTRIBUTIONS - COULOMB AMPLITUDE
 48 -0.43144485E-05 0.2797939E-04 -0.7199055E-05 0.2783942E-04 -0.6485193E-05 0.2564986E-04
 49 -0.2945286E-05 0.2020685E-04 0.1981937E-05 0.1197007E-04 0.2285245E-05 0.4363644E-05
 50 0.9975999E-06 0.1387087E-05 0.3664401E-06 0.4539757E-06 0.1263797E-06 0.1495558E-06

```

51   0.4115918E-07  0.4917498E-07  0.1254616E-07  0.1550942E-07  0.3479920E-08  0.4484606E-08
52   0.8614987E-09  0.1158921E-08  0.1897606E-09  0.2668946E-09  0.3769278E-10  0.5532170E-10
53   0.6863509E-11  0.1048498E-10  0.4011227E-12  0.6564278E-12
54
55       LEGENDR. COEFFICIENTS FOR SCATTERED NUCLEONS
56           ANGULAR DISTRIBUTIONS - NUCLEAR AMPLITUDE
57   0.2170835E-02  0.1412309E-02  0.6522240E-03  0.1489376E-03  -0.9879521E-04  -0.1874813E-03
58   -0.1411942E-03  -0.3952954E-04  0.2521289E-04  0.4118332E-04  0.3201004E-04  0.1829764E-04
59   0.8012941E-05  0.2296871E-05  -0.7746487E-08  -0.5016906E-06  -0.3702525E-06  -0.1738292E-06
60   -0.5883821E-07  -0.1288533E-07  -0.6759290E-10  0.1646849E-08  0.1021304E-08  0.4263068E-09
61   0.1424714E-09  0.4007164E-10  0.9650292E-11  0.1996839E-11  0.3528891E-12  0.5227283E-13
62   0.6176636E-14  0.4876127E-15
63
64       LEGENDR. COEFFICIENTS FOR SCATTERED NUCLEONS
65           ANGULAR DISTRIBUTIONS - NUCLEAR AMPLITUDE
66   0.9565691E-03  0.5102000E-03  0.8365503E-04  -0.1187958E-03  -0.1331185E-03  -0.5775174E-04
67   0.8367231E-05  0.2328133E-04  0.1339943E-04  0.3604671E-05  -0.7366372E-06  -0.1517552E-05
68   -0.1102538E-05  -0.5784097E-06  -0.2433012E-06  -0.8433366E-07  -0.2419922E-07  -0.5657427E-08
69   -0.1007560E-08  -0.1000858E-09  0.1361956E-10  0.1033220E-10  0.3232954E-11  0.7169172E-12
70   0.1174102E-12  0.1225515E-13  -0.8647102E-16  -0.3966461E-15  -0.1095979E-15  -0.1957308E-16
71   -0.2525476E-17  -0.2048621E-18
72
73       LEGENDR. COEFFICIENTS FOR SCATTERED NUCLEONS
74           ANGULAR DISTRIBUTIONS - NUCLEAR AMPLITUDE
75   0.1850992E-03  0.1030871E-03  0.5518601E-04  0.2319700E-04  0.1718877E-04  0.1318311E-04
76   0.2356545E-04  0.3151302E-04  0.2686733E-04  0.1675987E-04  0.9029487E-05  0.4320527E-05
77   0.1902438E-05  0.7826731E-06  0.3022264E-06  0.1093565E-06  0.3699940E-07  0.1171050E-07
78   0.3477649E-08  0.9727038E-09  0.2567319E-09  0.6393304E-10  0.1500060E-10  0.3310516E-11
79   0.6832691E-12  0.1307962E-12  0.2296452E-13  0.3643733E-14  0.5125194E-15  0.6208137E-16
80   0.6113328E-17  0.4108569E-18
81
82       LEGENDR. COEFFICIENTS FOR SCATTERED NUCLEONS
83           ANGULAR DISTRIBUTIONS - NUCLEAR AMPLITUDE
84   0.1398786E-03  0.6892511E-04  0.2506651E-04  0.5067118E-05  -0.4245684E-05  -0.4320062E-05
85   -0.1111258E-05  0.3199606E-06  0.5811792E-06  0.3402495E-06  0.1579071E-06  0.6471443E-07
86   0.2554638E-07  0.9748736E-08  0.3492891E-08  0.1151697E-08  0.3499297E-09  0.9929605E-10
87   0.2667402E-10  0.6819424E-11  0.1654575E-11  0.3784061E-12  0.8096309E-13  0.1607042E-13
88   0.2931545E-14  0.4867789E-15  0.7282979E-16  0.9703776E-17  0.1133861E-17  0.1133306E-18
89   0.9181377E-20  0.5028210E-21

```

11 Program SHEMMAN

As was mentioned before, the CC-calculations with coupling built on the soft-rotator model are self-consistent as parameters of non-axial soft nuclear Hamiltonian, which determine coupling, are first tested to predict collective levels of the nucleus. A code SHEMMAN adjusts such parameters comparing experimental and calculated levels. It uses the same search procedure as OPTMAN, but the χ^2 function is now the sum of squares of the calculated and experimental level energy differences divided by the squares of experimental energies. Here we describe input for nuclear Hamiltonian parameters adjustment using SHEMMAN code.

11.1 Input Data

Input data of SHEMMAN is described here. Data has the card image form. Units of the data are MeV.

- Record 1 - Any text information that identifies current calculations
- Record 2 - FORMAT(25I2)

NPRI , NUR , MEHAM , MESHA , MESHO , MEHAO

Switches describing adjustment and form of nuclear Hamiltonian

- **NPRI** - detailed output including a comparison of the experimental and calculated level energies; nuclear Hamiltonian parameters and the χ^2 value are written at each **NPRI** iteration during the search;
- **NUR** - number of experimental levels adjusted ($\text{NUR} \leq 20$);
- **MEHAM , MESHA , MESHO , MEHAO** - switches determining nuclear Hamiltonian model, with the meaning described in OPTMAN code input

- Record 3 FORMAT(6E12.7) Cards 3a, 3b, 3c

Parameters of non-axial nuclear Hamiltonian

HW , AMBO , AMGO , GAMO , BETO , BET4 - Card 3

BB42 , GAMG , DELG , BET3 , ETO , AMUO - Card 4

HWO , BB32 , GAMDE , DPAR , GSHPA - Card 5

The input format, sequence and meaning of the parameters are the same as in OPTMAN code - see description of OPTMAN input for details.

- Record 4 FORMAT(E10.4,6I2) Cards 4a, 4b,

Characteristics of nuclear levels

(ES(I), JU(I), NPI(I), NTU(I), NNB(I), NNG(I), NNO(I), I=1,NUR)

- **ES(I)** - energy of experimental level;
- **JU(I)** - spin of level (not multiplied by 2);
- **NPI(I)** - parity of level =+1 -for positive,=-1 -for negative;
- **NTU(I)** - the number of rotational energy solution τ ;
- **NNB(I)** - the number of β_2 oscillation function solution n_{β_2} ;
- **NNG(I)** - the number of γ oscillation function solution n_γ ;
- **NNO(I)** - the number of β_3 oscillation function solution n_{β_3} ;

meaning of these parameters are also described in OPTMAN input

- Record 5 - FORMAT(25I2)

Input of flags that determine which parameters of nuclear Hamiltonian will be adjusted, if **NPJ(I)=1**

the chosen parameter will be adjusted

(NPJ(I), I=1,16)

- NPJ(1) - flag for energy scale factor $\hbar\omega_0$ HW;
 - NPJ(2) - flag for nuclear softness $\mu_{\beta_{20}}$ AMBO;
 - NPJ(3) - flag for nuclear softness μ_{γ_0} AMGO;
 - NPJ(4) - flag for equilibrium non-axiality γ_0 GAMO;
 - NPJ(5) - flag for a_{42} BB42;
 - NPJ(6) - flag for non-axiality γ_4 GAMG;
 - NPJ(7) - flag for non-axiality δ_4 DELG;
 - NPJ(8) - flag for β_3 deformation ϵ_0 if MEHA0=2, β_{30} if MEHA0=3 BET3;
 - NPJ(9) - flag for β_3 non-axiality η ETO;
 - NPJ(10) - flag for β_3 softness μ_ϵ AMUO;
 - NPJ(11) - flag for energy scale factor of octupole oscillations $\hbar\omega_\epsilon$, used if MEHA0=1 HWO;
 - NPJ(12) - flag for a_{32} BB32;
 - NPJ(13) - flag not in use;
 - NPJ(14) - flag for energy splitting parameter δ_n DPAR;
 - NPJ(15) - flag no in use;
 - NPJ(16) - flag awaking γ transition calculations between levels (if this flag =1, other flags are ignored);
- Record 6 FORMAT(8D10.4) Cards 6a,
- (EP(I), I=1,NV)
- EP(I) - absolute accuracy for parameter with I^{th} flag=1, NV is equal to the number of flags=1;

This is the last card in input.

11.2 An Example of Input File

Here we present an input for ^{62}Ni nuclear Hamiltonian adjustment:

```

1  GAMBET   NI-62   BET3=BETO*KSI
2  200705010202
3  0.13346E+01 0.16260E+01 0.62668E+00 0.30681E+00 0.10280E+00 0.14883E-01
4  0.11933E-01 0.11365E+00 0.69740E+00 0.57435E+00 0.94804E-01 0.25984E+00

```

```

5  0.35000E+00 0.10000E-03 0.00000E+00 0.64753E+01 0.00000E+00
6  0.00000-0000+101000000  LEVELS OF Ni-62
7  1.17280-0002+101000000  ES(I),JU(I),NPI(I),NTU(I),NNB(I),NNG(I),NNO(I)
8  2.04840-0000+101010000
9  2.33610+0004+101000000
10 3.55270+0003+101000000
11 3.15770-0002+102000000
12 3.51850-0002+101010000
13 1 0 0 0 0 0 0 0 0 0 0 0 0 0 0 0
14 1.0000-05

```

Here we present output file for ^{62}Ni nuclear Hamiltonian adjustment

```

1  GAMBIT   NI-62   BET3=BETO*KSI
2  0.11728D+01  0.11301D+01  0.36419D-01  2   1   0   0   0
3  0.20484D+01  0.22176D+01  -0.82598D-01  0   1   1   0   0
4  0.23361D+01  0.24250D+01  -0.38044D-01  4   1   0   0   0
5  0.35527D+01  0.35381D+01  0.41162D-02  3   1   0   0   0
6  0.31577D+01  0.31577D+01  0.52481D-05  2   2   0   0   0
7  0.35185D+01  0.36217D+01  -0.29320D-01  2   1   1   0   0
8  0          0.174545825473537D-02
9  0.1334600D+01
10 0.11728D+01  0.11301D+01  0.36412D-01  2   1   0   0   0
11 0.20484D+01  0.22176D+01  -0.82606D-01  0   1   1   0   0
12 0.23361D+01  0.24250D+01  -0.38052D-01  4   1   0   0   0
13 0.35527D+01  0.35381D+01  0.41087D-02  3   1   0   0   0
14 0.31577D+01  0.31577D+01  -0.22448D-05  2   2   0   0   0
15 0.35185D+01  0.36217D+01  -0.29328D-01  2   1   1   0   0
16 0.11728D+01  0.10807D+01  0.78495D-01  2   1   0   0   0
17 0.20484D+01  0.21208D+01  -0.35325D-01  0   1   1   0   0
18 0.23361D+01  0.23191D+01  0.72838D-02  4   1   0   0   0
19 0.35527D+01  0.33836D+01  0.47603D-01  3   1   0   0   0
20 0.31577D+01  0.30198D+01  0.43671D-01  2   2   0   0   0
21 0.35185D+01  0.34635D+01  0.15627D-01  2   1   1   0   0
22 0.11728D+01  0.11202D+01  0.44834D-01  2   1   0   0   0
23 0.20484D+01  0.21982D+01  -0.73144D-01  0   1   1   0   0
24 0.23361D+01  0.24038D+01  -0.28978D-01  4   1   0   0   0
25 0.35527D+01  0.35072D+01  0.12814D-01  3   1   0   0   0
26 0.31577D+01  0.31301D+01  0.87385D-02  2   2   0   0   0
27 0.35185D+01  0.35900D+01  -0.20331D-01  2   1   1   0   0
28 1          0.147561991774612D-02
29 0.1322945D+01
30 0.13229E+01  0.16260E+01  0.62668E+00  0.30681E+00  0.10280E+00  0.14883E-01
31 0.11933E-01  0.11365E+00  0.69740E+00  0.57435E+00  0.94804E-01  0.25984E+00
32 0.35000E+00  0.10000E-03  0.00000E+00  0.64753E+01  0.00000E+00
33 1          0.136415233166913D-02
34 0.1311289D+01
35 0.13113E+01  0.16260E+01  0.62668E+00  0.30681E+00  0.10280E+00  0.14883E-01
36 0.11933E-01  0.11365E+00  0.69740E+00  0.57435E+00  0.94804E-01  0.25984E+00
37 0.35000E+00  0.10000E-03  0.00000E+00  0.64753E+01  0.00000E+00
38 1          0.136086330456320D-02

```

```

39      0.1308958D+01
40  0.13090E+01 0.16260E+01 0.62668E+00 0.30681E+00 0.10280E+00 0.14883E-01
41  0.11933E-01 0.11365E+00 0.69740E+00 0.57435E+00 0.94804E-01 0.25984E+00
42  0.35000E+00 0.10000E-03 0.00000E+00 0.64753E+01 0.00000E+00
43      1      0.136086253438106D-02
44      0.1308939D+01
45  0.13089E+01 0.16260E+01 0.62668E+00 0.30681E+00 0.10280E+00 0.14883E-01
46  0.11933E-01 0.11365E+00 0.69740E+00 0.57435E+00 0.94804E-01 0.25984E+00
47  0.35000E+00 0.10000E-03 0.00000E+00 0.64753E+01 0.00000E+00
48      1      0.136086216962804D-02
49      0.1308921D+01
50  0.13089E+01 0.16260E+01 0.62668E+00 0.30681E+00 0.10280E+00 0.14883E-01
51  0.11933E-01 0.11365E+00 0.69740E+00 0.57435E+00 0.94804E-01 0.25984E+00
52  0.35000E+00 0.10000E-03 0.00000E+00 0.64753E+01 0.00000E+00
53      1      0.136086214532893D-02
54      0.1308917D+01
55  0.13089E+01 0.16260E+01 0.62668E+00 0.30681E+00 0.10280E+00 0.14883E-01
56  0.11933E-01 0.11365E+00 0.69740E+00 0.57435E+00 0.94804E-01 0.25984E+00
57  0.35000E+00 0.10000E-03 0.00000E+00 0.64753E+01 0.00000E+00
58      1      0.136086213724699D-02
59      0.1308913D+01
60  0.13089E+01 0.16260E+01 0.62668E+00 0.30681E+00 0.10280E+00 0.14883E-01
61  0.11933E-01 0.11365E+00 0.69740E+00 0.57435E+00 0.94804E-01 0.25984E+00
62  0.35000E+00 0.10000E-03 0.00000E+00 0.64753E+01 0.00000E+00

```

11.3 Running the SHEMMAN Code

The code will first ask the name of input file, then code will suggest to give the name of the output file. While running, after each adjustment of χ^2 value, best Hamiltonian parameters and Hamiltonian parameters organized in the input format necessary for OPTMAN code will be given. After each NPRI adjustments detailed information about current search is outputted. In case where all NPJ(I)=0, initial information including χ^2 and level energies is printed and the code stops.

12 Conclusions

According to ISTC Project's Working Plan we modernized computational approaches of OPTMAN and SHEMMAN codes. New accurate numerical algorithms possible now due to available large computational resources are introduced, and user-friendly interface BEGIN for checking input of OPTMAN code was also developed. We developed two modernized algorithms for solution of coupled channels equations in scattering problem. First is the accurate system solution, which is 6-20 times faster than previously used one. Second quick solution algorithm is the iterative one with the improved convergence. We also improved the accuracy of matching procedure in case of charged scattered particles. All the algorithms are already included in the currently modernized code OPTMAN. User of it can choose among these algorithms when running optical calculations or as one of OPTMAN code options allow the code to apply optimal by time solution algorithm, depending of the number of couple equations, of the coupling

strength, incident particle energy, system spin. Physically-grounded dependence of the optical potential parameters on projectile energy was adopted to allow for an easy global optical potential search. Physical and mathematical ideas of the work were developed in close cooperation with our Collaborating Party. Current version of modernized OPTMAN code was used to find best fit nuclear optical parameters for ^{24}Mg , ^{26}Mg , ^{12}C , $^{28-30}\text{Si}$ and ^{52}Cr which are forwarded to Collaborative Party. They were already used for prediction of optical cross sections of natural Si, Mg and ^{12}C for Japanese high energy file evaluation - cooperative work with our Collaborating Party. Therefore, implementation of the Project already gives additional applicational results not planned by the Project Working Plan.

Acknowledgements

This work was carried out as ISTC Project B-521 with Japan as Financing Party. The authors are grateful to guidance of the late Dr. Y. Kikuchi who had started the collaboration among authors. They also thank members of JIENR and JAERI nuclear data center for helpful comments and supports. One of the authors, E. Soukhovitski, is grateful to JAERI for financial support of the work, offering an opportunity to stay at JAERI via foreign scientist invitation program and for the hospitality of Advance Science Research Center and Nuclear Data Center staff, that made this work possible.

References

- [1] A.I. Blokhin, A.V. Ignatjuk, V.N. Manokhin *et al.*, "BROND-2, Library of Recommended Evaluated Neutron Data, Documentation of Data Files", Yudernie Konstanty, issues 2+3 in English (1991).
- [2] T. Tamura, Rev. Mod. Phys. **37**, 679 (1965).
- [3] J. Raynal, "Optical Model and Coupled-Cannel Calculations in Nuclear Physics", IAEA SMR-9/8, IAEA (1970).
- [4] Y. V. Porodzinski $\ddot{\text{i}}$ and E. S. Sukhovitski $\ddot{\text{i}}$, Phys. of Atom. Nucl. **59**, 247 (1996).
- [5] Y. V. Porodzinski $\ddot{\text{i}}$ and E. S. Sukhovitski $\ddot{\text{i}}$, Sov. J. Nucl. Phys. **53**, 41 (1991).
- [6] Y. V. Porodzinski $\ddot{\text{i}}$ and E. S. Sukhovitski $\ddot{\text{i}}$, Sov. J. Nucl. Phys. **54**, 570 (1991).
- [7] E.S. Soukhovitski $\ddot{\text{i}}$ and S. Chiba, J. Nucl. Sci. Technol. **Suppl. 2**, 697(2002).
- [8] E. S. Sukhovitski $\ddot{\text{i}}$, O. Iwamoto, S. Chiba and T. Fukahori, J. Nucl. Sci. Technol. **37**, 120 (2000).
- [9] E. Sh. Soukhovitski, S. Chiba, J. Nucl. Sci. Technol., **Supple. 2**, 144 (2002).
- [10] S. Chiba, O. Iwamoto, Y. Yamanouti, M. Sugimoto, M. Mizumoto, K. Hasegawa, E. Sh. Sukhovitski $\ddot{\text{i}}$, Y. V. Porodzinski $\ddot{\text{i}}$, and Y. Watanabe, Nucl. Phys. A **624**, 305 (1997).
- [11] S. Chiba, O. Iwamoto, E. S. Sukhovitski $\ddot{\text{i}}$, Yu. Watanabe and T. Fukahori, J. Nucl. Sci. Technol. **37**, 498 (2000).
- [12] W. Sun, Y. Watanabe, E. Sh. Sukhovitski $\ddot{\text{i}}$, O. Iwamoto and S. Chiba, J. of Nucl. Sci. and Technol. **40**, 635 (2003).
- [13] E.S. Sukhovitski $\ddot{\text{i}}$, S. Chiba, J.-Y. Lee, B.-t. Kim and S.-W. Hong, J. Nucl. Sci. Technol. **40**, 69(2003).
- [14] J.Y. Lee, E. Sh. Sukhovitski $\ddot{\text{i}}$, Y.-O. Lee, J. Chang, S. Chiba and O. Iwamoto, J. Korean Phys. Soc. **38**, 88 (2001).
- [15] E.S. Sukhovitski $\ddot{\text{i}}$, S. Chiba, J.-Y. Lee, Y.-O. Lee, J. Chang, T. Maruyama and O. Iwamoto, J. Nucl. Sci. Technol. **39**, 816 (2002).
- [16] E.S. Sukhovitski $\ddot{\text{i}}$, Y.-O. Lee, J. Chang, S. Chiba and O. Iwamoto, Phys. Rev. C**62**, 044605 (2000).
- [17] S. Hama, B.C. Clark, E.D. Cooper, H.S. Sherif and R.L. Mercer, Phys. Rev. C **41**, 2737(1990).
- [18] R.L.B. Elton, Nuovo Cimento **XLII B**, 277 (1966).
- [19] D. G. Madland, A. J. Sierk, Proc. Int. Conf. on Nuclear Data for Science and Technology, vol 1, p 202, Trieste, 1997.

- [20] G. E. Brown and M. Rho, Nucl. Phys. **A372**, 397(1981).
- [21] E.S. Sukhovitskiĭ, G.B. Morogovskii, S. Chiba, O. Iwamoto and T. Fukahori, " *Physics and Numerical Methods of OPTMAN: a Coupled-channels Method Based on Soft-rotator Model for a Description of Collective Nuclear Structure and Excitations*" , JAERI-Data/Code 2004-002(2004).
- [22] A. Bohr and B. R. Mottelson, " *Nuclear Structure, Vol. II, Nuclear Deformations*" , p.195, W. A. Benjamin Inc. (1975).
- [23] A. S. Davydov, " *Vozbuzhdennye sostoyaniya atomnykh yader (Excited States of Atomic Nuclei)*" , Moscow: Atomizdat (1969).
- [24] P. O. Lipas and J. P. Davidson, Nucl. Phys. **26**, 80 (1961).
- [25] F. Todd Baker, Nucl. Phys. **A331**, 39 (1979).
- [26] S. G. Rohozinski and A. Sobczewski, Acta. Phys. Polon. B **12**, 1001 (1981).
- [27] I. M. Strutinsky, Atomic Energy **4**, 150 (1956).
- [28] S. Flugge, " *Practical Quantum Mechanics*" , Springer-Verlag, Berlin-Heidelberg-New York, 1971.
- [29] A.Ya. Dzyublik and V.Yu. Denisov: Yad. Fiz. **56**, 30(1993).
- [30] J.M. Eisenberg and W. Greiner: " *Nuclear Models*" , North-Holland, Amsterdam (1970).
- [31] A.S. Davydov and G.F. Filippov: Nucl. Phys. **8**, 237(1958).
- [32] M. Abramowitz and I.A. Stegun: " *Handbook of Mathematical Functions*" , Dover Publications, New York(1965).
- [33] R. H. Bassel, R. M. Drisko, and G. R. Satchler, Oak Ridge National Laboratory Report ORNL-3240, (1962).
- [34] J. Rainal, Phys. Rev. **C23**, 2571 (1980).
- [35] E. Sh. Sukhovitskiĭ, S. Chiba, O. Iwamoto and Y.V. Porodzinskii, Nucl. Phys. **A 640**, 19 (1998).
- [36] E. Sh. Sukhovitskiĭ, S. Chiba, O. Iwamoto, Nucl. Phys. **A 646**, 147 (1999).
- [37] Y. Kikuchi, INDC(FR)-5/L, 1972.
- [38] C. Störmer, Arch. Sci. Phys. **63** (1907).
- [39] J. Raynal, " *Equations couplées et DWBA*" , Report LYCEN,6804, Aussois (1968).
- [40] M.A. Melkonoff, J. Raynal, T. Sawada, Methods Comput. Phys., **6**, Academic Press, NY (1966).
- [41] P.E. Hodgson, " *The Optical Model of Elastic Scattering*" , The Clarendon Press, Oxford (1963).

- [42] ENDF-6 Formats Manual, Report IAEA-NDS-76, Rev. 6, April 2001, edited by V. McLane.
- [43] J.P. Delaroche, Y. Wang and J. Rappoport, Phys. Rev., **C39**, 391 (1989).
- [44] A.M. Lane, Phys. Rev.Lett. **8**, 171 (1962); A.M. Lane, Nucl. Phys. **35**, 676 (1962).
- [45] A. R. Barnett, Comp. Phys. Commun. **11**, 141, (1976).
- [46] P.G. Young, E.D. Arthur, M.B. Chadwick, Proc. IAEA Workshop Nucl. Reaction Data and Nucl. Reactor-Physics, Design and Safety, Triest, Italy, April 15- May 17, p.277 (1996).
- [47] M. Uhl, B. Strohmaire : “*STAPRE, A Computer Code for Particle Induced Activation Cross Sections and Related Quantities*”, IRK - 76/01, IRK Vienna (1976).
- [48] H.S. Wall : *Continued Fractions*, Van Nostard, New York (1948).
- [49] Yu.V. Porodzinskii, E. Sh. Sukhovitskii, Phys. Atom. Nucl. **55**, 1315 (1992).

国際単位系(SI)と換算表

表1 SI基本単位および補助単位

量	名称	記号
長さ	メートル	m
質量	キログラム	kg
時間	秒	s
電流	アンペア	A
熱力学温度	ケルビン	K
物質量	モル	mol
光度	カンデラ	cd
平面角	ラジアン	rad
立体角	ステラジアン	sr

表3 固有の名称をもつSI組立単位

量	名称	記号	他のSI単位による表現
周波数	ヘルツ	Hz	s ⁻¹
力	ニュートン	N	m·kg/s ²
圧力、応力	パスカル	Pa	N/m ²
エネルギー、仕事、熱量	ジュール	J	N·m
功率、放射束	ワット	W	J/s
電気量、電荷	クーロン	C	A·s
電位、電圧、起電力	ボルト	V	W/A
静電容量	ファラード	F	C/V
電気抵抗	オーム	Ω	V/A
コンダクタンス	ジーメンス	S	A/V
磁束	ウェーバ	Wb	V·s
磁束密度	テスラ	T	Wb/m ²
インダクタンス	ヘンリー	H	Wb/A
セルシウス温度	セルシウス度	°C	
光束度	ルーメン	lm	cd·sr
照度	ルクス	lx	lm/m ²
放射能	ベクレル	Bq	s ⁻¹
吸収線量	グレイ	Gy	J/kg
線量当量	シーベルト	Sv	J/kg

表2 SIと併用される単位

名称	記号
分、時、日	min, h, d
度、分、秒	°, ', "
リットル	l, L
トントン	t
電子ボルト	eV
原子質量単位	u

$$1 \text{ eV} = 1.60218 \times 10^{-19} \text{ J}$$

$$1 \text{ u} = 1.66054 \times 10^{-27} \text{ kg}$$

表4 SIと共に暫定的に維持される単位

名称	記号
オングストローム	Å
バーン	b
バール	bar
ガル	Gal
キュリ	Ci
レントゲン	R
ラド	rad
レム	rem

$$1 \text{ Å} = 0.1 \text{ nm} = 10^{-10} \text{ m}$$

$$1 \text{ b} = 100 \text{ fm}^2 = 10^{-28} \text{ m}^2$$

$$1 \text{ bar} = 0.1 \text{ MPa} = 10^5 \text{ Pa}$$

$$1 \text{ Gal} = 1 \text{ cm/s}^2 = 10^{-2} \text{ m/s}^2$$

$$1 \text{ Ci} = 3.7 \times 10^{10} \text{ Bq}$$

$$1 \text{ R} = 2.58 \times 10^{-4} \text{ C/kg}$$

$$1 \text{ rad} = 1 \text{ cGy} = 10^{-2} \text{ Gy}$$

$$1 \text{ rem} = 1 \text{ cSv} = 10^{-2} \text{ Sv}$$

表5 SI接頭語

倍数	接頭語	記号
10 ¹⁸	エクサ	E
10 ¹⁵	ペタ	P
10 ¹²	テラ	T
10 ⁹	ギガ	G
10 ⁶	メガ	M
10 ³	キロ	k
10 ²	ヘクト	h
10 ¹	デカ	da
10 ⁻¹	デシ	d
10 ⁻²	センチ	c
10 ⁻³	ミリ	m
10 ⁻⁶	マイクロ	μ
10 ⁻⁹	ナノ	n
10 ⁻¹²	ピコ	p
10 ⁻¹⁵	フェムト	f
10 ⁻¹⁸	アト	a

(注)

- 表1～5は「国際単位系」第5版、国際度量衡局1985年刊行による。ただし、1 eVおよび1 uの値はCODATAの1986年推奨値によった。
- 表4には海里、ノット、アール、ヘクタールも含まれているが日常の単位なのでここでは省略した。
- barは、JISでは流体の圧力を表す場合に限り表2のカテゴリーに分類されている。
- EC閣僚理事会指令ではbar、barnおよび「血圧の単位」mmHgを表2のカテゴリーに入れている。

換算表

力	N(=10 ⁵ dyn)	kgf	lbf
	1	0.101972	0.224809
	9.80665	1	2.20462
	4.44822	0.453592	1

$$\text{粘度 } 1 \text{ Pa}\cdot\text{s}(\text{N}\cdot\text{s}/\text{m}^2) = 10 \text{ P(ポアズ)} (\text{g}/(\text{cm}\cdot\text{s}))$$

$$\text{動粘度 } 1 \text{ m}^2/\text{s} = 10^4 \text{ St(ストークス)} (\text{cm}^2/\text{s})$$

圧力	MPa(=10 bar)	kgf/cm ²	atm	mmHg(Torr)	lbf/in ² (psi)
	1	10.1972	9.86923	7.50062 × 10 ³	145.038
力	0.0980665	1	0.967841	735.559	14.2233
	0.101325	1.03323	1	760	14.6959
	1.33322 × 10 ⁻⁴	1.35951 × 10 ⁻³	1.31579 × 10 ⁻³	1	1.93368 × 10 ⁻²
	6.89476 × 10 ⁻³	7.03070 × 10 ⁻²	6.80460 × 10 ⁻²	51.7149	1

エネルギー・仕事・熱量	J(=10 ⁷ erg)	kgf·m	kW·h	cal(計量法)	Btu	ft · lbf	eV	1 cal = 4.18605 J(計量法)
	1	0.101972	2.77778 × 10 ⁻⁷	0.238889	9.47813 × 10 ⁻⁴	0.737562	6.24150 × 10 ¹⁸	= 4.184 J (熱化学)
	9.80665	1	2.72407 × 10 ⁻⁶	2.34270	9.29487 × 10 ⁻³	7.23301	6.12082 × 10 ¹⁹	= 4.1855 J (15 °C)
	3.6 × 10 ⁶	3.67098 × 10 ⁵	1	8.59999 × 10 ⁵	3412.13	2.65522 × 10 ⁶	2.24694 × 10 ²⁵	= 4.1868 J(国際蒸気表)
	4.18605	0.426858	1.16279 × 10 ⁻⁶	1	3.96759 × 10 ⁻³	3.08747	2.61272 × 10 ¹⁹	仕事率 1 PS(仮馬力)
	1055.06	107.586	2.93072 × 10 ⁻⁴	252.042	1	778.172	6.58515 × 10 ²¹	= 75 kgf·m/s
	1.35582	0.138255	3.76616 × 10 ⁻⁷	0.323890	1.28506 × 10 ⁻³	1	8.46233 × 10 ¹⁸	= 735.499 W
	1.60218 × 10 ⁻¹⁹	1.63377 × 10 ⁻²⁰	4.45050 × 10 ⁻²⁶	3.82743 × 10 ⁻²⁰	1.51857 × 10 ⁻²²	1.18171 × 10 ⁻¹⁹	1	

放射能	Bq	Ci	吸収線量	Gy	rad
	1	2.70270 × 10 ⁻¹¹	1	100	
	3.7 × 10 ¹⁰	1	0.01	1	

照 射 線 量	C/kg	R
	1	3876
	2.58 × 10 ⁻⁴	1

線量当量	Sv	rem
	1	100
	0.01	1

(86年12月26日現在)

Programs OPTMAN and SHEMMAN Version 8 (2004)



古紙配合率100%
白色度70%の再生紙を使用しています